國立臺灣大學醫學院腦與心智科學研究所

碩士論文

Graduate Institute of Brain and Mind Sciences

College of Medicine

National Taiwan University

Master Thesis

雷特氏症之大腦結構改變與臨床表現的相關性

The brain microstructural change and its correlation with clinical presentations in Rett syndrome

詹子昀

Tz-Yun Jan

指導教授：李旺祚、曾文毅博士

Advisor: Wang-Tso Lee and Wen-Yih Isaac Tseng, Ph.D.

中華民國 106 年 07 月

July 2017

doi:10.6342/NTU201702958

目　錄

doi:10.6342/NTU201702958

Acknowledgement

雷特氏症，在我的生命歷程中就像呼吸一樣自然，當然吸到第一口氣時，也曾用盡全力地大哭過，但現在無疑是我生命中的一部份。

我很感謝子瞳用她的生命教導身邊的人關於人生的意義。雖然我沒當過一百分的姊姊，但她絕對是一百分的妹妹。當然我的爸媽，耀坤和秀鈴您們也辛苦了，謝謝您們總是無條件接受各種先斬後奏的決定，您們的付出與對我的信任，是我一輩子最珍貴的禮物。還有老詹，子晴，謝謝你一直嚇我，讓我在第一年就開始擔心畢不了業的各種事，你真的懂我，而我也畢業了，哈哈。

還要謝謝所有的家人阿嬤、大姑姑、小阿姨、爺爺與小姑姑幸福的一家，您們的支持是我身後最堅強的後盾。特別謝謝阿嬤和大姑姑，這兩年的生活起居都由您們照顧，讓我能吃飽睡暖（囤積脂肪）才能應付論文大魔王。

沒想到時間過得那麼快，還記得四年前拿著研究主題去友校找遍相關領域的老師，卻沒有人願意接下這個難題。當下真的覺得研究罕病，果然不是件容易的事。幸好在兩年前遇到李旺祚教授，第一次會談老師就欣快地答應一切，雖然我想做的內容並不是十分明確，但老師還是很細心指導。真的謝謝老師以及實驗室中的美蘭、倩文、學長、麗君和易瑾學姊。此外還要感謝曾文毅教授及實驗室的芊丰、長樂、致憲，在研究上給了我很多建議與分析技術上的指導，讓我能順利完成研究。還有台大影醫部的彭信逢醫師及團隊的護理師姊姊，您們的專業讓我們的掃描能順利進行。真心謝謝大家的協助，讓我圓了自小的夢想。

謝謝我愛的人，周和 Debbie，我曾懷疑這兩年若沒有你們，我是不是能夠平安撐過。周，我對你的感謝，就從六年多前的摩托車相遇開始，爾後就不必多說了，因為我必纏你一輩子。還有我最愛的北一籃乙，七七乳加陪著我成長，給我力量。

最後還要謝謝酒團、McDonald lab、乃綺（你總是讓我想起高中時遇到的那些特別的靈魂）、蕾雷家族、隔壁實驗室的各位學長學姊們、黑旋風及主人鱷魚子、腦心所曉雯、內湖康家、聖保祿 DC 及所有在這兩年遇到的人，不論是美國、日本、香港、上海、台灣，每次相遇都激發我的人生產生不同的變化。謝謝你們。

2016 與 2017 是不平凡的兩年，對我而言也是。
謝謝每個願意改變與接納不同的你們。因為有你，愛不罕見。

最後，真心希望這篇小小的論文能對雷特氏症的研究有所貢獻。

doi:10.6342/NTU201702958

中文摘要

研究背景:雷特氏症 (Rett syndrome) 是一種神經發展疾病，通常於六至十八個月發病，在這個階段患童會逐漸喪失溝通、認知及動作能力，取而代之的是反覆固著的手部刻板動作。部分患者在長大後會出現肌張力不全及類帕金森氏症的動作障礙，而再次影響到行動能力。在過去神經病理的檢查中發現，病患的大腦體積有明顯的減少，但相關研究甚少，結果也較不一致。

研究目的:為了瞭解疾病造成的大腦結構改變與臨床表現的相關性，本研究利用三種磁振造影技術，深入檢測患者的灰質體積與白質神經束變異之情形及次皮質中鐵離子的沉積變化，並進一步與臨床評估工具及問卷之結果作相關性比較。

研究方法:本研究共招募28位雷特氏症患者及32位年齡與性別相符的健康受試者，年齡範圍為2至27歲，並將受試者們以年齡10歲區分為兒童組與年長組，以利後續比較。腦部影像是透過一般性磁振造影 (magnetic resonance imaging, MRI) 、磁振擴散頻譜造影 (diffusion spectrum imaging, DSI) 與磁敏感加權造影 (susceptibility weighted imaging, SWI) 獲得影像結構資訊。腦部灰質體積乃利用Freesurfer軟體進行分析，而擴散頻譜造影資訊則透過全腦神經束自動分析 (tract-based automatic analysis) 得到擴散非等向性 (generalized Fractional Anisotropy, GFA) 數值，爾後再以此比較功能性神經束的完整性。磁敏感加權造影則是由訊號的對比率進行差異之比較，之後檢測與年齡及行為分數的相關性。

研究成果: 雷特氏症患者在灰質結構上依年齡呈現區域上的改變，兒童組在雙側額葉及頂葉都出現體積低於健康受試者的情形，而在年長組則為全腦的體積改變。在本研究中功能性神經束分為三大類: 語言、視知覺與動作，年長組在此三類神經束的擴散非等向性數值都是顯著低於控制組，而兒童組則保有較佳的完整性。與語言能力相關的弓狀束 (arcuate fasciculus) ，在有/無語言的兩群病患中呈現差異。而在視知覺相關的神經束中，病患的前

doi:10.6342/NTU201702958

聯合(anterior commissure) 完整性高於健康受試者，且與視覺動作整合分數呈中度正相關，而在連接兩側枕葉的神經束- 胼胝體壓部 (callosal fiber of splenium) ，也發現了相似的行為相關性。動作的部分則未發現相關的神經束與行為分數有相關。磁敏感加權造影的結果則顯示患者在紋狀體有較顯著的鐵離子沉積，而沉積情形與年齡相關。

研究結論: 在此研究中發現雷特氏症患者的大腦灰質與白質結構呈漸進式的變化。過去文獻曾指出患者的退化前期語言能力已有遲緩，根據此研究結果，弓狀束的完整性或許可作為日後語言能力的觀察目標，並進行追蹤研究。即使疾病造成嚴重的結構損害，在視知覺神經束與視動整合的相關性中，可以推測白質的完整性可能會藉由活動訓練而增加。另一方面，動作能力與動作相關神經束未見相關性，可能因為動作相關的網絡與機轉過為複雜有關。不過在基底核鐵離子沉積的發現，或許能提供另一個研究的方向，透過長期追蹤以更瞭解雷特氏症的疾病與腦部改變。

關鍵字: 雷特氏症，一般性磁振造影，磁振擴散頻譜造影，磁敏感加權造影，全腦神經束自動分析，腦部結構改變，鐵離子沉積

doi:10.6342/NTU201702958

Abstract

Objective: Rett syndrome (RTT) is a neurodevelopmental disease that primarily affects girls. It is characterized by trajectory changes in communication, cognition and motor functions. Researches in neuropathology showed some marked changes in total brain volume and cerebral size. To understand the disease-specific pathological changes of brain microstructures in RTT, we applied cortical volume data and tract-specific analysis to investigate the alteration of brain microstructure and utilized susceptibility weighted imaging (SWI) to detect abnormal iron accumulation.

Methods: We recruited 28 patients and 32 age- and sex-matched healthy controls. All of the scans were acquired by 3 tesla scanner with 32-channel phased array coil. MR imaging consists of sagittal T1-weighted and axial T2 fast spin-echo. A total of 102 diffusion encoding gradients with the maximum diffusion sensitivity were applied in diffusion spectrum imaging (DSI) and SWI sequence with flow compensation was used to acquire high-resolution imaging. Four cortical lobes were compared separately in two age groups for clarifying the regional difference. The volume data were analyzed and extracted from Freesurfer software. The generalized fractional anisotropy (GFA) value of targeted tracts were analyzed from tract-based automatic analysis (TBAA) and calculated by two sample t-test with Bonferroni correction. Signal intensity on the SWI were measured on subcortical regions and compared with health controls. Finally, Spearman's rank correlation coefficient was used in correlation between clinical presentation and brain microstructural alterations.

Results: The regional difference in gray matter showed significant decrease in bilateral frontal lobes and parietal lobes in younger patients and general decrease in four lobes in older patients. GFA values in speech-language related tracts were significantly reduced in older RTT patients. The alteration of speech-language-related tracts between the

doi:10.6342/NTU201702958

patients with/without speech was only observed in arcuate fasciculus. The comparison of visual perception-related tracts showed no difference in GFA values between younger groups, but showed severe reduction in older patients. Interestingly, the anterior commissure in both RTT groups showed higher GFA value than healthy controls and the integrity revealed a mild association with visual motor function. In addition, the motor-related fiber tracts in older RTT group showed lower GFA values, primarily located in frontal striatum and callosal fibers. However, the change of the fiber tracts with significant reduction was not correlated with the changes in motor scales. Furthermore, the contrast ratio in SWI showed significantly lower in striatum of RTT.

Discussion: To investigate the microstructural alteration in the different age, we found the progressive changes in the cerebral cortex with age and the reductions in fiber tracts. In the light of early delayed speech-language millstone in RTT and the association with speech ability and GFA values, the integrity of arcuate fasciculus can be a language marker for RTT and for follow-up research. The visual perception-related tracts were associated with visual motor function. These may prove the activity-driven increasing in white matter tracts, even suffering from the severe damage of disease. On the other hand, the cortico-basal ganglia-thalamo-cortical loop in RTT was generally impaired though without correlation with the behavioral data. The consequence may be related to complex neuron network and neuron dysfunction in movement. Moreover, we discovered the abnormal iron accumulation in RTT with uncertain reason. Therefore, a longitudinal cohort study is mandatory to elucidate the effect of the subtle change in basal ganglia.

Keywords: Rett syndrome; DSI; SWI; TBAA; regional difference; iron accumulation

doi:10.6342/NTU201702958

1. Introduction

1.1 Biology of brain in Rett syndrome

Rett syndrome (RTT) is an uncommon neurodevelopmental disease. Approximate 1/ 10,000 to 1/ 20,000 of girls are involved (Bienvenu et al., 2006; Laurvick et al., 2006; Virginia C. N. Wong & Li, 2007), and affect their whole life. Patients with RTT usually have relatively normal development before six to eighteen months, and gradually develop progressive problems in communication, learning, memory, motor coordination and neurodevelopment. Stereotyped hand movement may spontaneous appear with the loss of hand function. The first diagnosis of RTT was described by Andreas Rett in 1966 (Rett,1966;1986). The critical breakthrough in RTT comes from the discovery that inactivation of methyl-CpG-binding protein 2 (*MECP2*) gene located in X chromosome plays a primary cause of the disease (Amir, 1999). This finding provided an explanation for female prevalence in RTT. Because of being hemizygous, males with *MECP2* mutation usually suffered from more severe phenotype, such as congenital encephalopathy and shorten lifespan (Villard et al., 2000).

Based on a cross-national survey in Taiwan, about 70–90% of atypical and typical RTT patients were identified with *MECP2* mutation (Chin Wong, Hung, Jan, Lee, & Taiwan Rett Syndrome, 2017). Mutations of *MECP2* can result from missense, nonsense, insertions, deletions, or splice site mutation. The function of *MECP2* attracts the attention on its epigenetic mechanisms, which change gene expression by DNA methylation and histone tail modification resulting in repression of gene transcription. Using RTT mouse model, the target genes of *MECP2* have been highlighted their important roles in regulation and control of neuronal maturation, dendritic morphology, and synaptic

doi:10.6342/NTU201702958

transmission in development (Armstrong, 2005; Boggio, Lonetti, Pizzorusso, & Giustetto, 2010; Guy, Cheval, Selfridge, & Bird, 2011). MECP2 in human brain prominently expressed in mature neurons with the timing of the ontogeny of central nervous system. It increased dramatically in gestation and continued to the age in ten in the cerebral cortex (Shahbazian, Antalffy, Armstrong, & Zoghbi, 2002). Furthermore, the expression of this protein showed more consistent order with the establishment of synapses than with neuronal age (Johnston, Blue, & Naidu, 2005). Therefore, the importance of MeCP2 is not only revealed in early life, but also continuously modulates the neural function in adults (McGraw, Samaco, & Zoghbi, 2011). It is noteworthy to investigate the influence of RTT in whole life.

Although the mutation of *MECP2* is not the only etiology for RTT and the pathogenic mechanisms are complicated, the investigation of genetic and biological changes in brain is beneficial to our understanding of the disease.

1.2 Manifestations of clinical phenotypes in Rett syndrome

With absence of proper MECP2 function, the neuron cannot accelerate to the mature states, and the deficit with different time period might be presume to the correlation with a delayed onset of clinical presentation. Base on the observation of changes in behavioral and clinical phenotypes, RTT can be divided into four stages (Developmental stagnation, Rapid regression, Pseudo-stationary stage, and Late motor deterioration), even though symptoms may overspread between each stage (Hagberg, 2002; Hagberg & Witt-Engerstrom, 1986; Neul et al., 2010). Clinically, patients are relatively normal development before six months to one and half years old, despite the fact that some might be small head circumference in stage one. A microcephaly

doi:10.6342/NTU201702958

mentioned in several natural history of patient probably resulted from deceleration of head growth as two to four months of age in Rett syndrome (Chahrour & Zoghbi, 2007; Naidu, 1997; E. E. J. Smeets, Pelc, & Dan, 2011). Later, the development of patient appears progressive problems with communication, learning, co-ordination and neurodevelopment, and usually combined severe mental retardation. At stage two, usually happens in one to four years old, patients will appear typically stereotyped hand movement, instead of acquired skills in hand, and partial patients may lose their ability to walk or become gait abnormality with poor balance. Hand stereotypies as an obvious pattern in RTT is defined in involuntary, repetitive, rhythmic and patterned hand movements with predictable form and location. These compulsive automatisms disappear during sleep. In RTT, stereotypies often perform a midline and symmetric hand pattern (Chin Wong et al., 2017; Temudo, 2007) and through their whole life.

In contrast to devastating deterioration mentioned, in stage three, the development often become more stable with slowly progresses in motor regression between the ages of two to ten. Patients may decrease the stereotypic hand movements in intensity or frequency. Additionally, the remarkably communicational ability mainly with the eyes preserves and is used for social convention, requesting an object or information, making a choice, and answering (Bartl-Pokorny et al., 2013; Djukic & McDermott, 2012; Djukic, Valicenti McDermott, Mavrommatis, & Martins, 2012; Rose et al., 2013; Schwartzman, 2013; Urbanowicz, Downs, Girdler, Ciccone, & Leonard, 2016). The stage can last for decades, and some of the patients may stay in this stage for the rest of life. The last stage, patients suffer from motor deterioration with prominent features described as muscle weakness, rigidity, spasticity with gait. Patients reduced mobility due to extrapyramidal involvement over a long period and become wheel-chair dependent. Scoliosis and distal distortion appear apparently in this stage (Hagberg, 2005; Smeets et al., 2003). Few

doi:10.6342/NTU201702958

studies supported that RTT in middle age might present with general premature neuromuscular aging with lose a great deal of muscle strength, power even volume and change in texture of skin and hair. (Hagberg, 2005; Roze et al., 2007). The parkinsonian features shows more common in older girls with RTT, presented as dystonia, bradykinesia, hypomimia (FitzGerald, Jankovic, & Percy, 1990). The cause of parkinsonian features in latter stage is controversial and less clinical evidence, consequently, a well-designed research is in demand.

1.3 The alteration of cortical gray matter and white matter in normal children and adolescent

There is age-related change in brain development. The intracranial space grows exponentially from early childhood to early adolescent. Increasing volume in gray matter reaches the peak of growth trajectory at later childhood, thereafter, it decreases linearly by age (Courchesne et al., 2000). As a normal brain development, different cerebral lobes may grow with different sequence. In childhood, parietal cortex is the earliest mature lobe in brain and its growth follows a non-linear developmental curve to the peak at age10 in girls and age 11 in boys. About the same time, frontal lobe, thought to drive motivation of behavior and anticipate the consequences, reaches the peak of gray matter volume. Although some might argue that functional maturation in the dorsal lateral prefrontal lobe, served as a guard to control the impulse and to judge or make decisions, lately grows to adult level in adolescents. These two lobes follow a similar pattern of development, increasing during pre-adolescent to maximal size and decline slowly during post-adolescent stage. On the other hand, temporal lobe and occipital lobe peak later in post-adolescent at age 16 and 20, respectively (Giedd et al., 1999; Lenroot & Giedd, 2006). The developmental trajectory of cortical gray matter complies with a specific pattern for

doi:10.6342/NTU201702958

their primary functions. For instance, motor and sensory functions of frontal and parietal lobes mature earliest, and higher order association areas in superior temporal lobe, which integrate these primary functions, mature later (Lenroot & Giedd, 2006).

In contrast to the upset U shape of gray matter developmental curves, the volume of white matter of brain generally increases with the growth of axonal membranes, density, and axonal caliber with increased myelination. The fiber tracts may grow throughout childhood and adolescence and even to the age of young adults (Giedd et al., 1999; Krogsrud et al., 2016; Lenroot & Giedd, 2006). In addition, the developmental trend of fiber tracts may have more complex pattern than gray matter, including region-specific, task-specific, and population-specific differences. During the development of white matter fibers, synapse pruning is occurring to maintain the essential connectivity between different regions of the brain (Tierney & Nelson III, 2009). In general, the magnitude of the changes showed the pattern of posterior–anterior development. The projection fibers developed first, followed by commissural and then associational fibers (Schmithorst & Yuan, 2010). The development of white matter has less age-specific alteration, and the white matter integrity can be affected by different diseases. Therefore, the white matter integrity can prove a better observation for the effect of the diseases.

1.4 Neuroimaging findings in brain structure of Rett syndrome

Research in neuropathology has shown some marked changes in total brain volume and cerebral size in RTT. The reduced brain size was not attributed to atrophy but to poor neuronal soma size and dendritic arborizations in the cerebral cortex (Armstrong, Dunn, Antalffy, & Trived, 1995). Additionally, the reduction of pigmentation in the substantia nigra and the decreased dendritic territories in the thalamus, basal ganglia and amygdala were found in subcortical regions (Bauman, L., & Arin, 1995; Riederer et al., 1986).

doi:10.6342/NTU201702958

However, there is a paucity of information on the parameters of brain development in RTT.

Neuroimaging studies using magnetic resonance imaging (MRI) are a popular non-invasive tool for assessment of brain structure and function, connecting neural activity and clinical event. Many neuroimaging studies have shown a widespread decrease in gray matter and relative preservation of the posterior occipital region in RTT. Reiss et al. published the first volumetric MRI study of 14 Rett syndrome girls, which cut apart the brain into 16 regions. They suggested that the largest decreased cortical gray matter was in the frontal region even though with regional variation. Furthermore, the reduction in brain volume was more severe in gray matter than in white matter. The significant reduction was also observed in parietal, superior parietal-occipital region and basal ganglia in the subcortical areas (Murakami, Haas, Press, & Yeung-Courchesne, 1992; Reiss et al., 1993). Two small cohort studies in adolescent and adult patients have also shown the comparative reduction in frontal, temporal lobe and cerebellum (Bauman et al., 1995; Gotoh et al., 2001). The relation between decreased size of cerebellum and age was also demonstrated (Murakami et al., 1992), although there was no evidence of the progressive decrease in the cerebral cortex with age.

With the advance of MR technology, well tissue-segmentation method has been developed for more precision analysis. Carter et al. used the Talairach data processing and Voxel-Based Morphometry to seek the answer about the preferential volumetric reductions in RTT (Carter et al., 2008). Talairach data processing is based on a stereotactic principle to establish a standard atlas and grid. It subdivides the brain into more than one thousand sectors and tries to eliminate individual bias. Voxel-Based Morphometry also spatially normalize the brain regions to stereotactic patterns and provide information of voxel and clusters. In their study, they confirmed the reduction in

doi:10.6342/NTU201702958

the frontal lobe and also the dorsal parietal region with mild diffuse reduction in the cortical white matter.

However, studies related to the changes of white matter tracts in RTT are limited. In 1995, an autopsy study revealed the selective dendritic alteration in motor and frontal cortex in RTT girls (Armstrong et al., 1995). A magnetic resonance spectroscopic study also described the marked decreased *N*-acetyl-aspartate (NAA) in cortical white matter than in gray matter (Horska´ et al., 2000). The NAA is thought to be a neuronal marker, which is only present in mature neuronal and axon. The changes of white matter tracts in RTT can be revealed by diffusion tensor imaging (DTI), which estimates the diffusional motion of water molecules in the pixel of a brain imaging. The water molecular diffuses preferentially along axonal fiber directions. Therefore, the diffusion anisotropy can provide the information of the changes in fiber tracts (Mori & Barker, 1999; Pierpaoli & Basser, 1996). The first DTI study showed significant decrease of fractional anisotropy in the corpus callosum in RTT compared with the control. Although both RTT patients and the controls showed a gradual decrease by age in apparent diffusion coefficient (ADC), there was a greater decrease of ADC in controls (Izbudak et al., 2009).

Another DTI study also showed the significant reduction in frontal white matter, genu and splenium of corpus callosum, external and internal capsule, inferior fronto–occiptal fasciculus, and superior longitudinal fasciculus. The change of superior longitudinal fasciculus was correlated with the ability of speech in RTT (Mahmood et al., 2010). However, there were limited studies investigating the changes in motor system, the related tracts, and age difference in patients. It may arise from insufficient ROIs to track more fibers that are functional during the dynamic phase of development. Furthermore, the manual tractography is highly operator-dependent and heterogeneous when the individual subject is prone to reconstruction errors owing to complex fiber

doi:10.6342/NTU201702958

geometry and head motion artifacts. Therefore, a comprehensive and accurate registration method is needed to explore the whole view of brain structure in RTT.

1.5 The unknown storm in basal ganglia of Rett syndrome

The parkinsonian features may affect the later life of older individuals with RTT. Previous studies showed that the function of the striatum was correlated with the psychomotor deficit in *Mecp2*-knockout mice (Kao, Su, Carlson, & Liao, 2015; Su, Kao, Huang, & Liao, 2015). The reduction of pigmentation and neurons in the substantia nigra, where is related to Parkinson disease, and smaller volume of caudate nucleus were also discovered in post-mortem brain and MRI studies in patients with RTT (Bauman et al., 1995; Reiss et al., 1993). The time of the expression of MeCP2 protein in basal ganglia is similar to superficial cerebral cortex (Shahbazian et al., 2002), which means that the maturation of brain is relatively late in these regions. A longitudinal study showed that the peak of development in basal ganglia is in adolescent age (Wierenga et al., 2014). However, the dramatically increased density of striatal D2 receptor at an early stage of RTT patients (Chiron et al., 1993), which reached the peak at the age of ten (Meng, Obonai, & Takashima, 1998), might decrease the dopaminergic transmission and cause the extrapyramidal symptom. Although these putative factors had provided a cleaner view to understanding the disease, the correlation with clinical presentation is still unknown.

Recently, many studies have shown the alterations in basal ganglia of the individuals with Parkinson disease and related diseases. Some unnatural signal loss in substantial nigra, putamen, caudate nucleus and globus pallidus was found in T2* weighted imaging and susceptibility weighted imaging (SWI) in Parkinson disease (Feng et al., 2007; Hwang et al., 2015; Rossi et al., 2010; Schneider et al., 2016; Z. Wang, Luo, & Gao, 2016; Zhang et al., 2010). SWI is a three-dimensional gradient echo sequence

doi:10.6342/NTU201702958

with full flow compensation and high in-plane resolution. The characteristic of SWI is sensitive to iron and calcium because of the different susceptibilities. Substances with various susceptibilities can have distinct contrast of signals in imaging. This technique had been widely used in patients with micro-bleeding, stroke, axonal injury, cerebral mineralization, venous disease and neurodegenerative disease (Lee et al., 2012; Mittal, Wu, Neelavalli, & Haacke, 2009; Nandigam et al., 2009; Prell et al., 2015; Sehgal et al., 2005). Furthermore, other basal ganglia diseases and Huntington's disease also showed the intensity alteration in globus pallidus (Macerollo et al., 2014).

Intriguing, the hypointensity in SWI was also found in atypical RTT with WDR45 mutation. The patients with WDR45 mutations don't show progression in childhood, which is followed by global developmental regression with suddenly-onset dystonia-parkinsonism in adulthood. The disease, also called b-propeller protein-associated neurodegeneration (BPAN), showed the evident signal contrast in substantial nigra and globus pallidus in SWI (S. Crisp et al., 2013; S. J. Crisp et al., 2015; Hayflick et al., 2013; Ohba et al., 2014). The results not only demonstrate the possibility of abnormal iron deposition in RTT, who also suffer from similar regressive pattern, but also shed light on the possible parkinsonian feature in RTT.

Therefore, SWI may provide a non-invasive and iron-sensitivity measurement to many clinical diseases. It is also safe and can be applied in vivo. Given the property of SWI, it might be an appropriate assessment tool for the possible changes of brain iron concentration in RTT and can be applied to clarify the unknown storm in RTT.

doi:10.6342/NTU201702958

2. Rationale and Hypothesis

To our best knowledge, the major role of *MECP2*, which causes RTT, regulates the neuronal development, controls their maturation followed the sequence of CNS development, and even affects neural function in the adult. Mutation in *MECP2* may affect the maturation of neurons leading to a small size in volume; however, it is uncertain whether the degenerative process continuously affects the patients' brain throughout their life or only affects a certain period in their lifespan. In addition, the aforementioned evidence proved that the reduction of brain volume in patients with RTT is diffuse and variable, and the results of different studies were inconsistent, which may partly arise from different experimental design and age groups. Most of the previous studies focused on children and adolescents with RTT but not younger adults. There was also wide age range in previous studies leading to variable and heterogeneous results. Therefore, to investigate the development of microstructures of whole brain in RTT patients, we separated the present subjects into two groups, under ten years old and older than ten. We hypothesize that the regional difference of gray and white matter in RTT may be correlated with the sequential development in age.

RTT is a rare neurodevelopmental disease with a unique trajectory change in clinical phenotypes. Partial or complete loss of the acquired hand skills and communication, and impaired or absence of mobility are the main criteria of classical RTT (Neul et al., 2010). Therefore, it is crucial to clarify the preferential involvement of specific microstructures in brain in these patients. The development of white matter tracts is more task-specific than gray matter. They can help us to explore the functional-specific pathologic changes in brain and correlate the microstructural change with clinical phenotypes. In the present study, we focused on the motor, speech and visually related tracts because of the specific changes in regression of motor and speech function with well preservation of visual

doi:10.6342/NTU201702958

performance. The second hypothesis in this study is that the motor and speech-related tracts in RTT may be more affected compared with healthy controls. In contrast, the vision-related tracts are less affected. They are compatible with the clinical phenotypes in RTT.

In the later stage of RTT, parkinsonian features may appear with dystonia of distal part of four limbs suggesting the possible characteristic features of premature aging. These symptoms may be associated with nigrostriatal–dopaminergic pathway dysfunction and abnormal regulation of *MECP2* gene. However, these possible parkinsonian behaviors and early aging have never been investigated in prior studies in older individuals with RTT. Recently, several studies had mentioned the abnormal iron deposition in basal gang glia in neurodegenerative diseases, including Parkinson's disease, parkinsonism, and atypical Rett syndrome, and also in normal aging (D. Wang, Li, Wei, Li, & Dai, 2012; Xu, Wang, & Zhang, 2008). Individuals with RTT may also suffer from abnormal brain iron deposition leading to parkinsonian feature in older patients. SWI is a versatile imaging modality allowing measurement of physiological and pathological alterations of iron. Therefore, the last aim of this study is to estimate and to investigate the brain iron concentration and its correlations with age and clinical status in RTT.

doi:10.6342/NTU201702958

3. Material and Method

3.1 Study Participants

A total of 39 diagnosed RTT patients were invited to this study, age range from 2 to 27 years. All subjects were recruited from specific outpatient department for Rett syndrome in National Taiwan University hospital. The evaluation was executed with revised diagnostic criteria (Neul et al., 2010) by major neurologist (Lee W.T.).

As healthy controls, typically developing subjects with no other neurologic disease (e.g. psychiatric diagnoses, history of neurological impairment, neuropsychiatric conditions, clinical evidence of a genetic disorder) were enrolled. 32 gender-matched people were confirmed by the interview of typically behavioral development and paired to RTT patients by age within 6 months individually. All subjects were suitable for participation in a MRI study and right-hand dominance. For avoiding the motion-related artifact, patients with RTT and younger health control (age less than 4 years old) had to be sedated by chloral hydrate before executing MRI scanning.

While the subject was scanned, parents or caregivers were requested to finish the developmental and clinical questionnaires. Because the caregivers are not native English speaker, the English version questionnaires were simultaneously oral-translated in Chinese by researchers. The administration of the interview and clinical assessment (PDMS-2) often took 45 to 60 minutes. Subjects were brought to an empty and safe space to carry out the assessment for PDMS-2. The sequencing of subtests started from gross motor domains to fine motor domains. In order to guarantee the quality of the assessment, all of the evaluation were executed by occupational therapist (Jan, T.Y.). This study was approved by the institutional review board at the National Taiwan University Hospital in Taipei, Taiwan(201510011RINC).

doi:10.6342/NTU201702958

3.2 Image data acquisition and processing

MRI data were acquired for each participant with approximately 40-minutes acquisition time. In this study, we proposed to utilize conventional MR image, diffusion spectrum imaging (DSI), and Susceptibility weighted image (SWI) to acquire the information of brain structure in neural tissue, fiber integrity and metal concentration. All of the scans are acquired using a Siemens Tim Trio 3T scanner with 32 channel head coil at NTUH.

Sedation were implemented by nurses or doctors before 30 minutes from the scanning time. All participants lied on the examination table with head surrounded by foam cushions to restrict head movements and with body belt for safety. Within the scanning, heart rate and pulse oximetry were continuously monitored. The scan time including T1-weighted images, T2-weighted images DSI and SWI was approximately 40 minutes.

3.2.1 Conventional MR imaging:

The protocol of conventional MRI covered the whole brain consisted of sagittal T1-weighted and axial fast spin-echo T2-weighted imaging. To obtain anatomical reference and further calculation of gray matter volume, high-resolution T1-weighted imaging was performed by 3D magnetization-prepared rapid gradient echo sequence. The definition of the sagittal localizer was defined on the slice orientations of the axial images from the orientations parallel to the line between the anterior and posterior commissures. Thickness of transverse sections in 1.0 mm^3 was obtained parallel to the anterior and posterior commissure line and with repetition time (TR) = 2000, echo time (TE) =2.98 ms, flip angle = 9^o, field of view (FOV) read = 256x192 mm and the total number of slices per slab is 208. The fast spin echo sequence was acquired from 56 contiguous axial

doi:10.6342/NTU201702958

T2-weighted images with the TR= 9650 ms, TE = 103ms; field of view (FOV) = 200× 200 mm^2; and slice thickness = 2.5 mm.

Prior to data processing, all scans successfully passed a quality assurance, based on visual inspection for gross structural abnormalities by professor Tseng, W.Y. and were adjusted the definite coordinates using display methods on the Statistical Parametric Mapping 12 software package (SPM12; http://www.fil.ion.ucl.ac.uk/spm/software/spm12/) run in MATLAB 2016 (Mathworks, USA). Artifacts, poor directionality or image quality could potentially hamper image segmentation, therefore imaging data should be processing before analysis in software.

Imaging analysis: For extracting the volume in gray matter, FreeSurfer software package (v.6.0.0-64bit; Martinos Center for Biomedical Imaging, Boston, MA, USA) was used to create a three-dimensional model of the cortical surface and cortical thickness with area measurements.

The segmentation of cortical volume was performed using the FreeSurfer "recon-all" pipeline (http://surfer.nmr.mgh.harvard.edu), according to intensities and continuity information from full-head image to establish representations of the boundary of gray/white matter (surface) and pial surface. The standardized procedure of reconstruction and estimation is described as follow:

Motion correction in original imaging is the primary step to ensure the accuracy of T1 weighted images. Later, based on deformation procedure, non-brain tissue was removed according to estimated probability of each voxel. The rest tissue was edited the topological surface by automatically transformation to Talairach space and segmentation of volumetric structures for tessellation of the gray matter-white matter boundary (Fischl, 2004; Fischl et al., 2002). Following intensity gradients, an automated topology correction (Fischl, Liu, & Dale, 2001) and surface deformation were applied to optimally

doi:10.6342/NTU201702958

place the gray/white and gray/cerebrospinal fluid borders at the location for the greatest shift in intensity (Fischl & Dale, 2000). The automatic labeling method not only provided similar consequence to manual labeling in prior study but also showed low reproducibility errors and high precision(Fischl & Dale, 2000; Jovicich et al., 2006), therefore it is suitable for present research.

After the procedure of recon-all, FreeSurfer software provided a 'stats' folder contained information of gray matter thickness, pial surface and subcortical volumetric structures. Taking account of ease, consistency and accuracy for investigation of volume size in gray matter, Desikan-Killiany-Tourville (DKT) cortical labeling atlases (rh.aparc.DKTatlas.stats/ lh.aparc.DKTatlas.stats) were selected and extracting volumetric data to analyze. The DKT cortical labeling atlas was established from manual-labeled imaging with 101health people brain defined on Desikan-Killiany cortical parcellation atlas (Desikan et al., 2006) and developed an automated registration and label algorithm. DKT atlas comprise with total 31 cortical regions per hemisphere. For the better consistency, four cortical regions removed from the 35 labels of the DK protocol including bankstss, corpus callosum, frontal pole, and temporal pole(Klein & Tourville, 2012). To explore the local change in gray matter, 31 cortical regions were subdivided into four lobic group and comparing the difference in two age groups.

3.2.2 Diffusion spectrum imaging (DSI)：

DSI was developed to map fiber architectures in tissues by water diffusion with three dimensional MRI. It performed by a pulsed-gradient spin-echo diffusion echo planar imaging(EPI) sequence with twice-refocused balanced echo for reducing eddy-current distortions(Wedeen, Hagmann, Tseng, Reese, & Weisskoff, 2005). Due to the capacity to imaging the orientation of intravoxel fiber, DSI become a more specific

doi:10.6342/NTU201702958

method to detects the crossing fiber in white matter(Wedeen et al., 2008).DSI data were acquired with following parameters: TE = 130 ms, TR = 9600ms, in-plane spatial resolution = 2.5 × 2.5 mm^2, FOV = 200 x 200 mm^2, matrix size = 80 x 80 x 56 slices. A total of 102 diffusion encoding gradients with the maximum diffusion sensitivity, bmax = 4000 s/mm^2, were applied on the grid points in a half sphere of the 3D q-space with $|q| \leq 3.6$ units(Kuo, Chen, Wedeen, & Tseng, 2008).

Data preprocessing is crucial for reliable consequences. It prevents substantial in-scanner head motion due to comparatively long scanning time in DSI. Head motion may result in signal loss in the presence of strong diffusion-encoding gradients of diffusion weighted imaging, especially in higher b-value. A total of 5,712 images (56x102) in per subject were scrutinized by calculating the continuous signal distribution in the central square of each image. The signal of image deviating from continuous distribution was thought to be signal loss. Therefore, we applied an in-house algorithm developed by Huang, C.F. to repair the losing signal in per image and ensure the quality of acquisition data.

Imaging analysis: Owing to the property of the data in the q-space are real and symmetrical, the obtained half-sphere data were projected to fill the other half of the sphere. Additionally, mean apparent propagator (MAP) MRI framework offered a reconstruction model from 3D q-space signal and transfer it into diffusion propagators(Ozarslan et al., 2013). Generalized fractional anisotropy (GFA), a diffusion indices equivalent to FA in DTI, was calculated from diffusion propagators at each voxel. The acquisition value offers the anisotropic diffusion information of water molecules which may reflect the microstructural architectures and orientation of neural axon (Gorczewski, Mang, & Klose, 2009).

doi:10.6342/NTU201702958

A whole brain tracts analysis was applied the method developed by Chen et al, named Tract-based automatic analysis (Chen et al., 2015). TBAA were reconstructed on the NTU-DSI-122 template, a standard coordinate system with high quality resolution (Hsu, Lo, Chen, Wedeen, & Isaac Tseng, 2015) and constructed 76 fiber bundle by assigning 2 or 3 ROIs for each targeted tract. The streamlines of targeted tract should completely thread through the associated ROIs. After then, each defined fiber bundle was constructed on standard template and transformed diffusion datasets to individually native space. In the later computation, fiber bundles were interpolated into 100 steps and saved as the sampling coordinates of diffusion indices for reliable sampling of the microstructural properties along the tracts. Total 76 fiber tracts derived from TBAA in whole-brain were categorized into three groups: (a) association fibers (cortical-cortical connections), (b) projection fibers (spinal-cortical-, caudate-cortical, putaminal-cortical, and thalamic-cortical connections), and (c) commissural fibers (left-right hemispheric connections).

The procedure of TBAA method in our study is described as follow:

Total 60 DSI datasets with T1-weighted imaging (consist of 28 RTT patients and 32 health controls) were registered to create a study-specific template (SST) and then second- registered to NTU-DSI-122 template with two-step strategy separately.The two-step registration strategy combined the information of anatomical information provided by T1-weighted images and microstructural information provided by DSI dataset and enhance the registration for individual diffusion data.The output format of TBAA was called two-dimension (2D) connectogram for each subject's each diffusion index. The X and Y axes of connectogram indicated 76 predefined tract bundles and 100 steps along each tract bundles. The superposition of 2D connectogram from each subject generated a

doi:10.6342/NTU201702958

three-dimension (3D) connectogram. The value from connectogram were applied to further statistical analysis(Wu et al., 2015).

3.2.3 Susceptibility weighted image(SWI):

Tissues with different susceptibility can be distinguished from their contrast signal in sufficiently long echo times. SWI was applied in the principal to enhance imaging contrast for conventional (magnitude) imaging based on a high in-plane resolution. Three-dimensional gradient echo sequence with 3-direction flow compensation was used to acquire high- resolution imaging. On the other hand, phase imaging, reflecting the static magnetic field inhomogeneities, were utilized as a high-pass filter to mask the original magnitude imaging by multiplication. The obtained SWI perform a minimum intensity projection(mIP) over neighboring slices to facilitate sensitivity and improve the recognition of inhomogeneity (E. Mark Haacke, Xu, Cheng, & Reichenbach, 2004). Iron features as a paramagnetic element. In an external applied magnetic field, tissue with the iron will strengthen the local magnetic field and phase shift begin to differ from zero. As given a sufficient TE, tissue with more iron content shifts more phase to positive (in the left-handed system) from zero. The characteristic can be used to quantitatively determine the iron concentration of tissue. The property of SWI has been widely used in several diseases to detect the abnormality in tissue components (E. M. Haacke, Mittal, Wu, Neelavalli, & Cheng, 2009; Mittal et al., 2009). Therefore, we planned to use the sensitive techniques to gain the information about the mineralization in basal ganglia in the patient with RTT.

The SWI sequence with flow compensation comprised of the following parameters: TE=20ms, TR =28ms, FOV = 230x 230 mm, voxel size=0.8x0.7x1.6 mm and 72 slices per slab with 22.2% oversampling. The images were acquired in the

doi:10.6342/NTU201702958

transaxial plane, parallel to the anterior/posterior commissure (AC–PC) line. A high-pass filter was applied and analysis of signal intensity on the SWI images was recorded bilaterally according to the anatomical structures of region of interest(ROI) in the substantia nigra, caudate nuclei, putamen, globus pallidus and thalamus on the slice, where they were visualized best. Images were reviewed on a commercially available workstation in Siemens and read by a neuroradiologist (Peng, S. F.) for the presence of infarcts and hemorrhages.

Imaging analysis: One subject was removed from the analysis due to moderate motion artifact. Total 59 SWI imaging (28 individuals with RTT and 31healthy control) were estimated. Two quantitative analysis were applied to investigate the contrast of 5 ROIs: visually grading scale and contrast ratio. The visually grading scale was used to score the bilateral signal intensity in 5 ROIs comparing to CSF. The hypointensity was measured according to relatively grading scale by visual discrimination, ranging from 0 to 3 point (0: SI similar to CSF intensity; 1: mild hypointensiy; 2: moderate hypointensiy; 3= severe hypointensity)(Gupta, Saini, Kesavadas, Sarma, & Kishore, 2010). To compare the inhomogeneity, each ROI was measured bilaterally as S_{ROI} and calculated against the occipital white matter as contrast ratio. Signal intensity in occipital white matter was characterized with little variation in patients, so it is suitable to be a comparable baseline. The contrast ratio was calculated as "$CR=(S_{ROI}-S_O)/ S_O$ "(S_{ROI}: signal intensity of ROI structures, S_O: signal intensity of occipital WM). An experienced neuroradiologist (Peng, S. F.) analyzed all imaging independently by a defined radiological protocol.

doi:10.6342/NTU201702958

3.3 Questionnaire and assessment tool

The developmental questionnaire was designed to realize the performance of hand function, mobility, and speech in patients' daily life. Parent/ caregiver were requested to complete the questionnaire. The first part of form was used to survey the frequency of stereotyped movement and the trajectory of development in hand function and mobility. The second part was acquired for the information of hierarchical abilities in hand function, speech, and mobility. Each item of the independence and the performance in the past should also be recorded. Other 4 clinically quantitative questionnaires (RSBQ, RSSS, SSSI, and ADAMS) were available for the information of symptoms, emotion changes and social interaction of patients with RTT. The categories of developmental questionnaire included hand function, speech and gross motor scale as followed content.

Hand function:

The scale consists 8 level of observed hand skill. (Downs et al., 2010)(1) No observed hand function, (2) Able to hold at least one large object (cup, spoon, small ball or toy) >2s, (3) Assistance to grasp but able to pick up and hold at least one large object >2s, (4) Able to grasp, pick up and hold at least one large object >2s, (5) use a raking grasp to grasp, pick up and hold a small object >2s, (6) Can be a scissors, inferior pincer, or superior pincer grasp, (7) Skills for level 6 and able to transfer an object from one hand to the other. Accurate pre-shaping of the hand is not seen, and (8) Skills for level 7 and, when hand is approaching an object, hand orientation and size recognition closely approximates the position and size of the object.

Speech：

doi:10.6342/NTU201702958

The scale based on the capacity to speak categorized into 4 items. (1) Could speak in phrases or sentences, for example: I want to eat… (我要吃…), (2) Single words, for example: rice (飯飯),(3) Babbling, for example: “da da”, “a a”, and (4) Mute.

Gross Motor Scale:

The measurement includes 15 small items, and divided into three sub scales (sitting, standing and walking , and challenge), which is more suitable for administration in RTT group (Downs et al., 2016). The items grouped in “Sitting” group contains sitting on the floor, sitting on a chair, and sitting on a stool. Nine items grouped in “Standing and Walking” includes sit to stand, standing, walking, side stepping, turning, walking on a slope and stepping over an obstacle, due to the relation to weight bearing activities.

The rest items grouped by describing skills of moving from the floor to standing, picking up an object from the floor and running, named ‘Challenge’ group, because of the complexity of the skills.

Peabody Developmental Motor Scales:

For the purpose of collecting the results with reliability and validity (Connolly, McClune, & Gatlin, 2012), Peabody Developmental Motor Scales-2nd edition (PDMS-2) were applied to assess the gross motor and fine motor skills objectively(Folio & Fewell, 2000; Libertus & Landa, 2013). The assessment was usually used in clinical assessment and training and measure interrelated motor abilities that develop early in life. PDMS-2, a motor development program, consists of 6 subtests: *reflexes*, *stationary* (e.g. static balance and body control), *locomotion* (e.g. crawling, walking, running, hopping and jumping), *object manipulation* (e.g. catching, throwing and kicking a ball), *grasping* (e.g.

doi:10.6342/NTU201702958

holding, grasping, pincer grasp and manipulation in hand) and *visual-motor integration* (e.g. eye tracking, transfer objects and playing with cubes).

The items of reflexes were excluded since reflexes should be inhibited by cortical level in normal development and the evaluation was only applied in children younger than 11 months. For each item of the subtest, performance criteria are specified and scored on a 3-point scale, from zero to two. Administration should start in each category at a basal age level of the age, however, in this study, the basal level was adjusted to only define as the first level at which three consecutive items get a 2-score. The testing steps up to the ceiling age level, defined as the level at which 3 consecutive items get a 0-score. The raw scores were summed up by the item scores and transformed into standardized scores and standardized developmental motor quotients for the gross motor scale, fine motor scale and total score.

Rett Syndrome Behaviour Questionnaire

The Rett Syndrome Behaviour Questionnaire (RSBQ) is a measure in observation of typically pathological behaviors in individuals with RTT(Mount, Charman, Hastings, Reilly, & Cass, 2002). A total of 45 items were grouped into eight domains/subscales: (1) General Mood, (2) Breathing Problems, (3) Body Rocking and Expressionless Face, (4) Hand Behaviors, (5) Repetitive Face Movements, (6) Night-time Behaviors, (7) Fear/Anxiety, and (8) Walking/Standing). Each item was scored on a Likert scale of 0–2, based on how well the description fit to the behavior of patient. The rating scale is specific to RTT that covers a wide range of problem behaviors and clinical symptoms(Barnes et al., 2015; Kaufmann et al., 2012). According to description of symptoms, three domains (Body Rocking and Expressionless Face,

doi:10.6342/NTU201702958

Repetitive Face Movements Walking/Standing) were chose as dystonia index to estimate the degree of parkinsonian features.

Rett Syndrome Severity Scale

Rett Syndrome Severity Scale includes 7 domains: (1) frequency and manage-ability of seizures; (2) respiratory irregularities; (3) scoliosis; (4) ability to walk; (5) hand use; (6) speech; and (7) sleep. Each item was scored on a Likert scale of 0–3, based on how well the describes to the severity of symptoms. The classification of total scores in the 0–7 range correspond to the mild category, while scores of 8–14 and 15–21 are classified as moderate and severe, respectively (Kaufmann et al., 2012; Mahmood et al., 2010) .

Anxiety, Depression, and Mood Scale

Anxiety, Depression, and Mood Scale (ADAMS) is a developed instrument for assessing emotional domains in individuals with intellectual disability and RTT (Barnes et al., 2015; Esbensen, Rojahn, Aman, & Ruedrich, 2003). The measurement consists of 28 items, grouped into five sub- scales: (1) Manic/Hyperactive Behavior, (2) Depressed Mood, (3) Social Avoidance, (4) General Anxiety, (5) Obsessive Behavior. The total scores were summed up in four-point likert scale that combines frequency and severity ratings.

Ghuman–Folstein Screen for Social Interaction

Rett syndrome was categorized in autism spectrum disorder in DSM-4, because it share some feature with autism. Ghuman–Folstein Screen for Social Interaction is a value-screening instrument for particular concern of children with autism spectrum disorder, which can help to get more information about patients' behavior. It is a

doi:10.6342/NTU201702958

parent/caregiver-report questionnaire, emphasized reciprocal social interaction including joint attention skills, initiation of social interaction and the response to the environment and social context. It contains 54 items and each item is positive from 0 (almost never) to 3 (almost all the time). (Ghuman, Freund, Reiss, Serwint, & Folstein, 1998; Ghuman, Leone, Lecavalier, & Landa, 2011). Since people with RTT might suffer from initial movement impaired, which could affect the performance in social interaction. Besides sum of total score, behaviors which associated with eye-contact were retrieval for further comparison.

3.4 Statistical analysis

The distribution of demography in age, gender, gene mutation, years of education, handedness, speech-language ability and stage were presented in number and percentage in four group (younger RTT, older RTT, younger control and older control). The neuro-motor development scales in hand function and gross motor scale were expressed as number and percentage as well. The raw scores of Peabody developmental motor scale were transfer to age equivalent and standard score by official manual. Due to the norm was established from children with age zero to five years old, the raw score of individual with age over five were referenced from five years old norm. The performance difference in five subtests between younger RTT and older RTT were compared in independent T-test with raw scores for consistency. Questionnaires of RSBQ, RSSS, SSI and ADAMS were performed with the means, the standard deviations, also the p value calculated from independent T-test.

The first step of imaging data analysis was the confirmation of lateralization in cortical gray matter. Paired T-test was used on four cortical lobes between left and right hemisphere, additionally, laterality index (left-right/left+right) in RTT and control group

doi:10.6342/NTU201702958

were measured by unpaired T-test to indicate the cerebral asymmetry. In two age groups, separately, differences of four cortical lobes were analyzed using one-way ANCOVA between RTT and control groups. Statistic with age and total intracranial volume as covariates was utilized to minimize their effects on the study variables. To investigate structural feature in detail, total 31 regions of interest on per hemisphere were compared by independent T-test. The aforementioned analyses were adjusted with Bonferroni correction.

Owing to the property of white matter, the representations of fiber tracts were thought to be more associated with functional changes. The tract bundles related to speech-language, visual perception and motor were selected as target tracts for the clinical alteration of RTT. For the purpose of comparing the differences in fiber tracts, mean GFA value of white matter tract bundles, generated from TBAA, was used and analyzed by two sample T-test. Bonferroni correction was used to account for multiple comparisons. In addition, all patients were grouped by language ability (mute/preserved language) and mobility (sitting, standing, walking and challenging) for comparing to controls with Kruskal–Wallis H test in targeted tracts. Kruskal–Wallis H test is a nonparametric statistic, which is free from assumption of normal distribution. To determine the differences among the groups, Dunn's test was applied for post-hoc test as multiple comparisons. Furthermore, Spearman rank correlation were used to analyze the correlation between integrity of functional tract and the behavioral data in RTT.

The signal intensity of 5 ROIs (substantia nigra, caudate nuclei, putamen, globus pallidus and thalamus) were estimated in contrast ratio ($CR= (S_{ROI} - S_O)/ S_O$) and compared using Mann-Whitney U test between patients and controls. Clinical correlations between contrast ratio in 5 ROIs and behavioral data (transferred RSBQ score and the subtests of RSBQ including body rocking and expressionless face, repetitive

doi:10.6342/NTU201702958

face movements and walking/standing)) were applied in Spearman rank correlation due to non-linear pattern in behavior. On the other hand, linear regression was used to explore the association between iron concentrations of basal ganglia and age from RTT and control.

All statistical analyses were computed by using IBM SPSS Statistics 22 (SPSS Inc., Chicago, Illinois, USA) and P value with less than 0.05 was considered to have significant difference.

doi:10.6342/NTU201702958

4. Results

4.1 Demography

Data from 39 individuals with RTT were obtained first, and 11 were excluded due to atypical phenotype or incomplete information. The excluded subjects included 4 Rett-like variant patients, 3 atypical RTT patients with CDKL5 mutation and 4 with unsuccessful sedation. Therefore, a total of 28 individuals with typical RTT (27 females and 1 male) and 32 age and gender-matched healthy control were enrolled for analysis. Patients were divided into younger group and older group by the criteria age of 10.

There was no significantly statistical difference in age, mean year of rehabilitation (education), and gender in RTT group and control group (Table 1). There was merely one 15-year-old boy with RTT in present study. *MECP2* mutation was found in 24 (86%) of 28 of typical RTT. Four did not find any gene mutation. Due to regression of hand function, most of the patients presented without dominant handedness. The other RTT patients and all controls had right-handed dominance. Six (50%) of 12 younger RTT stayed in stage 2, and the rest of youngers were regressed to stage 3 (33%) or stage 4 (17%). On the other hand, 12 (75%) of the 16 older patients were regressed to stage 4, and the other four were in stage 3. Total six patients in this study could speak with words (less than 5 words). Of these, one was in older group, aged 21 years, and the others were younger girls (Table 1.).

4.2 Behavioral results in neuro-motor development and clinical presentations between two age groups in Rett syndrome

After comparing the raw scores of motor development in PDMS-2, there is no difference between two RTT groups. However, considering the reference of age-norm, the standard scores of fine motor and gross motor in older group were significantly lower than the youngers (fine motor: $p = 0.02$, gross motor: $p = 0.03$). The age equivalence of

doi:10.6342/NTU201702958

RTT patients showed that performance of fine motor in all older RTT patients was equal to children with age under 1 year, except for two patients with 17 years (age equivalence of grasping = 12M) and 21 years (age equivalence of visual motor = 18M). Two of younger RTT with 4 years showed better performance in age equivalence from 18 months to 36 months. The motor development of other young girls displayed more variability. The performance of locomotion seemed to preserve better than stationary and object manipulation in both RTT groups (Table 2).

The distribution of gross motor scale for RTT showed that approximately one third (0.33) of young girls could achieve "challenge" level, but there was no older RTT patients did it (Table 3). Five (40%) of younger RTT patients showed the ability of standing and walking and three (25%) of them could sit on different height level. In older RTT group, 13 (81%) of 16 patients achieved "standing and walking" level and one could sit in three situations. Two (13%) of 16 patients could not sit independently. The number of each item did not show progressive increase or decrease because the remained motor functions in RTT may be heterogeneous and did not follow the sequence of development.

In hand function level (Table 4), 43% of older patients and 25% of young patients had no observed hand function, while 25% of younger RTT and 34% of older RTT patients were able to hold the large object; for example, nursing bottle. In youngers, three (0.25%) could adjust the hand movement for different objects, eight (67%) patients presented their hand function in deterioration and three (0.25%) patients maintain their hand function. On the other hand, two (12.5%) of older patients could transfer objects and one (6.2%) older patient could adjust the hand movement. Eleven (69%) of older patients regressed in hand function and five (31%) patients maintained, even though two (12%) of them had not developed in any hand function.

doi:10.6342/NTU201702958

Rett syndrome behavior questionnaire showed no difference between two RTT groups ($p = 0.65$), and there was no significant difference in ADAMS ($p = 0.45$). However, Rett syndrome severe score indicated that the older group showed significantly more severe in scoliosis and speech impairment than younger group (total score: $p=0.03$, scoliosis: $p = 0.01$, and speech: $p = 0.02$). In addition, younger RTT patients exhibited higher frequency in social interaction ($p = 0.03$) and expression by eye contact when parents were angry ($p < 0.01$), or happy ($p = 0.02$), and showed the interest in other children ($p = 0.01$) (Table 5).

4.3 Volume changes in cortical lobe between Rett syndrome and control in two group

To explore the development of brain structure in RTT, the trajectory of development was fitted by quadratic regression. For establishing a better-fitting model, we created age square as new variable. The development of total intracranial volume in RTT showed a decreasing slope before age 15 ($b1 = -8.72$, $p = 0.655$). Comparing to total intracranial volume, the trajectory of gray matter displayed a well-fitting with age in two groups and the curve represented a dramatic decreasing in RTT before 10 years (b1: -15.48, b2:0.351, adjusted $R2 = 0.299$, $p = 0.012$) and continues a plateau in adolescent and early adult. The curve of healthy controls showed a tardily increasing and followed by a slowly decreasing curve (b1: 1.99, b2: -0.162, adjusted $R2 = 0.206$, $p = 0.035$). The trajectory of development in white matter showed a different pattern, although there is no significance in the regression model ($p = 0.136$). Both of two groups showed an increasing curve (control: b1: 16.47, b2: -2.95, adjusted $R2 = 0.664$, $p<0.000$; RTT: b1: 5.28, b2: -0.109, adjusted $R2 = 0.148$); however, the development of RTT represent a gradually increased pattern (Figure. 1 and Figure.2).

doi:10.6342/NTU201702958

To investigate the regional difference in gray matter, four cortical lobes were compared separately by ANCOVA in two age groups (age and TIV as covariates). Patients with younger age showed significantly decreased in bilateral frontal lobes (corrected p-value: R:0.044; L:0.028) and bilateral parietal lobes (corrected p-value: R0.004; L:0.032). Patients with older age suffered from a global decrease in four lobes (Table 9. and Table 10.) and showed a significant decrease in bilateral parietal lobes (corrected p-value: R:0.003; L:0.003) and right temporal lobe (corrected p-value: R:0.032) (Table 6.). There is no hemisphere difference in four cortical lobes of RTT; however, the data of control groups showed the larger volume in right parietal lobe (Table 7). Comparison of laterality index in two age groups, there was no difference between RTT and control (Table 8). The trajectory of bilateral lobes demonstrated the similar pattern with total gray matter in RTT and the volume decreased before teens (Figure 3. and Figure 4.).

4.4 Microstructural changes in speech-language related fiber tracts.

Because the speech-language function is well-known with left-dominance, it is important to get whole information about the microstructural alteration of bilateral tracts. Therefore, we compared eight of speech-language-related fiber tracts and its contralateral tracts between RTT and controls. There was no significant difference in GFA values in bilateral corticospinal tracts corticospinal tract connecting to primary motor cortex of mouth component (L: p value = 0.14; R: p value = 0.36) between older RTT group and older control group. The other fiber tracts showed significantly decreasing GFA in bilateral hemisphere in older RTT group, including arcuate fasciculus (left/right: $p < 0.0001$/ < 0.0001), frontal aslant tract (left/right: p=0.0226/0.0005), perpendicular fasciculus (left/right: $p < 0.0001$/ < 0.0001), superior longitudinal fasciculus 3 (left/right: $p = 0.0007$/ < 0.0001), and uncinate fasciculus (left/right: $p < 0.0001$/ < 0.0001). The

doi:10.6342/NTU201702958

superior temporal part of callosal fibers, connecting bilateral superior temporal lobes, the GFA value was also shown to have significant decrease in older RTT group ($p < 0.0001$). Most speech-language-related fiber tracts still showed significant decrease after Bonferroni correction, except for left frontal aslant tract. In younger RTT group, there was only one fiber tract showed significant decrease in GFA value, which remained significant difference after Bonferroni correction (left perpendicular fasciculus, $p = 0.0003$) (Table 11. and Figure 13.).

4.5 Microstructural changes in visual perception-related fiber tracts.

The comparison of visual perception-related tracts showed no difference in GFA values between younger groups. Interestingly, the anterior commissure in both RTT groups showed higher GFA value than healthy controls (young RTT group/control: 0.231±0.03/ 0.227±0.03, $p = 0.779$; older RTT group/control: 0.214 ±0.02/ 0.194±0.03, $p = 0.016$). However, the other tracts in older RTT group showed significant decrease after Bonferroni correction. The occipital lobe connected tracts included superior longitudinal fasciculus 2 (left/right: p= 0.0003/ <0.0001), optic radiation of thalamic radiation (from thalamus projected to superior occipital gyrus, left/right: $p = 0.0001/0.0069$), precuneus part of callosal fiber (connecting bilateral precuneus, $p = 0.0001$) and splenium part of callosal fiber (connecting bilateral occipital lobe, $p = 0.0002$) showed the significant decreasing in GFA values in older RTT. (Table 12. and Figure 14).

4.6 Microstructural changes in motor function related-fiber tracts.

The motor function is relatively complicated and involves many cortical regions such as prefrontal cortex, premotor cortex, primary motor cortex, supplementary motor area and also the subcortical area. Therefore, we compared the tracts connected to the aforementioned areas. There was no difference in younger groups, except callosal fiber

doi:10.6342/NTU201702958

connecting bilateral orbitofrontal lobe (OFC). However, the motor-related fiber tracts in older RTT group showed lower GFA values, primarily located in frontal striatum connected tracts and callosal fibers. The significant reductions in GFA values were in fiber tracts connecting frontal striatum to orbitofrontal gyrus (left/right: $p = 0.0001/ <0.0001$), fiber tracts connecting frontal striatum to motor precentral gyrus (left/right: $p <0.0001/ 0.0006$), callosal fibers connecting bilateral dorsal lateral prefrontal cortex (DLPFC) ($p <0.0001$), callosal fibers connecting ventral lateral prefrontal cortex (VLPFC) ($p <0.0001$), callosal fibers connecting supplementary motor area (SMA) ($p = 0.0001$), callosal fibers connecting motor precentral gyrus ($p <0.0001$), and callosal fibers connecting paracentral lobes ($p <0.0001$). The tracts originated from brainstem to primary motor cortex showed difference in components of hand (left: $p = 0.028$), trunk (left/right: $p =0.049/ 0.003$), and neck (left/right: $p=0.019/ 0.036$). The fiber tracts connected to lateral prefrontal in older RTT group showed reduction in bilateral connecting fibers from frontal striatum to DLPFC (left/right: $p <0.004 / 0.013$), left connecting fiber from frontal striatum to VLPFC ($p = 0.008$), left thalamic radiation to DLPFC part ($p = 0.021$), and bilateral thalamic radiation to VLPFC (left/right: $p = 0.028/ 0.023$) (Table13 and Figure 15.).

4.7 The correlation between functional change and white matter integrity

For further investigating of microstructure changes in speech-language-related tracts and the functional change, patients could speak were grouped as "with speech" (n=6). Other mute patients were selected by matching age and gender, and grouped as" without speech" (n=6). These two groups were compared to age- and gender-matched controls by Kruskal-Wallis H test (Figure 5., Figure 6. and Table 14.).

doi:10.6342/NTU201702958

There is no difference in GFA value between patients with speech and control group. The significant reduction between patients without speech and controls were observed in arcuate fasciculus (p = 0.003), perpendicular fasciculus (p = 0.001), superior longitudinal fasciculus 3 (p = 0.033), uncinate fasciculus (p = 0.033), and callosal fiber of superior temporal lobule (p = 0.033). The alteration of speech-language-related tracts between the patients with/without speech was only observed in arcuate fasciculus (p = 0.027).

Patients with RTT preserved the ability of visual pointing, but the integrities of visual perception-related tracts were worse in older RTT. After calculating by Spearman's correction, no significant correlation between the screen for social integration and mean GFA value of targeted tracts was found. In another visual-motor scale, a subtest of PDMS-2 showed the moderate correlation with anterior commissure (R = 0.531; P = 0.034) and splenium part of callosal fiber (R = 0.607; P = 0.013) (Figure 7. and Table 15.).

To investigate the relationship between the microstructural alteration and motor function in older groups, patients were divided into "Patient with mobility" and "Patient without mobility" according to gross motor scale and compared to age-matched healthy controls. The fiber tracts with significant reduction were chosen to analyze the relationship between motor function and motor-related tracts. The results showed no difference between patients in "with mobility" and "without mobility" group in selected tracts. However, these two groups showed significant reduction than controls, respectively (Table 18., Figure 8. And Figure 9.). Additionally, the change of the fiber tracts with significant reduction was not correlated with the changes in gross motor scale and hand function scale (Table 16. and Table 17.).

4.8 The alteration of signal intensity in basal ganglia and the correlation with age and behavior

doi:10.6342/NTU201702958

Contrast ratio and visual grading scale were applied to detect the abnormality of iron deposition in RTT. To confirm the normal distribution of visual scores and contrast ratio of 5 ROIs, F-test was used. The results showed that there were non-normality in 5 ROIs (p value of visually grading scale: substantia nigra (SN): 0.0001, caudate nucleus (CA): 0.084, putamen (PU):0.09, and globus pallidus (GP): 0.04 ; p-value of contrast ratio: contrast ratio of substantia nigra :0.002, contrast ratio of caudate nucleus: <0.0001, contrast ratio of putamen:0.002, contrast ratio of globus pallidus: 0.005, contrast ratio of thalamus (TH): <0.0001), therefore non-parametric statistics was applied in the comparison of further analysis.

In Table 19, the controls had lower visual grading scale (0 or 1), and two women (age 21 and 27) showed slightly hypointensity in globus pallidus with score of 2. There was no hypointensity detected in thalamus whether in control group or in patients. The significant differences were shown in substantia nigra (p=0.007) and globus pallidus (p=0.0043). In these two regions, patients showed higher hypointensity (SN: RTT/control: 1.286±0.763/ 0.844±0.369; GP: RTT/control: 1.429±0.69/ 0.969±0.474). In contrast, the contrast ratio showed different results in the striatum. Patients with RTT were shown to be significantly lower than controls in putamen ($p < 0.0001$) and caudate nucleus ($p < 0.0001$) after Bonferroni correction. The same phenomenon of signal intensity was shown in globus pallidus (Table 20 and Figure 10.). On the other hand, the contrast ratio of 5 ROIs changed with age in both groups, and the coefficient R showed the negatively moderate correlation (Figure 11). Therefore, the association of age and signal intensity was similar to the previous study. Nevertheless, the data of RTT patients scattered widely with great heterogeneity. Since the adult patients with RTT may show dystonia and parkinsonian feature, and the abnormal iron accumulation has been found in patients with Parkinson's disease and atypical RTT, the symptoms selected from Rett syndrome

doi:10.6342/NTU201702958

behaviour questionnaire were further analyzed with contrast ratio in five ROIs. The results showed that there was significantly negative correlations in caudate nucleus ($p = 0.033$) and thalamus ($p = 0.025$) (Figure 12).

doi:10.6342/NTU201702958

5. Discussion

The present study is the first RTT study considering the effect of age difference on brain microstructural changes and their correlation with clinical features. Most of the previous RTT researches combined the imaging data of both children and adults, and analyzed the association of behavior without standardized assessment. Hence, the results yielded from those studies might be variable and heterogeneous with low-reliability behavioral observation during clinical evaluation. Therefore, proper grouping of the participants is mandatory due to the difference of developmental trajectory with age and the clinical characteristics in RTT. Therefore, in the present study, we separated our patients into two age groups, younger group and older group, and compared the brain microstructural changes with age- and gender-matched healthy controls. Additionally, we evaluated the clinical features not only with standardized assessment tool (PDMS-2) but also with several questionnaires in both RTT groups. These comprehensive evaluations offered the complete information toward clinical observation.

5.1 Demographic data in Rett syndrome

RTT was reported to be associated with mutation in the methyl-CpG-binding protein 2 (*MECP2*) gene (Amir, 1999). Worldwide data showed that 70–90% RTT patients revealed this mutation (Bourdon et al., 2001; Wong, Hung, Jan, Lee, & Taiwan Rett Syndrome, 2017; M. R. Li, Pan, Bao, Zhang, & Wu, 2007; Vacca et al., 2000). In our data, we found 85% of patients had *MECP2* mutation, which is consistent with previous studies. Our data were collected from 28 RTT subjects, aging from two to twenty seven. Twelve females were grouped in "Younger" and fifteen females and one man were grouped in "Older". Nearly all individuals with RTT were females, owing to the location of *MECP2* gene on X-chromosome. Although higher gender coherence is desired

doi:10.6342/NTU201702958

optimally, in this study, we did not remove the male subject. Instead, we enrolled an age-matched male in control group, as an assumption that the influence of *MECP2* mutation might be more severe than the interference in gender. The observation of handedness revealed only a few subjects with right-handed dominance. Most of the patients lost their hand function, which was replaced by stereotypic movement. Therefore, it was hard to report the handedness in this group. The regression also showed in speech-language function. In Japan, a study with ninety-nine cases indicated that more than half of patients could speak some words, and nearly fifteen percent spoke two-word sentence (Uchino, Suzuki, Hoshino, Nomura, & Segawa, 2001). However, patients in our study showed low language function than previous studies. A total of 6 patients could speak with vocabulary in mainly bilabial words ("ba ba", "ma ma", "bao bao"). The number of the meaningful words was less and there was no sentence in our subjects. Therefore, we divided the patients into two groups (word or mute) when we analyzed their relationship with speech-related tracts, replacing the original categories in the questionnaire.

The raw scores of neurodevelopmental assessment in five subtests demonstrated no difference between two RTT groups, but the standard scores of fine motor and gross motor showed significant difference. This might be inferred to as the floor effect in norm-reference. In this study, standard scores of patients aged over five were collated in 6-year-old norm-reference. This was because of the influence of disease, patients experienced early regression in childhood, and were unable to achieve age-appropriate milestone of development. Age equivalent in Table 2 illustrated the obvious difference in neuro-motor performance in RTT cohort. It also showed the developmental restriction in both groups. The Rett syndrome gross motor scale (Table 3) supported the limitation of performance in the gross motor in older age. On the other hand, some patients with older age preserved their hand function in simple grasping skill, but not in manipulation skill. The hand

doi:10.6342/NTU201702958

function also did not improve as that of younger female subjects (Table 2 and Table 4). Although, questionnaires supported the deterioration of clinical severity in older RTT group, the symptoms of emotion component revealed a releasing trend with increasing age.

Improving eye contact in the stable stage is a well-known alteration in social behavior. Children with RTT showed isolated social behaviors and the features of autism in an early stage, and hence, erroneous diagnosis of infantile autism frequently occurred (Hagberg, 2002; Mount, Charman, Hastings, Reilly, & Cass, 2003). After the end of regression, the behavior of eye contact and joint attention increased for communication and functioned as the basic intention and desire. Parents with RTT reported that patients with well function usually develop a primitive language by "eye pointing" to replace their lost ability in speech and fine motor for communication. Furthermore, the visual pattern enhanced increasingly in school age and adolescents (Djukic & McDermott, 2012; Djukic, Valicenti McDermott, Mavrommatis, & Martins, 2012; Schwartzman, Velloso Rde, D'Antino, & Santos, 2015). However, in our study older patients had lower scores in social interaction. There might be two reasons for this result. First, the items in the questionnaire for evaluating social interaction were mainly motor related, thus yielding lower scores reflecting patients with motor limitation, not the visual ability in RTT patients (Ghuman, Leone, Lecavalier, & Landa, 2011; Kaufmann et al., 2012). The severe motor regression restricted performance in responding to the environment and people, and the subtle visual alteration might be ignored from observation by caregivers. Second, Schwartzman and his colleague applied the eye-tracking technique and discovered a negative correlation between age and social participation, in which adult patients gazed shorter time at human stimuli (face) than non-human stimuli. The researchers of the study further explained that this manifestation may result from the long-term restriction of

doi:10.6342/NTU201702958

patients' social context and social interest. Considering patients' vulnerable physiological status, parents or caregivers tend to establish a regular and rigid environment for the patients (Schwartzman, Velloso Rde, D'Antino, & Santos, 2015).

In the present study, most of the patients suffered from motor regression and pseudo-stationary periods, but it was difficult to determine their progression stage by age. Generally, the younger group performed better in the neuromotor development and social components, but there was no significant difference in two age groups. In addition, the symptoms seemed to extenuate in the older age.

5.2 Brain volume changes in Rett syndrome are consistent to developmental sequence in cortical lobe

Due to the heterogeneous explanation of volume change in previous RTT research, we tried to investigate the brain structural alteration based on a biological view. From a global view of the development of brain, the gray matter volume showed a trend of increase from early teen age for the control group, followed by a gradual decrease in volume from 750 to 700 mm^3. In contrast, the volume decreased dramatically from 650 to 500 mm^3 in patients with RTT, and remained steady during adolescent period and adult age. Besides white matter volume showed a tardy development till adulthood. The volume-changing track in RTT patients indicated the immature brain structure and insufficient nutrition for maintenance in both gray matter and white matter, which was consistent with the function of *MECP2* and its downstream genes (Guy, Cheval, Selfridge, & Bird, 2011; Li & Pozzo-Miller, 2014; McGraw, Samaco, & Zoghbi, 2011).

According to the theory of sequential expression of MECP2, the hypothesis was established on the regional difference of gray and white matter in RTT with correlation to the sequential development in age. Comparing to healthy controls, the difference

doi:10.6342/NTU201702958

showed from parietal and frontal lobe which should mature at age of early teen, and the decreasing volume diffused to whole-brain lobes. The hemisphere difference was discovered in the parietal lobe of control, but with a further analysis, the laterality index showed no difference between groups.

We emphasized the alteration of gray matter in RTT were associated with the increasing age with lacking expression of MECP2 and related proteins, even though most of the previous studies discussing the brain volume and performance. In our study, patients were recruited from age of 2 to 26 and provided the important information of development of the brain. Nevertheless, the alteration in aging is also critical to clarify the pathology of the disease. Therefore, a longitudinal study is necessary for following the trail of volume change in the older patients. Alternatively, studying in an aging cohort is useful to elucidate mechanisms and define the biomarkers in RTT.

5.3 The changes in clinical presentations are related to functional fiber tracts

Considering the task-specific characteristics in white matter, fiber tracts were preferred to be used to explore the functional-specific pathologic changes in brain, and to correlate the microstructural change with clinical phenotypes. We selected three domains of clinical phenotypes due to its specific alterations with stages in RTT.

Losing of speech ability and motor function is the major criteria of RTT, which appears in regression stage, and there is increasing visual ability after the late regression stage. Nevertheless, the relationship between the clinical changes and alterations of brain microstructure has not been reported in previous RTT studies. Therefore, in the present study we picked up 7 speech-language-related fiber tracts and their contralateral tracts: arcuate fasciculus, perpendicular fasciculus, frontal aslent tract, superior longitudinal fasciculus, uncinate fasciculus, mouth part of corticospinal tract and superior temporal part of callosal fiber of (Bernstein & Liebenthal, 2014; Broce, Bernal, Altman, Tremblay,

doi:10.6342/NTU201702958

& Dick, 2015; Friederici, 2009; Hage & Nieder, 2016; Kronfeld-Duenias, Amir, Ezrati-Vinacour, Civier, & Ben-Shachar, 2016; Marchina et al., 2011).

Speech is a lateralized function, mainly arising from the left hemisphere. In the younger patients, the significant decrease of water anisotropy was in left perpendicular fasciculus. The association fiber, also named Wernicke perpendicular or vertical occipital fasciculus, is running vertically and interconnecting areas of parietal, temporal, and occipital (Bartsch, Geletneky, & Jbabdi, 2013). Although the function of perpendicular fasciculus remains unclear, it is assumed that the region of the brain connected is related to higher order function of language. Conversely, the older patients were found to have significant reduction of fiber integrity in all speech-language related tracts and their contralateral tract, except for the corticospinal tract of mouth. Previous studies showed that the integrity of tracts decreased severely with increasing age. To get the information between the integrity of tracts and the clinical presentation, we performed post-hoc analysis among speech subgroup. The findings showed that GFA in left arcuate fasciculus had significant difference between patients with and without speech group. Arcuate fasciculus is direct connecting segments in Broca's area and in Wernicke's area, where are located at the inferior parietal lobule and superior-temporal gyrus and sulcus. As a dorsal stream of model of speech and language processing, arcuate fasciculus plays a critical role in translating acoustic information into articulatory linguistic representations and involved at the level of phonological, lexical, syntactic, semantic and pragmatic (Catani & Mesulam, 2008; Hope, Seghier, Prejawa, Leff, & Price, 2016; López-Barroso et al., 2013; Marchina et al., 2011). The multilevel presentation of the tract was supported in evolutionary view, a review article reported that human showed higher connection than non-language primate in the dorsal stream (Friederici, 2009). Other age-related studies showed that the arcuate fasciculus was found to have high relationship with age than other

doi:10.6342/NTU201702958

language tracts and the density mainly increased during childhood and early adolescent (Broce, Bernal, Altman, Tremblay, & Dick, 2015; Paus et al., 1999). The same reduction in GFA in arcuate fasciculus was shown in the study of autism spectrum disorder (Chiang, Chen, Lin, Tseng, & Gau, 2017; Moseley et al., 2016), even though the reduction was also indicated in the right hemisphere.

In accordance with previous studies, lower diffusion indices were detected in superior longitudinal fasciculus. We compared the GFA value among patients categorized by speech capacity and controls in SLF3, which serves as phonological processing and has relationship with dysarthria and language impairment (Makris et al., 2005; Maldonado, Moritz-Gasser, & Duffau, 2011; Nagae et al., 2012). Patients without language showed the significant reduction of GFA than controls, but there was no difference between the patients with single word and controls. The last result was different from the previous studies (Mahmood et al., 2010). It might arise from the age distribution of the patients with language and the component of selected tracts.

Five of younger patients preserves speech ability, but there was only one older patient preserved the speech capacity. The integrity of white matter preserves better in patients in the childhood stage. Therefore, the reduction of diffusion index was not significant in the present study in patients with single words. Besides, for an accurate comparison, we selected SLF3 as target tract, which connecting inferior frontal gyrus of opercular part and angular gyrus. This specific ROIs selection of SLF also influences the results in small cohort comparison. Interestingly, several language-related tracts like UF and perpendicular fasciculus also had alterations in microstructure, which may arise from early speech delay in RTT patients. In the light of clinical observation, most girls with typical RTT did not achieve early speech-language millstone and performed atypical patterns in the speech-language domain on the pre-regression period (Bartl-Pokorny et

doi:10.6342/NTU201702958

al., 2013; Marschik et al., 2013; Marschik et al., 2012). In fact, the patients with language usually accompanied with better development in other domains, although it is difficult to reliably identify the disease before obvious regression in motor development. The integrity of white matter in language may provide a diagnostic marker to facilitate early identification and speculate the prognosis.

The preservation of eye contact was often reported in RTT studies, with an increasing trend in school age and adolescent patients (Djukic & McDermott, 2012; Djukic, Valicenti McDermott, Mavrommatis, & Martins, 2012; Schwartzman, Velloso Rde, D'Antino, & Santos, 2015). Although the diffusion data of white matter showed that the visual perception tracts maintained its integrity in younger patients, it was reduced in older patients. A general decreasing tendency appeared in occipital lobe-connected tracts, including SLF2, optict radiation of halamic radiation, the precuneus part of callosal fiber and splenium part of callosal fiber. Furthermore, the alteration of microstructure was concordant with the clinical observation in our data, in which the younger patients performed better in social interaction. Although the microstructure of white matter was affected by the disease, the result of the study indicated the integrity of callosal splenium was positively correlated with visual-motor integration. Hence, the reason for the subtle alteration in white matter microstructure may result from plasticity through visually social interaction or rehabilitation activities in daily life (Scholz, Klein, Behrens, & Johansen-Berg, 2009).

Interestingly, the fiber integrity of anterior commissure (AC) showed higher GFA value in the older group than the corresponding control group, and illustrated a positive correlation with the scores of visual-motor integration. According to previous studies, AC seemed to hold a compensatory role functioning as multisensory integration and linkage between vision, attention and action in individuals with callosal agenesis and dysfunction

doi:10.6342/NTU201702958

of corpus callosum (Risse, LeDoux, Springer, Wilson, & Gazzaniga, 1978; van Meer et al., 2016; Winter & Franz, 2014). Besides, Preilowski suggested that patients with anterior-part commissurotomy performed poorly in bilateral motor-learning tasks (Preilowski, 1972).

The function of AC in RTT remains unclear. We assumed a similar compensatory mechanism would appear in RTT patients for the following reasons. First, the reduction of corpus callosum has been indicated in several RTT studies (Carter et al., 2008; Gotoh et al., 2001; Murakami, Haas, Press, & Yeung-Courchesne, 1992; Reiss et al., 1993), and the increasing integration in AC may be found in callosal agenesis patients. Second, after white matter analysis, the visual perception-related fiber tracts showed the significant decrease. However, an eye tracking study demonstrated that the visual stimuli with preferential attention to novelty operate a similar processing between RTT patients and typical children (Djukic, Valicenti McDermott, Mavrommatis, & Martins, 2012). Therefore, another pathway is presumed to exist for the visual function in RTT patients. Third, the substituted visual pathways were mentioned in research with callosal agenesis, utilizing tractography to examine posterior part of the AC, in identifying whether the connection of AC would prolong to primary visual cortex (van Meer et al., 2016). All studies might support the abnormal increase of GFA in AC. However, the actual role of AC in RTT needs further investigation to clarify its connection with visual cortex when more precise visual perception evaluation can be done by advanced techniques.

The regression in early stage of RTT caused the long-term motor deficit (Downs et al., 2010; Downs et al., 2016; FitzGerald, Jankovic, & Percy, 1990; Roze et al., 2007), and in older age they suffered from severely movement impairment and abnormal extrapyramidal involvement (Charman et al., 2002; FitzGerald et al., 1990; Hagberg & Witt-Engerstrom, 1986; Lane et al., 2011; Johnston, Blue, & Naidu, 2005; Martínez et

doi:10.6342/NTU201702958

al., 2013; Parisi, 2016; E. Smeets et al., 2003; Smeets, Pelc, & Dan, 2011). The unusual development in motor functions was often mentioned to be related to dopaminergic systems in RTT (Chiron et al., 1993; Kao, Su, Carlson, & Liao, 2015; Segawa, 2005; Su, Kao, Huang, & Liao, 2015). Therefore, for investigation of the change in motor function, we selected the cortico-basal ganglia-thalamo-cortical loop to execute the comparison. This loop serves as the dopaminergic modulation for inhibiting or exciting motor instructions (Braak & Del Tredici, 2008; Parent & Hazrati, 1995; Silkis, 2001). Moreover, we added the anterior part of the corpus callosum into consideration. The functions of callosal fibers act as the communications for the bilaterally executive functions and motor functions (Aboitiz & Montiel, 2003; Liu et al., 2010; Rosenbloom, Sassoon, Fama, Sullivan, & Pfefferbaum, 2008).

Our studies showed that the integrity of fiber tracts conserved well in younger subjects with RTT. On the contrary, it was reduced in several fiber bundles in older patients. The most common affected regions were in commissural fibers where connecting hemispheres, the genu, DLPFC, VLPFC, SMA, motor precentral and paracentral gyrus parts of callosal fiber. They showed the significant reduction in older patients. In the cortico-basal ganglia-thalamo-cortical loop, the cortico-striatum tracts connecting frontal striatum to orbitofrontal gyrus and motor precentral gyrus showed significant decreased, but the thalamic-cortical tracts and corticospinal tracts merely showed the lower reduction after Bonferroni correction. Moreover, the correlation between clinical presentation and tract integrity was not found in present data, and the density of motor-related fibers were also not different between patients with and without mobility after post-hoc comparisons, even though there were difference between healthy controls and two locomotion groups in older patients.

doi:10.6342/NTU201702958

We postulated that the reductions of GFA values in the cortico-basal ganglia-thalamo-cortical loop and commissural fibers in older subjects might arise from several reasons. The expression of MeCP2 developed with temporal differences in cortex and subcortical area. For instance, the expression of MeCP2 in basal ganglia developed later than cerebral cortex (Shahbazian, Antalffy, Armstrong, & Zoghbi, 2002). Once the neurons develop without sufficient MeCP2, poor neuronal soma size and insufficient dendritic arborizations may occur. Although the impaired development of striatum and thalamus in RTT patients were only mentioned sporadically in the past (Bauman, L., & Arin, 1995; Reiss et al., 1993), and there was no evidence of microstructural difference in older age. The delayed neuronal dysfunction in striatum and thalamus might result in the structural alteration and reduced fiber density in the cortico-basal ganglia-thalamo-cortical loop in our study.

However, the present results showed insufficient relations between clinical presentations and fiber integrity in motor-related tracts. The production of a single movement may involve many complicated procedures, including the functions of neurotransmitters. The motor dysfunctions in RTT patients exit in both structural level and molecular level (Chiron et al., 1993; Kao et al., 2015; Segawa, 2005; Su et al., 2015). Therefore, the demyelination or the poor density in fiber tracts is inadequate to describe the presentations in motor function. Other possible reasons were the limited number of RTT patients in the present study, and bad motor quality in preserved mobility patients. Although subjects with mobility could walk independently, the atypical gait patterns and imbalance were usually observed (Downs et al., 2015; Downs et al., 2016; FitzGerald et al., 1990; Hagberg, 2002; Neul et al., 2010; E. Smeets et al., 2003). The abnormal locomotion may be affected by the injuries of complex neuron network or an infrequent iron deposition in striatum, which was showed in some atypical patients (Crisp et al.,

doi:10.6342/NTU201702958

2013; Crisp et al., 2015; Hayflick et al., 2013; Ohba et al., 2014; Rossi et al., 2010). Consequently, the detection for unusual iron deposition in basal ganglia is essential to elucidate the secondary motor regression in older patients.

5.4 Abnormal iron accumulation in Rett syndrome

The finding in SWI images was separated into two parts: the comparison in visually grading scale and contrast ratio. In the light of the left-hand system, the phase difference might cause by paramagnetic element: iron deposition. Therefore, the accumulation in SWI could be detect by degree of signal loss in visual judgement or computation by software. The result of visually grading scale exhibited the significant increasing of hypointensity in substantia nigra and globus pallidus, accompanied with growing trend in the striatum. Although the iron status of the brain in RTT patients was not mentioned before, the results of visually grading data were consistent with visual findings of atypical RTT patients with WDR45-mutation (Crisp et al., 2013; Crisp et al., 2015; Ohba et al., 2014). Nevertheless, the further identification of contrast ratio displayed significant dephasing in striatum merely. The different results might be enlightened on methodology distinction. Although the application of visual grading scale discovered the hypointensities in striatum, it did not consider the signal noise ratio in each imaging, which might lead to deviation in visual judgement.

The iron accumulation in substantia nigra and globus pallidus raises quickly before twenty years of life, but striatum deposits maximally after the middle age of life (Ramos, 2014). In present data, patients and healthy control demonstrated the similarly age-related distribution of contrast ratio in the deep brain, but individuals with RTT demonstrated generally lower ratios. Additionally, the only meaningful result in correlation with parkinsonian feature showed in the caudate nucleus, even though clinical features appeared unobvious aggravation at this timing. Because the iron accumulation in striatum

doi:10.6342/NTU201702958

usually occurs in normal middle-aged adults (Hagberg, 2005; Roze et al., 2007), the present results may indicate that iron accumulation in the striatum of RTT patients was more related to early aging. Hence, the abnormal iron accumulation in the present study can be thought to be a biomarker of early aging. To clarify the assumption, a longitudinal follow-up study with additional patients is desired to gain better knowledge and understanding of the progress of brain iron accumulation in RTT.

On the other hand, the relation with the parkinsonian features in older girls with RTT (FitzGerald et al., 1990) should not be ignored. As we know, dysfunctional iron regulation and aggregation may result in oxidative stress and cell death (Hagemeier, Geurts, & Zivadinov, 2012). Whether the abnormal iron expression acts a primary or secondary role in dystonia remains unclear. Therefore, other pathological mechanisms involved in RTT still needs further evaluation.

5.5 Limitations

Despite we applied three advanced imaging techniques to explore the brain microstructure in RTT patients, the present study still had a few limitations. First, lacking the specific template for children is a major problem in our study. We recruited patients with wide range of age for observing the alteration in the different stages. However, the data might be affected by the properties of microstructure in normal development, such as lack of intensity contrast between neighboring tissues. Even though we applied the high resolution and high-quality imaging for this study, the effect with pulled children' data into adults' anatomical template might provide an insufficiently accurate of the spatial transform for fitting individual scan.

Second, the standardized assessment tool suffered from floor effect. Patients with RTT were scored below the standard scores basal. We chose PDMS-2 as a developmental

doi:10.6342/NTU201702958

evaluation for the items concerned more suitable for the motor development of patients and the age norm-referenced help us to acquire more information about age equivalent of performance. But the floor effect and the age limitation of norm-referenced made the results hard to be explained and difficult to be compared with controls.

Additionally, one of our research goals was to explore the association between iron accumulation and the clinical presentation of the parkinsonian feature. However, there was insufficient information in our data about the symptoms of parkinsonian and dystonia. The study merely applied scores of sub items with the parkinsonian-like description in the behavioral questionnaire (RSBQ). We expect a more sensitive and specific evaluation for the future study. The last, although RTT is a rare neurodevelopment disease, a longitudinal cohort study is necessary to get more robust information of development and pathology alteration for RTT research.

doi:10.6342/NTU201702958

6. Conclusions

As the first RTT study to investigate the microstructural alteration in the different age, we found the progressive changes in the cerebral cortex with age and the reductions in fiber tracts. Although the researches related to fiber bundle integrity in RTT are scarce, we attempted to clarify the association between clinical presentations and development of function related tracts from the present data. The integrity of arcuate fasciculus showed difference in three speech-diverse groups, indicating that it can be a language marker for RTT and for follow-up research. The visual perception-related tract in the callosal fiber of splenium and anterior commissure showed mild microstructural alterations with visual motor function. These may prove the activity-driven increasing in white matter tracts, even suffering from the severe damage of disease. On the other hand, the cortico-basal ganglia-thalamo-cortical loop in RTT was generally impaired though without correlation with the behavioral data. The consequence may be related to complex neuron network and neuron dysfunction in movement. Moreover, we discovered the abnormal iron accumulation in RTT patients with uncertain reason. Therefore, a longitudinal cohort study is mandatory to elucidate the effect of the subtle change in basal ganglia.

doi:10.6342/NTU201702958

7. Reference

Aboitiz, F., & Montiel, J. (2003). One hundred million years of interhemispheric communication: the history of the corpus callosum. Brazilian journal of medical and biological research, 36(4), pp.409-420.

Amir, R. E., Van den Veyver, I.B., Wan, M., Tran, C.Q., Francke, U. and Zoghbi, H.Y. (1999). Rett syndrome is caused by mutations in X-linked MECP2, encoding methyl-CpG-binding protein 2. Nature genetics, 23(2), 185-188.

Armstrong, D. D. (2005). Neuropathology of Rett Syndrome. Journal of Child Neurology, 20(9).

Armstrong, D., Dunn, J. K., Antalffy, B., & Trived, R. (1995). Selective dendritic alteration in the cortex of Rett Syndrome. Journal of Neuropathology and Experimental Neurology, 54(2), 195-201.

Barnes, K. V., Coughlin, F. R., O'Leary, H. M., Bruck, N., Bazin, G. A., Beinecke, E. B., . . . Kaufmann, W. E. (2015). Anxiety-like behavior in Rett syndrome: characteristics and assessment by anxiety scales. J Neurodev Disord, 7(1), 30. doi:10.1186/s11689-015-9127-4

Bartl-Pokorny, K. D., Marschik, P. B., Sigafoos, J., Tager-Flusberg, H., Kaufmann, W. E., Grossmann, T., & Einspieler, C. (2013). Early socio-communicative forms and functions in typical Rett syndrome. Res Dev Disabil, 34(10), 3133-3138. doi:10.1016/j.ridd.2013.06.040

Bartsch, A. J., Geletneky, K., & Jbabdi, S. (2013). The temporoparietal fiber intersection area and Wernicke perpendicular fasciculus. Neurosurgery, 73(2), pp.E381-E382. doi:10.1371/journal.pone.0049451

Bauman, M. L., L., K. T., & Arin, D. M. (1995). Pervasive neuroanatomic abnormalities of the brain in three cases of Rett's syndrome. Neurology, 45, 1581-1586.

Bernstein, L. E., & Liebenthal, E. (2014). Neural pathways for visual speech perception. Front Neurosci, 8, 386. doi:10.3389/fnins.2014.00386

Bienvenu, T., Philippe, C., De Roux, N., Raynaud, M., Bonnefond, J. P., Pasquier, L., . . . Villard, L. (2006). The Incidence of Rett Syndrome in France. Pediatric Neurology, 34(5), 372-375. doi:10.1016/j.pediatrneurol.2005.10.013

Boggio, E. M., Lonetti, G., Pizzorusso, T., & Giustetto, M. (2010). Synaptic determinants of rett syndrome. Front Synaptic Neurosci, 2, 28. doi:10.3389/fnsyn.2010.00028

Bourdon, V., Philippe, C., Labrune, O., Amsallem, D., Arnould, C., x000E, . . . Jonveaux, P. (2001). A detailed analysis of the MECP2 gene: prevalence of

doi:10.6342/NTU201702958

recurrent mutations and gross DNA rearrangements in Rett syndrome patients. Human Genetics, 108(1), 43-50. doi:10.1007/s004390000422

Braak, H., & Del Tredici, K. (2008). Cortico-basal ganglia-cortical circuitry in Parkinson's disease reconsidered. Exp Neurol, 212(1), 226-229. doi:10.1016/j.expneurol.2008.04.001

Broce, I., Bernal, B., Altman, N., Tremblay, P., & Dick, A. S. (2015). Fiber tracking of the frontal aslant tract and subcomponents of the arcuate fasciculus in 5-8-year-olds: Relation to speech and language function. Brain Lang, 149, 66-76. doi:10.1016/j.bandl.2015.06.006

Carter, J. C., Lanham, D. C., Pham, D., Bibat, G., Naidu, S., & Kaufmann, W. E. (2008). Selective cerebral volume reduction in Rett syndrome: a multiple-approach MR imaging study. AJNR Am J Neuroradiol, 29(3), 436-441. doi:10.3174/ajnr.A0857

Catani, M., & Mesulam, M. (2008). The arcuate fasciculus and the disconnection theme in language and aphasia: history and current state. Cortex, 44(8), 953-961. doi:10.1016/j.cortex.2008.04.002

Chahrour, M., & Zoghbi, H. Y. (2007). The story of Rett syndrome: from clinic to neurobiology. Neuron, 56(3), 422-437. doi:10.1016/j.neuron.2007.10.001

Charman, T., Cass, H., Owen, L., Wigram, T., Slonims, V., Weeks, L., . . . Reilly, S. (2002). Regression in individuals with Rett syndrome. Brain & Development, 24, 281-283.

Chen, Y. J., Lo, Y. C., Hsu, Y. C., Fan, C. C., Hwang, T. J., Liu, C. M., . . . Tseng, W. Y. (2015). Automatic whole brain tract-based analysis using predefined tracts in a diffusion spectrum imaging template and an accurate registration strategy. Hum Brain Mapp, 36(9), 3441-3458. doi:10.1002/hbm.22854

Chiang, H. L., Chen, Y. J., Lin, H. Y., Tseng, W. I., & Gau, S. S. (2017). Disorder-Specific Alteration in White Matter Structural Property in Adults With Autism Spectrum Disorder Relative to Adults With ADHD and Adult Controls. Hum Brain Mapp, 38(1), 384-395. doi:10.1002/hbm.23367

Chin Wong, L., Hung, P. L., Jan, T. Y., Lee, W. T., & Taiwan Rett Syndrome, A. (2017). Variations of stereotypies in individuals with Rett syndrome: A nationwide cross-sectional study in Taiwan. Autism Res. doi:10.1002/aur.1774

Chiron, C., Bulteau, C., Loc'h, C., Raynaud, C., Garreau, B., Syrota, A., & Maziere, B. (1993). Dopaminergic D2 receptor SPECT imaging in Rett syndrome: increase of specific binding in striatum. Journal of nuclear medicine, 34(10), 1717-1721.

doi:10.6342/NTU201702958

Connolly, B. H., McClune, N. O., & Gatlin, R. (2012). Concurrent validity of the Bayley-III and the Peabody Developmental Motor Scale-2. Pediatr Phys Ther, 24(4), 345-352. doi:10.1097/PEP.0b013e318267c5cf

Courchesne, E., Chisum, H. J., Townsend, J., Cowles, A., Covington, J., Egaas, B., . . . Press, G. A. (2000). Normal brain development and aging: quantitative analysis at in vivo MR imaging in healthy volunteers. Radiology, 216(3), 672-682.

Crisp, S. J., Meyer, E., Gregory, A., Archer, H., Hayflick, S., Kurian, M. A., & Silva, R. (2015). WDR45 Mutation in Atypical Rett Syndrome with Brain Iron Accumulation. . Movement Disorders Clinical Practice, 2(1), 81-83. doi:10.1002/mdc3.12120

Crisp, S., Meyer, E., Gregory, A., Archer, H., Hayflick, S., Kurian, M. A., & de Silva, R. (2013). A Rett-Look-Alike with Brain Iron Accumulation. Journal of Neurology, Neurosurgery & Psychiatry, 84(11), e2.154-e152. doi:10.1136/jnnp-2013-306573.38

Desikan, R. S., Segonne, F., Fischl, B., Quinn, B. T., Dickerson, B. C., Blacker, D., . . . Killiany, R. J. (2006). An automated labeling system for subdividing the human cerebral cortex on MRI scans into gyral based regions of interest. Neuroimage, 31(3), 968-980. doi:10.1016/j.neuroimage.2006.01.021

Djukic, A., & McDermott, M. V. (2012). Social preferences in Rett syndrome. Pediatr Neurol, 46(4), 240-242. doi:10.1016/j.pediatrneurol.2012.01.011

Djukic, A., Valicenti McDermott, M., Mavrommatis, K., & Martins, C. L. (2012). Rett syndrome: basic features of visual processing-a pilot study of eye-tracking. Pediatr Neurol, 47(1), 25-29. doi:10.1016/j.pediatrneurol.2012.04.009

Downs, J., Bebbington, A., Jacoby, P., Williams, A. M., Ghosh, S., Kaufmann, W. E., & Leonard, H. (2010). Level of purposeful hand function as a marker of clinical severity in Rett syndrome. Dev Med Child Neurol, 52(9), 817-823. doi:10.1111/j.1469-8749.2010.03636.x

Downs, J., Leonard, H., Jacoby, P., Brisco, L., Baikie, G., & Hill, K. (2015). Rett syndrome: establishing a novel outcome measure for walking activity in an era of clinical trials for rare disorders. Disabil Rehabil, 37(21), 1992-1996. doi:10.3109/09638288.2014.993436

Downs, J., Stahlhut, M., Wong, K., Syhler, B., Bisgaard, A. M., Jacoby, P., & Leonard, H. (2016). Validating the Rett Syndrome Gross Motor Scale. PLoS One, 11(1), e0147555. doi:10.1371/journal.pone.0147555

Esbensen, A. J., Rojahn, J., Aman, M. G., & Ruedrich, S. (2003). Reliability and Validity of an Assessment Instrument for Anxiety, Depression, and Mood

doi:10.6342/NTU201702958

among Individuals with Mental Retardation. Journal of Autism and Developmental Disorders, 33(6), 617-629.

Feng, F., You, H., Hu, L., Wang, H., L., Z. F., Jin, Z. Y., & Cui, L. Y. (2007). Preliminary study of susceptibility-weighted imaging in differentiation of multiple system atrophy and idiopathic Parkinson disease. Chinese Medicine Imaging Technology, 23(6).

Fischl, B. (2004). Automatically Parcellating the Human Cerebral Cortex. Cerebral Cortex, 14(1), 11-22. doi:10.1093/cercor/bhg087

Fischl, B., & Dale, A. M. (2000). Measuring the thickness of the human cerebral cortex from magnetic resonance images. Proceedings of the National Academy of Sciences, 97(20), 11050-11055.

Fischl, B., Liu, A., & Dale, A. M. (2001). Automated manifold surgery: constructing geometrically accurate and topologically correct models of the human cerebral cortex. IEEE transactions on medical imaging, 20(1), 70-80.

Fischl, B., Salat, D. H., Busa, E., Albert, M., Dieterich, M., Haselgrove, C., . . . Montillo, A. (2002). Whole brain segmentation: automated labeling of neuroanatomical structures in the human brain. Neuron, 33(3), 341-355.

FitzGerald, P. M., Jankovic, J., & Percy, A. K. (1990). Rett Syndrome and Associated Movement Disorders. Movement Disorders, 5(3), 195-202.

Folio, M. R., & Fewell, R. R. (2000). Peabody developmental motor scales: Examiner's manual. Pro-ed.

Friederici, A. D. (2009). Pathways to language: fiber tracts in the human brain. . Trends in cognitive sciences, 13(4), 175-181. doi:0.1016/j.tics.2009.01.001

Ghuman, J. K., Freund, L., Reiss, A., Serwint, J., & Folstein, S. (1998). Early detection of social interaction problems: development of a social interaction instrument in young children. Journal of Developmental & Behavioral Pediatrics, 19(6), 411-419.

Ghuman, J. K., Leone, S. L., Lecavalier, L., & Landa, R. J. (2011). The screen for social interaction (SSI): a screening measure for autism spectrum disorders in preschoolers. Res Dev Disabil, 32(6), 2519-2529. doi:10.1016/j.ridd.2011.07.008

Giedd, J. N., Blumenthal, J., Jeffries, N. O., Castellanos, F. X., Liu, H., Zijdenbos, A., . . . Rapoport, J. L. (1999). Brain development during childhood and adolescence: a longitudinal MRI study. . Nature neuroscience, 2(10), 861-863.

Gorczewski, K., Mang, S., & Klose, U. (2009). Reproducibility and consistency of evaluation techniques for HARDI data. MAGMA, 22(1), 63-70. doi:10.1007/s10334-008-0144-0

doi:10.6342/NTU201702958

Gotoh, H., Suzuki, I., Maruki, K., Mitomo, M., Hirasawa, K., & Sasaki, N. (2001). Magnetic resonance imaging and clinical findings examined in adulthood-studies on three adults with Rett syndrome. Brain & Development, 23, S118-S121.

Guy, J., Cheval, H., Selfridge, J., & Bird, A. (2011). The role of MeCP2 in the brain. Annu Rev Cell Dev Biol, 27, 631-652. doi:10.1146/annurev-cellbio-092910-154121

Hagberg, B. (2002). Clinical manifestations and stages of Rett syndrome. Ment Retard Dev Disabil Res Rev, 8(2), 61-65. doi:10.1002/mrdd.10020

Hagberg, B. (2005). Rett Syndrome: Long-Term Clinical Follow- Up Experience Over Four Decades. J Child Neurol, 20, 722-727.

Hagberg, B., & Witt-Engerstrom, I. (1986). Rett Syndrome: A suggested staging system for describing impairment profile with increasing age towards adolescene. American Journal of Medical Genetics, 24, 47-59.

Hage, S. R., & Nieder, A. (2016). Dual Neural Network Model for the Evolution of Speech and Language. Trends Neurosci, 39(12), 813-829. doi:10.1016/j.tins.2016.10.006

Hagemeier, J., Geurts, J. J., & Zivadinov, R. (2012). Brain iron accumulation in aging and neurodegenerative disorders. Expert review of neurotherapeutics, 12(12), 1467-1480. doi:0.1586/ern.12.128

Hayflick, S. J., Kruer, M. C., Gregory, A., Haack, T. B., Kurian, M. A., Houlden, H. H., . . . Hogarth, P. (2013). beta-Propeller protein-associated neurodegeneration: a new X-linked dominant disorder with brain iron accumulation. Brain, 136(Pt 6), 1708-1717. doi:10.1093/brain/awt095

Hope, T. M., Seghier, M. L., Prejawa, S., Leff, A. P., & Price, C. J. (2016). Distinguishing the effect of lesion load from tract disconnection in the arcuate and uncinate fasciculi. Neuroimage, 125, 1169-1173. doi:10.1016/j.neuroimage.2015.09.025

Horska´, A., Naidu, S., Herskovits, E. H., Wang, P. Y., Kaufmann, W. E., & Barker, P. B. (2000). Quantitative 1H MR spectroscopic imaging in early Rett syndrome. American Academy of Neurology, 715-728.

Hsu, Y. C., Lo, Y. C., Chen, Y. J., Wedeen, V. J., & Isaac Tseng, W. Y. (2015). NTU-DSI-122: A diffusion spectrum imaging template with high anatomical matching to the ICBM-152 space. Hum Brain Mapp, 36(9), 3528-3541. doi:10.1002/hbm.22860

Hwang, I., Sohn, C. H., Kang, K. M., Jeon, B. S., Kim, H. J., Choi, S. H., . . . Kim, J. H. (2015). Differentiation of Parkinsonism-Predominant Multiple System Atrophy from Idiopathic Parkinson Disease Using 3T Susceptibility-Weighted

doi:10.6342/NTU201702958

MR Imaging, Focusing on Putaminal Change and Lesion Asymmetry. AJNR Am J Neuroradiol, 36(12), 2227-2234. doi:10.3174/ajnr.A4442

Izbudak, I., Farage, L., Bonekamp, D., Zhang, W., Bibat, G., Mori, S., . . . Horska, A. (2009). Diffusion tensor imaging findings in Rett syndrome patients . In Proceedings of the 17th ISMRM Scientific Meeting, Honolulu, HI.

J.B. Lane, H.-S. Lee, L.W. Smith, P. Cheng, A.K. Percy, D.G. Glaze, . . . J.P. Krischer. (2011). Clinical severity and quality of life in children and adolescents with Rett syndrome. Neurology, 15, 1812-1818.

Johnston, M. V., Blue, M. E., & Naidu, S. (2005). Rett Syndrome and Neuronal Development. Journal of Child Neurology, 20(9), 759-763.

Jovicich, J., Czanner, S., Greve, D., Haley, E., van der Kouwe, A., Gollub, R., . . . Dale, A. (2006). Reliability in multi-site structural MRI studies: effects of gradient non-linearity correction on phantom and human data. Neuroimage, 30(2), 436-443. doi:10.1016/j.neuroimage.2005.09.046

Kao, F. C., Su, S. H., Carlson, G. C., & Liao, W. (2015). MeCP2-mediated alterations of striatal features accompany psychomotor deficits in a mouse model of Rett syndrome. Brain Struct Funct, 220(1), 419-434. doi:10.1007/s00429-013-0664-x

Kaufmann, W. E., Tierney, E., Rohde, C. A., Suarez-Pedraza, M. C., Clarke, M. A., Salorio, C. F., . . . Naidu, S. (2012). Social impairments in Rett syndrome: characteristics and relationship with clinical severity. J Intellect Disabil Res, 56(3), 233-247. doi:10.1111/j.1365-2788.2011.01404.x

Klein, A., & Tourville, J. (2012). 101 labeled brain images and a consistent human cortical labeling protocol. Front Neurosci, 6, 171. doi:10.3389/fnins.2012.00171

Krogsrud, S. K., Fjell, A. M., Tamnes, C. K., Grydeland, H., Mork, L., Due-Tonnessen, P., . . . Walhovd, K. B. (2016). Changes in white matter microstructure in the developing brain--A longitudinal diffusion tensor imaging study of children from 4 to 11years of age. Neuroimage, 124(Pt A), 473-486. doi:10.1016/j.neuroimage.2015.09.017

Kronfeld-Duenias, V., Amir, O., Ezrati-Vinacour, R., Civier, O., & Ben-Shachar, M. (2016). The frontal aslant tract underlies speech fluency in persistent developmental stuttering. Brain Struct Funct, 221(1), 365-381. doi:10.1007/s00429-014-0912-8

Kuo, L. W., Chen, J. H., Wedeen, V. J., & Tseng, W. Y. (2008). Optimization of diffusion spectrum imaging and q-ball imaging on clinical MRI system. Neuroimage, 41(1), 7-18. doi:10.1016/j.neuroimage.2008.02.016

doi:10.6342/NTU201702958

Lane, J. B., Lee, H. S., Smith, L. W., Cheng, P., Percy, A. K., Glaze, D. G., . . . Annese, F. (2011). Clinical severity and quality of life in children and adolescents with Rett syndrome. Neurology, 77(20), 1812-1818.

Laurvick, C. L., de Klerk, N., Bower, C., Christodoulou, J., Ravine, D., Ellaway, C., . . . Leonard, H. (2006). Rett syndrome in Australia: a review of the epidemiology. J Pediatr, 148(3), 347-352. doi:10.1016/j.jpeds.2005.10.037

Lee, J. H., Yang, T. I., Cho, M., Yoon, K. T., Baik, S. K., & Han, Y. H. (2012). Widespread cerebral cortical mineralization in Wilson's disease detected by susceptibility-weighted imaging. J Neurol Sci, 313(1-2), 54-56. doi:10.1016/j.jns.2011.09.031

Lenroot, R. K., & Giedd, J. N. (2006). Brain development in children and adolescents: insights from anatomical magnetic resonance imaging. Neurosci Biobehav Rev, 30(6), 718-729. doi:10.1016/j.neubiorev.2006.06.001

Li, M. R., Pan, H., Bao, X. H., Zhang, Y. Z., & Wu, X. R. (2007). MECP2 and CDKL5 gene mutation analysis in Chinese patients with Rett syndrome. J Hum Genet, 52(1), 38-47. doi:10.1007/s10038-006-0079-0

Li, W., & Pozzo-Miller, L. (2014). BDNF deregulation in Rett syndrome. Neuropharmacology, 76 Pt C, 737-746. doi:10.1016/j.neuropharm.2013.03.024

Libertus, K., & Landa, R. J. (2013). The Early Motor Questionnaire (EMQ): a parental report measure of early motor development. Infant Behav Dev, 36(4), 833-842. doi:10.1016/j.infbeh.2013.09.007

Liu, I. C., Chiu, C. H., Chen, C. J., Kuo, L. W., Lo, Y. C., & Tseng, W. Y. (2010). The microstructural integrity of the corpus callosum and associated impulsivity in alcohol dependence: a tractography-based segmentation study using diffusion spectrum imaging. Psychiatry Res, 184(2), 128-134. doi:10.1016/j.pscychresns.2010.07.002

López-Barroso, D., Catani, M., Ripollés, P., Dell'Acqua, F., Rodríguez-Fornells, A., & de Diego-Balaguer, R. (2013). Word learning is mediated by the left arcuate fasciculus. Proceedings of the National Academy of Sciences, 110(32), 13168-13173.

Macerollo, A., Perry, R., Stamelou, M., Batla, A., Mazumder, A. A., Adams, M. E., & Bhatia, K. P. (2014). Susceptibility-weighted imaging changes suggesting brain iron accumulation in Huntington’s disease: an epiphenomenon which causes diagnostic difficulty. European Journal of Neurology, 21, E16-E17. doi:0.1111/ene.12298

Mahmood, A., Bibat, G., Zhan, A. L., Izbudak, I., Farage, L., Horska, A., . . . Naidu, S. (2010). White matter impairment in Rett syndrome: diffusion tensor

doi:10.6342/NTU201702958

imaging study with clinical correlations. AJNR Am J Neuroradiol, 31(2), 295-299. doi:10.3174/ajnr.A1792

Makris, N., Kennedy, D. N., McInerney, S., Sorensen, A. G., Wang, R., Caviness, V. S., Jr., & Pandya, D. N. (2005). Segmentation of subcomponents within the superior longitudinal fascicle in humans: a quantitative, in vivo, DT-MRI study. Cereb Cortex, 15(6), 854-869. doi:10.1093/cercor/bhh186

Maldonado, I. L., Moritz-Gasser, S., & Duffau, H. (2011). Does the left superior longitudinal fascicle subserve language semantics? A brain electrostimulation study. Brain Struct Funct, 216(3), 263-274. doi:10.1007/s00429-011-0309-x

Marchina, S., Zhu, L. L., Norton, A., Zipse, L., Wan, C. Y., & Schlaug, G. (2011). Impairment of speech production predicted by lesion load of the left arcuate fasciculus. Stroke, 42(8), 2251-2256. doi:10.1161/STROKEAHA.110.606103

Marschik, P. B., Kaufmann, W. E., Sigafoos, J., Wolin, T., Zhang, D., Bartl-Pokorny, K. D., . . . Johnston, M. V. (2013). Changing the perspective on early development of Rett syndrome. Res Dev Disabil, 34(4), 1236-1239. doi:10.1016/j.ridd.2013.01.014

Marschik, P. B., Pini, G., Bartl-Pokorny, K. D., Duckworth, M., Gugatschka, M., Vollmann, R., . . . Einspieler, C. (2012). Early speech-language development in females with Rett syndrome: focusing on the preserved speech variant. Dev Med Child Neurol, 54(5), 451-456. doi:10.1111/j.1469-8749.2012.04123.x

Martínez, A. R., Turon, M., Callejón-Póo, L., Sole, E., Armstrong, J., & Pineda, M. (2013). Treatment Response in Behaviour Disorders in Rett Syndrome. Journal of Behavioral and Brain Science, 03(02), 217-224. doi:10.4236/jbbs.2013.32023

McGraw, C. M., Samaco, R. C., & Zoghbi, H. Y. (2011). Adult Neural Function Requires MeCP2. Science, 333, 8-9. doi:10.1126/science.1206593]

Meng, S. Z., Obonai, T., & Takashima, S. (1998). A developmental study of the dopamine D2R receptors in the human basal ganglia and thalamus. Early human development,, 51(1), 23-30.

Mittal, S., Wu, Z., Neelavalli, J., & Haacke, E. M. (2009). Susceptibility-weighted imaging: technical aspects and clinical applications, part 2. AJNR Am J Neuroradiol, 30(2), 232-252. doi:10.3174/ajnr.A1461

Mori, S., & Barker, P. B. (1999). Diffusion magnetic resonance imaging: its principle and applications. The Anatomical Record, 257(3), 102-109.

Moseley, R. L., Correia, M. M., Baron-Cohen, S., Shtyrov, Y., Pulvermuller, F., & Mohr, B. (2016). Reduced Volume of the Arcuate Fasciculus in Adults with High-Functioning Autism Spectrum Conditions. Front Hum Neurosci, 10, 214. doi:10.3389/fnhum.2016.00214

doi:10.6342/NTU201702958

Mount, R. H., Charman, T., Hastings, R. P., Reilly, S., & Cass, H. (2002). The Rett Syndrome Behaviour Questionnaire (RSBQ): re¢ning the behavioural phenoty. Journal of Child Psychology and Psychiatry, 43(8), 1099-1110.

Mount, R. H., Charman, T., Hastings, R. P., Reilly, S., & Cass, H. (2003). Feature of autism in Rett syndrome and severe mental retardation. Journal of Autism and Developmental Disorders, 33(4), 435-442. doi:10.1023/a:1025066913283

Murakami, J. W., Courchesne, E., , Haas, R. H., Press, G. A., & Yeung-Courchesne, R. (1992). Cerebellar and cerebral abnormalities in Rett syndrome: a quantitative MR analysis. American journal of roentgenology, 159(1), 177-183.

Nagae, L. M., Zarnow, D. M., Blaskey, L., Dell, J., Khan, S. Y., Qasmieh, S., . . . Roberts, T. P. (2012). Elevated mean diffusivity in the left hemisphere superior longitudinal fasciculus in autism spectrum disorders increases with more profound language impairment. AJNR Am J Neuroradiol, 33(9), 1720-1725. doi:10.3174/ajnr.A3037

Naidu, S. (1997). Rett Syndrome: A disorder affecting early brain growth. American Neurological Association.

Nandigam, R. N., Viswanathan, A., Delgado, P., Skehan, M. E., Smith, E. E., Rosand, J., . . . Dickerson, B. C. (2009). MR imaging detection of cerebral microbleeds: effect of susceptibility-weighted imaging, section thickness, and field strength. AJNR Am J Neuroradiol, 30(2), 338-343. doi:10.3174/ajnr.A1355

Neul, J. L., Kaufmann, W. E., Glaze, D. G., Christodoulou, J., Clarke, A. J., Bahi-Buisson, N., . . . RettSearch, C. (2010). Rett syndrome: revised diagnostic criteria and nomenclature. Ann Neurol, 68(6), 944-950. doi:10.1002/ana.22124

Ohba, C., Nabatame, S., Iijima, Y., Nishiyama, K., Tsurusaki, Y., Nakashima, M., . . . Matsumoto, N. (2014). De novo WDR45 mutation in a patient showing clinically Rett syndrome with childhood iron deposition in brain. J Hum Genet, 59(5), 292-295. doi:10.1038/jhg.2014.18

Ozarslan, E., Koay, C. G., Shepherd, T. M., Komlosh, M. E., Irfanoglu, M. O., Pierpaoli, C., & Basser, P. J. (2013). Mean apparent propagator (MAP) MRI: a novel diffusion imaging method for mapping tissue microstructure. Neuroimage, 78, 16-32. doi:10.1016/j.neuroimage.2013.04.016

Parent, A., & Hazrati, L. N. (1995). Functional anatomy of the basal ganglia. I. The cortico-basal ganglia-thalamo-cortical loop. Brain Research Reviews, 20(1), pp.91-127.

doi:10.6342/NTU201702958

Parisi, L., Di Filippo, T. and Roccella, M. (2016). The quality of life in girls with Rett syndrome. Mental Illness, 8(1). doi:0.4081/mi.2016.6302

Paus, T., Zijdenbos, A., Worsley, K., Collins, D. L., B, lumenthal, J., Giedd, J. N., . . . Evans, A. C. (1999). Structural maturation of neural pathways in children and adolescents: in vivo study. . Science, 283(5409), pp.1908-1911. doi:0.1126/science.283.5409.1908

Pierpaoli, C., & Basser, P. J. (1996). Toward a quantitative assessment of diffusion anisotropy. . Magnetic resonance in Medicine, 36(6), 893-906.

Preilowski, B. F. (1972). Possible contribution of the anterior forebrain commissures to bilateral motor coordination. Neuropsychologia, 10(3), 267-277.

Prell, T., Hartung, V., Tietz, F., Penzlin, S., Ilse, B., Schweser, F., . . . Grosskreutz, J. (2015). Susceptibility-weighted imaging provides insight into white matter damage in amyotrophic lateral sclerosis. PLoS One, 10(6), e0131114. doi:10.1371/journal.pone.0131114

Ramos, P., Santos, A., Pinto, N.R., Mendes, R., Magalhães, T. and Almeida, A., . (2014). Iron levels in the human brain: a post-mortem study of anatomical region differences and age-related changes. Journal of Trace Elements in Medicine and Biology, 28(1), pp.13-17.

Reiss, A. L., Faruque, F., Naidu, S., Abrams, M., Beary, T., Bryan, R. N., & Moser, H. (1993). Neuroanatomy of Rett Syndrome: A VolumetIric Imaging Study. Ann Neurol, 34.

Riederer, P., Weiser, M., Wichart, I., Schmidt, B., Killian, W., Rett, A., & Opitz, J. M. (1986). Preliminary Brain Autopsy Findings in Progredient Rett Syndrome. American J Med Genet, 24, 305-315.

Risse, G. L., LeDoux, J., Springer, S. P., Wilson, D. H., & Gazzaniga, M. S. (1978). The anterior commissure in man: Functional variation in a multisensory system. Neuropsychologia, 16(1), 23-31.

Rose, S. A., Djukic, A., Jankowski, J. J., Feldman, J. F., Fishman, I., & Valicenti-McDermott, M. (2013). Rett syndrome: an eye-tracking study of attention and recognition memory. Dev Med Child Neurol, 55(4), 364-371. doi:10.1111/dmcn.12085

Rosenbloom, M. J., Sassoon, S. A., Fama, R., Sullivan, E. V., & Pfefferbaum, A. (2008). Frontal Callosal Fiber Integrity Selectively Predicts Coordinated Psychomotor Performance in Chronic Alcoholism. Brain Imaging Behav, 2(2), 74-83. doi:10.1007/s11682-007-9017-9

Rossi, M., Ruottinen, H., Elovaara, I., Ryymin, P., Soimakallio, S., Eskola, H., & Dastidar, P. (2010). Brain Iron Deposition and Sequence Characteristics in Parkinsonism. Investigative Radiology, 45(12), 795-802.

doi:10.6342/NTU201702958

Roze, E., Cochen, V., Sangla, S., Bienvenu, T., Roubergue, A., Leu-Semenescu, S., & Vidaihet, M. (2007). Rett syndrome: an overlooked diagnosis in women with stereotypic hand movements, psychomotor retardation, Parkinsonism, and dystonia? Mov Disord, 22(3), 387-389. doi:10.1002/mds.21276

Schmithorst, V. J., & Yuan, W. (2010). White matter development during adolescence as shown by diffusion MRI. Brain Cogn, 72(1), 16-25. doi:10.1016/j.bandc.2009.06.005

Schneider, E., Ng, K. M., Yeoh, C. S., Rumpel, H., Fook-Chong, S., Li, H. H., . . . Chan, L. L. (2016). Susceptibility-weighted MRI of extrapyramidal brain structures in Parkinsonian disorders. Medicine (Baltimore), 95(26), e3730. doi:10.1097/MD.0000000000003730

Scholz, J., Klein, M. C., Behrens, T. E., & Johansen-Berg, H. (2009). Training induces changes in white-matter architecture. Nat Neurosci, 12(11), 1370-1371. doi:10.1038/nn.2412

Schwartzman, J. S. (2013). The use of eye-gaze technology in girls with rett syndrome. Pediatr Neurol, 48(2), 159. doi:10.1016/j.pediatrneurol.2012.10.007

Schwartzman, J. S., Velloso Rde, L., D'Antino, M. E., & Santos, S. (2015). The eye-tracking of social stimuli in patients with Rett syndrome and autism spectrum disorders: a pilot study. Arq Neuropsiquiatr, 73(5), 402-407. doi:10.1590/0004-282X20150033

Segawa, M. (2005). Early motor disturbances in Rett syndrome and its pathophysiological importance. Brain Dev, 27 Suppl 1, S54-S58. doi:10.1016/j.braindev.2004.11.010

Sehgal, V., Delproposto, Z., Haacke, E. M., Tong, K. A., Wycliffe, N., Kido, D. K., . . . Reichenbach, J. R. (2005). Clinical applications of neuroimaging with susceptibility-weighted imaging. J Magn Reson Imaging, 22(4), 439-450. doi:10.1002/jmri.20404

Shahbazian, M. D., Antalffy, B., Armstrong, D. L., & Zoghbi, H. Y. (2002). Insight into Rett syndrome: MeCP2 levels display tissue- and cell-specific differences and correlate with neuronal maturation. Human Molecular Genetics, 11(2).

Silkis, I. (2001). The cortico-basal ganglia-thalamocortical circuit with synaptic plasticity. II. Mechanism of synergistic modulation of thalamic activity via the direct and indirect pathways through the basal ganglia. Biosystems, 59(1), pp.7-14.

Smeets, E. E. J., Pelc, K., & Dan, B. (2011). Rett Syndrome. Molecular Syndromology, 2(3-5), 113-127. doi:10.1159/000337637

doi:10.6342/NTU201702958

Smeets, E., Schollen, E., Moog, U., Matthijs, G., Herbergs, J., Smeets, H., . . . Fryns, J. P. (2003). Rett syndrome in adolescent and adult females: clinical and molecular genetic findings. Am J Med Genet A, 122A(3), 227-233. doi:10.1002/ajmg.a.20321

Su, S. H., Kao, F. C., Huang, Y. B., & Liao, W. (2015). MeCP2 in the rostral striatum maintains local dopamine content critical for psychomotor control. J Neurosci, 35(15), 6209-6220. doi:10.1523/JNEUROSCI.4624-14.2015

Temudo, T., Oliveira, P., Santos, M., Dias, K., Vieira, J., Moreira, A., Calado, E., Carrilho, I., Oliveira, G., Levy, A. and Barbot, C. (2007). Stereotypies in Rett syndrome: Analysis of 83 patients with and without detected MECP2 mutations. 68, 1183-1187. doi:0.1212/01.wnl.0000259086.34769.78

Tierney, A. L., & Nelson III, C. A. (2009). Brain development and the role of experience in the early years. . Zero to three, 30(2), 9.

Uchino, J., Suzuki, M., Hoshino, K., Nomura, Y., & Segawa, M. (2001). Development of language in Rett syndrome. Brain & Development, 23, s233-s235.

Urbanowicz, A., Downs, J., Girdler, S., Ciccone, N., & Leonard, H. (2016). An Exploration of the Use of Eye Gaze and Gestures in Females With Rett Syndrome. J Speech Lang Hear Res, 59(6), 1373-1383. doi:10.1044/2015_JSLHR-L-14-0185

Vacca, M., Filippini, F., Budillon, A., Rossi, V., Mercadante, G., Manzati, E., . . . Hultén, M. (2000). Mutation analysis of the MECP2 gene in British and Italian Rett syndrome females. Journal of Molecular Medicine, 78(11), 648-655. doi:10.1007/s001090000155

van Meer, N., Houtman, A. C., Van Schuerbeek, P., Vanderhasselt, T., Milleret, C., & Ten Tusscher, M. P. (2016). Interhemispheric Connections between the Primary Visual Cortical Areas via the Anterior Commissure in Human Callosal Agenesis. Front Syst Neurosci, 10, 101. doi:10.3389/fnsys.2016.00101

Villard, L., Kpebe, A., Cardoso, C., Chelly, J., Tardieu, M., & Fontes, M. (2000). Two affected boys in a Rett syndrome family: Clinical and molecular findings. Neurology, 55(8), 1188-1193. doi:10.1212/wnl.55.8.1188

Virginia C. N. Wong, & Li, a. S. Y. H. (2007). Rett Syndrome: Prevalence Among Chinese and a Comparison of MECP2 Mutations of Classic Rett Syndrome With Other Neurodevelopmental Disorders. Journal of Child Neurology, 22(12), 1397-1400.

doi:10.6342/NTU201702958

Wang, D., Li, W. B., Wei, X. E., Li, Y. H., & Dai, Y. M. (2012). An investigation of age-related iron deposition using susceptibility weighted imaging. . PLoS One, 7(11), 50706 .

Wang, Z., Luo, X. G., & Gao, C. (2016). Utility of susceptibility-weighted imaging in Parkinson's disease and atypical Parkinsonian disorders. Transl Neurodegener, 5, 17. doi:10.1186/s40035-016-0064-2

Wedeen, V. J., Hagmann, P., Tseng, W. Y., Reese, T. G., & Weisskoff, R. M. (2005). Mapping complex tissue architecture with diffusion spectrum magnetic resonance imaging. Magn Reson Med, 54(6), 1377-1386. doi:10.1002/mrm.20642

Wedeen, V. J., Wang, R. P., Schmahmann, J. D., Benner, T., Tseng, W. Y., Dai, G., . . . de Crespigny, A. J. (2008). Diffusion spectrum magnetic resonance imaging (DSI) tractography of crossing fibers. Neuroimage, 41(4), 1267-1277. doi:10.1016/j.neuroimage.2008.03.036

Wierenga, L., Langen, M., Ambrosino, S., van Dijk, S., Oranje, B., & Durston, S. (2014). Typical development of basal ganglia, hippocampus, amygdala and cerebellum from age 7 to 24. Neuroimage, 96, 67-72. doi:10.1016/j.neuroimage.2014.03.072

Winter, T. J., & Franz, E. A. (2014). Implication of the anterior commissure in the allocation of attention to action. Front Psychol, 5, 432. doi:10.3389/fpsyg.2014.00432

Wu, C. H., Hwang, T. J., Chen, Y. J., Hsu, Y. C., Lo, Y. C., Liu, C. M., . . . Isaac Tseng, W. Y. (2015). Primary and secondary alterations of white matter connectivity in schizophrenia: A study on first-episode and chronic patients using whole-brain tractography-based analysis. Schizophr Res, 169(1-3), 54-61. doi:10.1016/j.schres.2015.09.023

Xu, X., Wang, Q., & Zhang, M. (2008). Age, gender, and hemispheric differences in iron deposition in the human brain: an in vivo MRI study. Neuroimage, 40(1), 35-42. doi:0.1016/j.neuroimage.2007.11.017

Zhang, J., Zhang, Y., Wang, J., Cai, P., Luo, C., Qian, Z., . . . Feng, H. (2010). Characterizing iron deposition in Parkinson's disease using susceptibility-weighted imaging: an in vivo MR study. Brain Res, 1330, 124-130. doi:10.1016/j.brainres.2010.03.036

doi:10.6342/NTU201702958

8. Tables

Table 1. Demographic characteristic and clinical status.

	Younger group			Older group		
	RTT	**Control**	**p value**	**RTT**	**Control**	**p value**
Age	5.463±2.30	5.694±1.80	0.786	19.203±5.08	19.813±5.46	0.733
Number	12	12		16	20	
Gender (M/F)	0/12	0/12		1/15	1/19	0.871
MECP2 mutation	11	-		13	-	
Mean years of rehabilitation/education	3.1	2.1	0.19	14.6	15.6	0.47
Handedness (R-L)	3-0	12-0		3-0	20-0	
Speech: words/mute	5/7	12/0	?	1/15	20/0	?
Rett syndrome stage (# /%)						
Stage 2	6 50%			0		
Stage 3	4 33%			12 75%		
Stage 4	2 17%			4 25%		

doi:10.6342/NTU201702958

Table 2. Comparison of Peabody Developmental Motor Scales in raw scores between two RTT groups and the norm-referenced age equivalent.

	Younger RTT N=12	Older RTT N=16	
Stationary	32.58±6.6	30.38±6.8	0.40
Under 1y	9	15	
1-2yrs	1	1	
2-3yrs	2	0	
Locomotion	62±33.7	55.75±29.3	0.60
Under 1yr old	5	6	
1-2yrs	6	10	
2-3yrs	1	0	
Object manipulation	4.16±8.9	0.5±1.09	0.11
Under 1yr old	8	13	
1-2yrs	3	3	
2-3yrs	1	0	
Grasping	18.5±17.04	16.93±14.6	0.79
Under 1yr old	8	15	
1-2yrs	2	1	
2-3yrs	2	0	
Visual-motor	34.5±29.1	25.68±19.3	0.34
Under 1yr old	9	15	
1-2yrs	3	1	
2-3yrs	0	0	
Standard score-gross motor*	3.17±1.95	2.07±0.25	0.03
Standard score-fine motor*	6.83±4.5	4.06±1.1	0.02

* p value <0.05, showed the significant difference

doi:10.6342/NTU201702958

Table 3. The comparison of clinical performance in gross motor scale between younger and older group in RTT patients.

		Young RTT		Older RTT	
		Number	%	Number	%
	Cannot sitting and walking			**2**	**0.13**
No.	**Sitting**	**3**	**0.25**	**1**	**0.06**
1	**Sitting on the floor**	11	0.92	11	0.69
2	**Sitting on a chair**	11	0.92	14	0.88
3	**Sitting on a stool**	10	0.83	11	0.69
	Standing and Walking	**5**	**0.42**	**13**	**0.82**
4	**Sit to stand**	5	0.42	5	0.31
5	**Standing (3sec)**	9	0.75	12	0.75
6	**Standing (10sec)**	9	0.75	12	0.75
7	**Standing (20sec)**	8	0.67	12	0.75
8	**Walking**	8	0.67	10	0.63
9	**Side stepping**	3	0.25	3	0.19
10	**Turning**	7	0.58	6	0.38
11	**Walking on a slope**	4	0.33	6	0.38
12	**Stepping over an obstacle**	5	0.42	2	0.13
	Challenge	**4**	**0.33**	**0**	**0**
13	**Moving from the floor to standing**	4	0.33	0	0
14	**Picking up an object from the floor**	3	0.25	0	0
15	**Running**	4	0.33	0	0

doi:10.6342/NTU201702958

Table 4. Hand function level of Rett syndrome comparing in two groups.

	Younger group	Older group
Number	**12**	**16**
Hand function scale	N(%)	N(%)
1. No observed hand function	3(0.25)	7(0.438)
2. Able to hold at least one large object	3(0.25)	4(0.25)
3. Assistance to grasp but able to pick up and hold at least one large object >2s	1(0.083)	0
4. Able to grasp, pick up and hold at least one large object >2s	0	1(0.062)
5. Use a raking grasp to grasp, pick up and hold a small object >2s	1(0.083)	1(0.062)
6. Can be a scissors, inferior pincer, or superior pincer grasp	1(0.083)	0
7. Able to transfer an object from one hand to the other	0	2(0.125)
8. Hand orientation and size recognition closely approximates the position and size of the object	3(0.25)	1(0.062)
Number of patient present the hand function in deterioration	8(0.67)	11(0.69)
Number of patient maintain their hand function	3(0.25)	5(0.31)
Number of patient present the hand function in progress	1(0.08)	0

doi:10.6342/NTU201702958

Table 5. The comparison of clinical performance in four questionnaires between younger and older group in RTT patients.

Questionnaire		Younger group n=12 Mean	SD	Older group n=16 Mean	SD	p value
RSBQ	**Sum**	**46.75 ± 14.42**		**44.56 ± 11.21**		**0.65**
	General mood	7.08 ± 3.20		6.94 ± 3.09		0.90
	Breathing problems	2.83 ± 2.48		3.00 ± 1.97		0.84
	Hand behavior	8.92 ± 1.78		8.50 ± 1.97		0.57
	Repetitive face movement	3.42 ± 1.73		3.38 ± 1.31		0.94
	Body rocking & expressionless face	6.58 ± 2.57		6.25 ± 1.81		0.69
	Night-time Behaviors	2.58 ± 1.31		1.75 ± 1.61		0.16
	Fear/ Anxiety	4.33 ± 2.64		3.69 ± 2.21		0.49
	Walking standing	2.17 ± 1.47		2.50 ± 1.26		0.52
	Behavior with no domain	8.83 ± 2.48		8.56 ± 1.97		0.75
RSSS	**Sum**	**9.17 ± 3.51**		**12.00 ± 2.90**		**0.03***
	Frequency & manageability of seizure	0.50 ± 0.80		0.69 ± 0.87		0.56
	Respiratory irregularities	0.92 ± 0.90		0.88 ± 0.89		0.90
	Scoliosis	0.58 ± 0.90		1.88 ± 1.31		0.01*
	Ability to walk	1.42 ± 1.16		1.88 ± 1.09		0.29
	Hand use	2.08 ± 0.90		2.50 ± 0.73		0.19
	Speech	2.58 ± 0.51		2.94 ± 0.25		0.02*
	Sleep	1.08 ± 0.51		1.25 ± 0.93		0.58
SSI	**Sum**	**58.00 ± 31.90**		**36.94 ± 16.46**		**0.03***
	When you talk to her/him	2.17 ± 0.94		1.94 ± 0.85		0.51
	When you return home	2.33 ± 1.07		1.63 ± 0.81		0.06
	During meal	1.75 ± 1.06		1.63 ± 0.72		0.71
	Happy#	2.25 ± 1.22		1.25 ± 0.93		0.02*
	Angry#	2.25 ± 1.14		1.13 ± 0.72		<0.01**
	Show the interest in other child	2.33 ± 0.89		1.50 ± 0.73		0.01*
ADAMS	**Sum**	**23.58 ± 11.34**		**26.94 ± 11.33**		**0.45**

#Can your child tell from the look on your face or tone on your voice when you are
* p value <0.05
** p value <0.01

doi:10.6342/NTU201702958

Table 6. Regional gray matter volume difference in two age group of Rett syndrome compared to health control (one-way ANCOVA, age and TIV as covariate).

Younger Group	Control		Rett					
	Mean	SD	Mean	SD	F	P value	corr. P value	Levene's test
TIV cm3	1354.86 ±	94.16	1166.37 ±	104.36		0.0001		
R_Frontal lobe**	82253.91 ±	2335.08	71571.67 ±	2335.08	7.872	0.011	0.044	0.984
L_Frontal lobe**	82615.13 ±	2348.82	71008.2 ±	2348.82	9.185	0.007	0.028	0.309
R_Parietal lobe**	67835.36 ±	1799.09	56758.3 ±	1799.09	14.259	0.001	0.004	0.16
L_Parietal lobe**	65054.01 ±	2102.14	55046.15 ±	2102.14	8.525	0.008	0.032	0.912
R_Temporal lobe	48507.00 ±	1555.63	46490.58 ±	1555.63	0.632	0.436	1.744	0.699
L_Temporal lobe	48924.64 ±	1397.56	45800.69 ±	1397.56	1.879	0.186	0.744	0.912
R_Occipital lobe	26356.10 ±	833.99	244114 ±	933.99	2.42	0.135	0.54	0.288
L_Occipital lobe	25979.59 ±	951.59	24240.15 ±	951.59	1.257	0.276	1.104	0.836

Older Group	Control		Rett					
	Mean	SD	Mean	SD	F	P value	corr. P value	Levene's test
TIV cm3	1333.04 ±	109.05	999.65 ±	117.7		1.5218E-10		
R_Frontal lobe*	78865.21 ±	2495.76	67120.92 ±	2964.83	5.983	0.02	0.08	0.007
L_Frontal lobe*	77774.37 ±	2457.25	68291.96 ±	2919.08	4.038	0.053	0.016	0.064
R_Parietal lobe**	61076.48 ±	2021.9	48701.71 ±	2401.91	10.121	0.003	0.012	0.221
L_Parietal lobe**	59424.82 ±	2050.6	48354.47 ±	2436	7.875	0.008	0.032	0.771
R_Temporal lobe**	50006.21 ±	1496.46	41932.23 ±	1777.71	7.866	0.008	0.032	0.006
L_Temporal lobe*	49369.22 ±	1555.21	43065.71 ±	1847.51	4.439	0.043	0.172	0.002
R_Occipital lobe*	24720.91 ±	834.95	20951.98 ±	991.87	5.506	0.025	0.1	0.584
L_Occipital lobe*	24170.40 ±	775.32	20540 ±	921.03	5.924	0.021	0.084	0.722

* p value <0.05

** corrected p value <0.05

doi:10.6342/NTU201702958

Table 7. Hemisphere difference in four cortical lobes (compared by paired T - test).

	Younger group		Older group	
	Control	**Rett**	**Control**	**Rett**
Frontal lobe	0.4152	0.6204	0.5512	0.8715
Parietal lobe	<0.0001* R>L	0.2183	0.0010* R>L	0.2071
Temporal lobe	0.3828	0.3116	0.2569	0.7601
Occipital lobe	0.5750	0.9027	0.0839	0.0629

doi:10.6342/NTU201702958

Table 8. The comparison of laterality index (Left-Right)/(Left+Right) in two age groups.

	Younger group			Older group		
	Control	Rett		Control	Rett	
	Mean ± SD	Mean ± SD	P value	Mean ± SD	Mean ± SD	P value
Frontal lobe	0.002 ± 0.009	-0.005 ± 0.031	0.477	-0.001 ± 0.010	0.001 ± 0.027	0.741
Parietal lobe	-0.023 ± 0.013	-0.014 ± 0.034	0.423	-0.010 ± 0.015	-0.011 ± 0.030	0.894
Temporal lobe	0.006 ± 0.023	-0.010 ± 0.036	0.218	0.003 ± 0.013	-0.004 ± 0.033	0.395
Occipital lobe	-0.004 ± 0.022	-0.001 ± 0.035	0.772	-0.010 ± 0.026	-0.015 ± 0.033	0.584

doi:10.6342/NTU201702958

Table 9. Comparison of 31 ROIs in two hemispheres between Rett syndrome and health control in younger group.

	Young group								
	Left					Right			
	Control		Rett			Control		Rett		
	mean	SD	mean	SD	corr. P value	mean	SD	mean	SD	corr. P value
Frontal lobe										
Superior frontal	26584 ± 2246		19830 ± 3019		**0.000**	28064 ± 3497		21786 ± 3664		**0.009**
Rostral middle frontal	13732 ± 1794		9611 ± 1553		**0.000**	13190 ± 1513		9143 ± 1696		**0.000**
Caudal middle frontal	7525 ± 1293		5636 ± 1145		**0.031**	7173 ± 943.2		5229 ± 1058		**0.003**
Pars orbitalis	2154 ± 365.6		1638 ± 324		**0.042**	2245 ± 283.4		1632 ± 326.8		**0.002**
Pars opercularis	4646 ± 450.5		3590 ± 528		**0.001**	5089 ± 841.8		3745 ± 646		**0.007**
Pars triangularis	5209 ± 778		3481 ± 664.2		**0.000**	4462 ± 428.1		3272 ± 668.5		**0.001**
Precentral	13774 ± 1595		10965 ± 1431		**0.005**	13412 ± 1575		10887 ± 1154		**0.006**
Medial orbitofrontal	5081 ± 847.5		4146 ± 800.1		**0.338**	4629 ± 423.9		3690 ± 509.8		**0.002**
Lateral orbitofrontal	9043 ± 1070		6978 ± 1201		**0.006**	9107 ± 892.5		7072 ± 1134		**0.002**
Parietal lobe										
Superior parietal	13200 ± 1860		9783 ± 2131		**0.012**	13518 ± 1939		9901 ± 1829		**0.003**
Inferior parietal	14646 ± 1114		10944 ± 2475		**0.003**	17628 ± 1424		13385 ± 3101		**0.009**
Supramarginal	12120 ± 1343		8936 ± 2057		**0.006**	11237 ± 1228		7858 ± 1689		**0.000**
Paracentral	4681 ± 381.5		3805 ± 452.9		**0.001**	4730 ± 572.5		3431 ± 361.2		**0.000**
Precuneus	11889 ± 1657		8498 ± 1708		**0.002**	13177 ± 1477		9311 ± 1675		**0.000**
Postcentral	12112 ± 1037		9487 ± 1537		**0.002**	11568 ± 1553		8850 ± 1281		**0.004**
Temporal lobe										
Transverse temporal	1271 ± 144.9		1035 ± 236.7		**0.233**	1058 ± 180.1		820.5 ± 187.8		**0.141**

doi:10.6342/NTU201702958

Superior temporal	18048 ± 1876	13814 ± 2481	**0.003**	17065 ± 2132	13500 ± 2622	**0.043**
Middle temporal	15486 ± 2240	10586 ± 2060	**0.000**	15988 ± 2780	11288 ± 2161	**0.004**
Fusiform	8432 ± 1478	6380 ± 1358	**0.057**	7885 ± 1236	6245 ± 1111	**0.076**
Inferior temporal	10759 ± 1894	8914 ± 1675	**0.594**	11433 ± 1256	9716 ± 1870	**0.463**
Occipital lobe						
Lateral occipital	13014 ± 1427	10478 ± 2037	**0.058**	13094 ± 1357	10631 ± 1848	**0.037**
Cuneus	5048 ± 705.6	3922 ± 846.9	**0.057**	4674 ± 479.6	3637 ± 795.5	**0.026**
Lingual	7783 ± 972.1	5989 ± 1166	**0.015**	7995 ± 916.5	6022 ± 1580	**0.035**
Pericalcarine	2150 ± 408.1	1835 ± 517.1	**3.480**	2425 ± 337.6	1992 ± 543.9	**0.884**
Limbic lobe						
Parahippocampal	2103 ± 282.2	1635 ± 280.7	**0.016**	1988 ± 210.8	1568 ± 271.4	**0.011**
Entorhinal	1464 ± 382	1331 ± 347.9	**11.840**	1430 ± 341.6	1257 ± 263.8	**5.575**
Rostral anterior cingulate	3292 ± 652.2	2571 ± 486.9	**0.174**	2480 ± 493.5	1896 ± 466.2	**0.215**
Caudal anterior cingulate	7525 ± 1293	5636 ± 1145	**0.031**	7173 ± 943.2	5229 ± 1058	**0.003**
Posterior cingulate	4088 ± 537.4	2894 ± 561.5	**0.001**	4058 ± 596.4	2925 ± 461.7	**0.001**
Isthmus of cingulate	3067 ± 383.4	2260 ± 473.8	**0.004**	2938 ± 269.1	2192 ± 514.3	**0.006**
Insula	6245 ± 701.5	4875 ± 730	**0.003**	6262 ± 672.1	4993 ± 602.9	**0.002**

doi:10.6342/NTU201702958

Table 10. Comparison of 31 ROIs in two hemispheres between Rett syndrome and health control in older group.

	Old group								
	Left					Right			
	Control		Rett			Control		Rett		
	mean	SD	mean	SD	corr. P value	mean	SD	mean	SD	corr. P value
Frontal lobe										
Superior frontal	23394 ± 3080		15816 ± 3882		**0.000**	25403 ± 3457		16922 ± 3614		**0.000**
Rostral middle frontal	11301 ± 2038		7313 ± 1833		**0.000**	10872 ± 2333		7198 ± 2111		**0.000**
Caudal middle frontal	6698 ± 1332		4247 ± 1094		**0.000**	5983 ± 1000		3697 ± 992.8		**0.000**
Pars orbitalis	1935 ± 226.3		1386 ± 424.4		**0.000**	2042 ± 259.5		1514 ± 435.1		**0.002**
Pars opercularis	4321 ± 948.2		2879 ± 814.1		**0.000**	4468 ± 1099		2788 ± 619.6		**0.000**
Pars triangularis	4337 ± 951.3		2962 ± 824.4		**0.001**	4217 ± 992.8		2758 ± 844.7		**0.001**
Precentral	12921 ± 1268		8544 ± 1688		**0.000**	12346 ± 1087		8281 ± 1723		**0.000**
Medial orbitofrontal	4412 ± 525.8		3189 ± 625.8		**0.000**	4190 ± 561.9		3056 ± 770.2		**0.000**
Lateral orbitofrontal	8397 ± 875.2		5801 ± 1363		**0.000**	8430 ± 757.3		5805 ± 1271		**0.000**
Parietal lobe										
Superior parietal	10639 ± 1590		7148 ± 1981		**0.000**	10885 ± 1251		7167 ± 1824		**0.000**
Inferior parietal	12764 ± 1559		7992 ± 1988		**0.000**	14782 ± 2174		9278 ± 2303		**0.000**
Supramarginal	10166 ± 2050		6457 ± 1901		**0.000**	9337 ± 1385		6019 ± 1563		**0.000**
Paracentral	4218 ± 565.8		2966 ± 636.7		**0.000**	3900 ± 470.8		2883 ± 624.8		**0.000**
Precuneus	9725 ± 1180		6451 ± 1344		**0.000**	10452 ± 1268		6928 ± 1499		**0.000**
Postcentral	10596 ± 1540		6978 ± 1259		**0.000**	9841 ± 1532		6530 ± 1539		**0.000**
Temporal lobe										
Transverse temporal	1140 ± 262.6		834.7 ± 215		**0.014**	855.4 ± 117.3		650.5 ± 169.2		**0.003**
Superior temporal	15668 ± 1883		10694 ± 2697		**0.000**	15126 ± 1520		10563 ± 2572		**0.000**
Middle temporal	13544 ± 1982		8494 ± 2366		**0.000**	13698 ± 1540		8655 ± 1647		**0.000**
Fusiform	7621 ± 1088		5000 ± 1446		**0.000**	7537 ± 984.1		5086 ± 1306		**0.000**
Inferiortemporal	11574 ± 1566		7558 ± 1591		**0.000**	11951 ± 1326		7792 ± 1847		**0.000**

doi:10.6342/NTU201702958

Occipital lobe						
Lateral occipital	11505 ± 1208	7805 ± 1418	**0.000**	11528 ± 1358	7989 ± 1559	**0.000**
Cuneus	4159 ± 611.9	2883 ± 683.8	**0.000**	3900 ± 508.8	2812 ± 579.7	**0.000**
Lingual	5945 ± 953.9	4349 ± 927.8	**0.000**	6275 ± 939.9	4585 ± 854.3	**0.000**
Pericalcarine	1823 ± 404.8	1441 ± 355.8	**0.163**	2091 ± 367	1627 ± 408.6	**0.029**
Limbic lobe						
Parahippocampal	2021 ± 347.5	1406 ± 304.8	**0.000**	1854 ± 285	1424 ± 306.7	**0.003**
Entorhinal	1453 ± 314.8	1089 ± 257.9	**0.016**	1509 ± 245.7	1120 ± 326.1	**0.006**
Rostral anterior cingulate	3223 ± 510.5	2037 ± 467.5	**0.000**	2271 ± 281.9	1576 ± 363	**0.000**
Caudal anterior cingulate	6698 ± 1332	4247 ± 1094	**0.000**	5983 ± 1000	3697 ± 992.8	**0.000**
Posterior cingulate	3320 ± 605.3	2247 ± 444.2	**0.000**	3416 ± 551.9	2278 ± 478.6	**0.000**
Isthmus of cingulate	2558 ± 411.3	1747 ± 356.7	**0.000**	2391 ± 397.1	1637 ± 341.2	**0.000**
Insula	5754 ± 643.2	4075 ± 819.8	**0.000**	5870 ± 644.9	4249 ± 917.6	**0.000**

doi:10.6342/NTU201702958

Table 11. Comparison of GFA values in language related tracts and its contralateral tracts between Rett syndrome and health control in two groups.

	Younger group					Older group				
	Control		Rett			Control		Rett		
	Mean	SD	Mean	SD	p value	Mean	SD	Mean	SD	p value
Speech-language related tracts										
AF_L	0.356 ±	0.03	0.332 ±	0.03	0.0561	0.441 ±	0.03	0.353 ±	0.05	0.0000 **
AF_R	0.355 ±	0.03	0.322 ±	0.03	0.0215 *	0.429 ±	0.03	0.342 ±	0.05	0.0000 **
Frontal aslent tract_L	0.414 ±	0.03	0.420 ±	0.04	0.6796	0.473 ±	0.03	0.441 ±	0.05	0.0226 *
Frontal aslent tract_R	0.333 ±	0.03	0.355 ±	0.04	0.1511	0.401 ±	0.03	0.351 ±	0.04	0.0005 **
Perpendicular fasciculus_L	0.280 ±	0.02	0.239 ±	0.03	0.0003 **	0.319 ±	0.03	0.258 ±	0.04	0.0000 **
Perpendicular fasciculus_R	0.267 ±	0.04	0.251 ±	0.05	0.3701	0.330 ±	0.03	0.252 ±	0.04	0.0000 **
SLF3_L	0.366 ±	0.05	0.336 ±	0.04	0.0986	0.425 ±	0.04	0.367 ±	0.05	0.0007 **
SLF3_R	0.308 ±	0.05	0.286 ±	0.04	0.2314	0.381 ±	0.04	0.303 ±	0.04	0.0000 **
UF_L	0.286 ±	0.02	0.261 ±	0.03	0.0245 *	0.344 ±	0.02	0.261 ±	0.04	0.0000 **
UF_R	0.288 ±	0.03	0.265 ±	0.03	0.0902	0.343 ±	0.03	0.263 ±	0.05	0.0000 **
CST of mouth_L	0.541 ±	0.03	0.545 ±	0.04	0.8007	0.596 ±	0.01	0.582 ±	0.04	0.1449
CST of mouth_R	0.522 ±	0.04	0.533 ±	0.04	0.4672	0.578 ±	0.02	0.569 ±	0.04	0.3619
CF of superior temporal lobule	0.454 ±	0.04	0.437 ±	0.04	0.2694	0.538 ±	0.03	0.447 ±	0.06	0.0000 **

* $p < 0.05$ Significant difference between patients of Rett syndrome and controls
** $p < 0.05$ Significant difference between patients of Rett syndrome and controls and survived after Bonferroni correction.

Abbreviations: R: right; L: left; AF: arcuate fasciculus; SLF: superior longitudinal fasciculus; UF: uncinate fasciculus; CST: corticospinal tract;
CF: callosal fibers

doi:10.6342/NTU201702958

Table 12. Comparison of GFA values in visual perception related tracts between Rett syndrome and health control in two groups.

	Younger group				Older group			
	Control		Rett		Control		Rett	
	Mean SD		Mean SD	p value	Mean SD		Mean SD	p value
Visual perception related tracts								
SLF2_L	0.350 ± 0.04		0.325 ± 0.04	0.1317	0.410 ± 0.04		0.350 ± 0.05	0.0003 **
SLF2_R	0.356 ± 0.04		0.324 ± 0.03	0.0636	0.420 ± 0.04		0.336 ± 0.04	0.0000 **
TR of optic_L	0.426 ± 0.05		0.400 ± 0.04	0.1560	0.490 ± 0.02		0.442 ± 0.04	0.0001 **
TR of optic_R	0.405 ± 0.05		0.378 ± 0.03	0.1224	0.456 ± 0.02		0.423 ± 0.04	0.0069 **
AC	0.227 ± 0.03		0.231 ± 0.03	0.7799	0.194 ± 0.03		0.214 ± 0.02	0.0166 *
CF of precuneus	0.386 ± 0.06		0.345 ± 0.05	0.0843	0.478 ± 0.08		0.368 ± 0.06	0.0001 **
CF of splenium	0.387 ± 0.03		0.380 ± 0.06	0.6830	0.480 ± 0.03		0.409 ± 0.06	0.0002 **

* $p < 0.05$ Significant difference between patients of Rett syndrome and controls

** $p < 0.05$ Significant difference between patients of Rett syndrome and controls and survived after Bonferroni correction.

Abbreviations: R: right; L: left; SLF: superior; TR: thalamic radiation; AC: arcuate fasciculus; CF: callosal fibers

doi:10.6342/NTU201702958

Table 13. Comparison of GFA values in motor related tracts between Rett syndrome and health control in two groups.

	Younger group					Older group				
	Control		Rett			Control		Rett		
Motor related tracts	**Mean**	**SD**	**Mean**	**SD**	**p value**	**Mean**	**SD**	**Mean**	**SD**	**p value**
CST of Hand_L	0.468 ±	0.03	0.476 ±	0.03	0.4848	0.521 ±	0.02	0.503 ±	0.03	0.0286 *
CST of Hand_R	0.529 ±	0.04	0.532 ±	0.03	0.8320	0.582 ±	0.02	0.565 ±	0.03	0.0511
CST of M1_L	0.555 ±	0.04	0.552 ±	0.03	0.8441	0.597 ±	0.02	0.576 ±	0.04	0.0493 *
CST of M1_R	0.506 ±	0.03	0.510 ±	0.03	0.7585	0.560 ±	0.03	0.529 ±	0.03	0.0034 *
CST of toe_L	0.532 ±	0.03	0.533 ±	0.03	0.9589	0.570 ±	0.02	0.556 ±	0.04	0.1621
CST of toe_R	0.526 ±	0.04	0.534 ±	0.04	0.6122	0.575 ±	0.02	0.554 ±	0.04	0.0502
CST of Geniculate fibers_L	0.448 ±	0.02	0.461 ±	0.03	0.2249	0.513 ±	0.02	0.490 ±	0.03	0.0196 *
CST of Geniculate fibers_R	0.462 ±	0.03	0.481 ±	0.03	0.1160	0.525 ±	0.03	0.502 ±	0.04	0.0362 *
FS of OFC_L	0.295 ±	0.03	0.278 ±	0.04	0.2457	0.369 ±	0.03	0.302 ±	0.06	0.0001 **
FS of OFC_R	0.296 ±	0.03	0.282 ±	0.04	0.2869	0.379 ±	0.03	0.299 ±	0.06	0.0000 **
FS of DLPFC_L	0.410 ±	0.04	0.404 ±	0.04	0.6907	0.459 ±	0.03	0.417 ±	0.05	0.0043 *
FS of DLPFC_R	0.420 ±	0.04	0.419 ±	0.04	0.9666	0.470 ±	0.03	0.431 ±	0.06	0.0137 *
FS of VLPFC_L	0.347 ±	0.02	0.355 ±	0.04	0.5607	0.398 ±	0.02	0.359 ±	0.06	0.0084 *
FS of VLPFC_R	0.283 ±	0.03	0.280 ±	0.04	0.8679	0.313 ±	0.02	0.290 ±	0.06	0.1131
FS of motor precentral_L	0.381 ±	0.03	0.388 ±	0.03	0.5606	0.448 ±	0.03	0.396 ±	0.04	0.0000 **
FS of motor precentral_R	0.364 ±	0.03	0.379 ±	0.03	0.2978	0.432 ±	0.03	0.380 ±	0.05	0.0006 **
TR of VLPFC_L	0.280 ±	0.03	0.276 ±	0.03	0.7403	0.320 ±	0.03	0.291 ±	0.05	0.0284 *
TR of VLPFC_R	0.352 ±	0.03	0.360 ±	0.04	0.5248	0.404 ±	0.02	0.365 ±	0.07	0.0239 *
TR of DLPFC_L	0.443 ±	0.03	0.459 ±	0.03	0.2252	0.502 ±	0.03	0.469 ±	0.05	0.0201 *
TR of DLPFC_R	0.441 ±	0.04	0.458 ±	0.03	0.2315	0.501 ±	0.02	0.475 ±	0.05	0.0527
TR of precentral_L	0.440 ±	0.03	0.448 ±	0.02	0.4855	0.469 ±	0.02	0.461 ±	0.04	0.4678
TR of precentral_R	0.446 ±	0.04	0.454 ±	0.03	0.5339	0.486 ±	0.03	0.463 ±	0.04	0.0565
CF of genu	0.447 ±	0.04	0.375 ±	0.05	0.0007 **	0.466 ±	0.04	0.341 ±	0.10	0.0000 **
CF of DLPFC	0.443 ±	0.04	0.412 ±	0.04	0.0483	0.497 ±	0.04	0.401 ±	0.07	0.0000 **
CF of VLPFC	0.427 ±	0.04	0.407 ±	0.04	0.1968	0.498 ±	0.04	0.386 ±	0.07	0.0000 **
CF of SMA	0.506 ±	0.04	0.502 ±	0.04	0.7779	0.591 ±	0.03	0.520 ±	0.06	0.0001 **

doi:10.6342/NTU201702958

CF of motor precentral	0.464 ± 0.04	0.475 ± 0.04	0.4533	0.556 ± 0.03	0.487 ± 0.05	0.0000 **
CF of paracentral	0.498 ± 0.04	0.490 ± 0.04	0.6684	0.595 ± 0.03	0.509 ± 0.05	0.0000 **

* $p < 0.05$ Significant difference between patients of Rett syndrome and controls

** $p < 0.05$ Significant difference between patients of Rett syndrome and controls and survived after Bonferroni correction.

Abbreviations: R: right; L: left; VLPFC/DLPFC: ventral/dorsal lateral prefrontal cortex; SMA: supplementary motor area; FS: frontal striatum; TR: thalamic radiation; CST: corticospinal tract; CF: callosal fibers

doi:10.6342/NTU201702958

Table 14. The comparisons of speech-language related tracts among ability of speech subgroups (age-matched).

					Post hoc test adjusted P value		
	Control	**Patient with speech**	**Patient without speech**	**p value**	**Without speech _ With speech**	**Without speech _ control**	**With speech_ control**
	n=6	n=6	n=6				
Mean age	10.26±6.8	9.035±6.5	8.80±6.6	0.925			
AF_L	0.390±0.04	0.364±0.03	0.304±0.01	0.002	0.027*	0.003**	1
Frontal aslent tract_L	0.436±0.47	0.447±0.02	0.397±0.04	0.097	-	-	-
Perpendicular fasciculus_L	0.303±0.01	0.265±0.02	0.218±0.01	0.001	0.121	0.001**	0.373
SLF3_L	0.391±0.05	0.378±0.03	0.316±0.04	0.032	0.194	0.033*	1
UF_L	0.316±0.04	0.277±0.02	0.230±0.03	0.004	0.218	0.003**	0.439
CST of mouth_R	0.559±0.04	0.573±0.02	0.530±0.42	0.52	-	-	-
CST of mouth_L	0.543±0.04	0.588±0.02	0.535±0.05	0.558	-	-	-
CF of superior temporal lobule	0.483±0.05	0.456±0.02	0.407±0.03	0.032	0.194	0.033*	1

Abbreviations: R: right; L: left; AF: arcuate fasciculus; SLF: superior longitudinal fasciculus; UF: uncinated fasciculus; CST: corticospinal tract; CF: callosal fibers

* $p < 0.05$ Significant difference

** $p < 0.01$ Significant difference

doi:10.6342/NTU201702958

Table 15. The correlation between visual perception related tracts and visual motor performance in older RTT patients (Spearman correlation).

		SSI sum	Sum of 6 items in SSI	Visual-motor integration	
SSI sum	R	1	0.647	0.335	
	Sig.	-	0.007	0.205	
Sum of 6 items in SSI	R	0.647	1	0.603	
	Sig.	0.007	-	0.013	*
Visual-motor integration	R	0.335	0.603	1	
	Sig.	0.205	0.013	-	
L_SLF2	R	0.14	0.118	0.361	
	Sig.	0.605	0.664	0.169	
R_SLF3	R	0.103	0.223	0.336	
	Sig.	0.705	0.385	0.201	
L_TR of optic	R	-0.161	0.012	0.29	
	Sig.	0.552	0.065	0.275	
R_TR of optic	R	-0.311	-0.271	0.174	
	Sig.	0.241	0.31	0.519	
AC	R	-0.112	0.228	0.531	
	Sig.	0.681	0.395	0.034	*
CF of precuneus	R	0.35	0.314	0.435	
	Sig.	0.184	0.236	0.092	
CF of splenium	R	0.155	0.22	0.607	
	Sig.	0.567	0.414	0.013	*

* $p < 0.05$ Significant

doi:10.6342/NTU201702958

Table 16. The correlation between motor related tracts and clinical presentation of gross motor scale and hand function scale in younger RTT patients.

		Hand function	GM scale
Hand function	R	1	0.673
	Sig.	-	0.017*
GM scale	R	-0.673	1
	Sig.	0.017*	-
L_CST of hand	R	-0.408	-0.136
	Sig.	0.188	0.674
L_CST of M1	R	-0.301	-0.064
	Sig.	0.342	0.843
R_CST of M1	R	-0.211	0.029
	Sig.	0.51	0.91
L_Geniculate fibers	R	-0.319	-0.114
	Sig.	0.313	0.724
R_Geniculate fibers	R	-0.075	0.036
	Sig.	0.816	0.912
L_FS of OFC	R	-0.075	-0.121
	Sig.	0.816	0.707
R_FS of OFC	R	-0.329	-0.286
	Sig.	0.296	0.369
L_FS of VLPFC	R	-0.15	-0.1
	Sig.	0.641	0.757
L_FS of DLPFC	R	-0.304	-0.479
	Sig.	0.336	0.115
R_FS of DLPFC	R	-0.272	-0.35
	Sig.	0.392	0.265
L_FS of motor precentral gyrus	R	-0.44	-0.393
	Sig.	0.152	0.206
R_FS of motor precentral gyrus	R	-0.054	-0.043
	Sig.	0.868	0.895
L_TR of VLPFC	R	-0.136	-0.283
	Sig.	0.674	0.373
R_TR of VLPFC	R	-0.379	-0.512
	Sig.	0.225	0.089
L_TR of DLPFC	R	-0.393	-0.322
	Sig.	0.206	0.307
CF of genu	R	0.114	0.465
	Sig.	0.724	0.127
CF of DLPFC	R	-0.093	0.204
	Sig.	0.774	0.525
CF of VLPFC	R	-0.221	-0.079
	Sig.	0.489	0.808
CF of SMA	R	-0.186	-0.093
	Sig.	0.563	0.774
CF of motor precentral gyrus	R	-0.286	-0.276
	Sig.	0.368	0.386
CF of paracemtral	R	0.014	-0.025
	Sig.	0.965	0.938

doi:10.6342/NTU201702958

Table 17. The correlation between motor related tracts and clinical presentation of gross motor scale and hand function scale in older RTT patients.

		Hand function	GM scale
Hand function	R	1	0.328
	Sig.	-	0.215
GM scale	R	0.328	1
	Sig.	0.215	-
L_CST of hand	R	-0.277	0.115
	Sig.	0.299	0.673
L_CST of M1	R	-0.049	0.186
	Sig.	0.856	0.491
R_CST of M1	R	-0.034	0.16
	Sig.	0.9	0.555
L_Geniculate fibers	R	-0.025	0.076
	Sig.	0.925	0.78
R_Geniculate fibers	R	0.075	0.2
	Sig.	0.784	0.458
L_FS of OFC	R	0.224	0.064
	Sig.	0.405	0.815
R_FS of OFC	R	0.121	0.02
	Sig.	0.656	0.941
L_FS of VLPFC	R	0.151	0.248
	Sig.	0.578	0.355
L_FS of DLPFC	R	-0.092	-0.053
	Sig.	0.734	0.846
R_FS of DLPFC	R	0.042	0.04
	Sig.	0.878	0.882
L_FS of motor precentral gyrus	R	0.291	0.098
	Sig.	0.275	0.719
R_FS of motor precentral gyrus	R	0.295	0.046
	Sig.	0.267	0.864
L_TR of VLPFC	R	0.133	0.009
	Sig.	0.623	0.974
R_TR of VLPFC	R	0.178	0.131
	Sig.	0.509	0.628
L_TR of DLPFC	R	-0.139	-0.227
	Sig.	0.607	0.399
CF of genu	R	0.221	0.411
	Sig.	0.41	0.113
CF of DLPFC	R	0.166	0.176
	Sig.	0.54	0.515
CF of VLPFC	R	0.203	0.276
	Sig.	0.451	0.301
CF of SMA	R	0.121	0.042
	Sig.	0.656	0.878
CF of motor precentral gyrus	R	0.02	0.107
	Sig.	0.941	0.692
CF of paracemtral	R	0.125	0.252
	Sig.	0.643	0.347

doi:10.6342/NTU201702958

Table 18. The comparisons of motor related tracts among mobility subgroups in older group.

					Post hoc test with adjusted P value		
	Control	**Patient With mobility**	**Patient Without mobility**	**p value**	**Can't walk_ Can walk**	**Can't walk_ Control**	**Can walk_ control**
	n=7	n=10	n=6				
Mean age	19.26±2.8	19.45±5.2	18.79±5.2	0.953	-	-	-
FS of OFC_L	0.307±0.06	0.362±0.04	0.291±0.06	0.54	-	-	-
FS of OFC_R	0.305±0.06	0.386±0.04	0.287±0.68	0.008*	1	0.02*	0.22
FS of motor precentral_L	0.402±0.04	0.452±0.02	0.386±0.30	0.022*	1	0.023*	0.128
FS of motor precentral_R	0.385±0.05	0.434±0.04	0.369±0.04	0.052	-	-	-
CF of DLPFC	0.410±0.06	0.502±0.03	0.384±0.07	0.006*	1	0.01*	0.025*
CF of VLPFC	0.395±0.05	0.510±0.04	0.370±0.08	0.001*	1	0.004*	0.005*
CF of SMA	0.529±0.04	0.596±0.03	0.505±0.07	0.016*	1	0.041*	0.032*
CF of motor precentral	0.496±0.04	0.566±0.03	0.472±0.06	0.008*	1	0.017*	0.024*
CF of paracentral	0.524±0.04	0.600±0.03	0.482±0.05	0.002*	0.834	0.002*	0.024*

Abbreviations: R: right; L: left; VLPFC/DLPFC: ventral/dorsal lateral prefrontal cortex; SMA: supplementary motor area; FS: frontal striatum; CST: corticospinal tract; CF: callosal fibers

doi:10.6342/NTU201702958

Table 19. The comparison of visually grading scale in 5 ROIs of basal ganglia between Rett syndrome patients and control (Mann Whitney U test).

	RTT	Control	
	Mean ± SD	Mean ± SD	p value
Substantia nigra	1.286 ± 0.763	0.844 ± 0.369	0.007**
Caudate nucleus	0.500 ± 0.509	0.375 ± 0.492	0.334
Putamen	0.286 ± 0.460	0.125 ± 0.336	0.124
Globus pallidus	1.429 ± 0.690	0.969 ± 0.474	0.0043**
Thalamus	0.000 0.000	0.000 0.000	1

* $p < 0.05$ Significant difference between patients Rett syndrome and controls
** $p < 0.05$ Significant difference between patients Rett syndrome and controls and survived after Bonferroni correction.

doi:10.6342/NTU201702958

Table 20. The comparison of contrast ratio in 5 ROIs of basal ganglia between Rett syndrome patients and control (Mann Whitney U test).

	Control N=31	RTT N=28	
ROIs	**Mean ± SD**	**Mean ± SD**	**P value**
Age	15.38 ± 8.15	13.31 ± 8.03	0.334
Substantia nigra	-0.1547 ± 0.11	-0.2371 ± 0.20	0.219
Caudate nucleus	0.0001 ± 0.10	-0.2557 ± 0.29	<0.0001**
Putamen	0.0542 ± 0.12	-0.2218 ± 0.22	<0.0001**
Globus Pallidus	-0.1256 ± 0.11	-0.2444 ± 0.18	0.010**
Thalamus	0.3139 ± 0.12	0.0539 ± 0.32	0.288

* $p < 0.05$ Significant difference between patients Rett syndrome and controls
** $p < 0.05$ Significant difference between patients Rett syndrome and controls and survived after Bonferroni correction.

doi:10.6342/NTU201702958

9. Figure

Figure 1. The different trajectories of development in total intracranial volume. The decline trajectory of development in RTT patients was fitted by quadratic regression with age as independent variable; in contrast, the normal development in healthy control showed an increasing trend ($R^2 = 0.241$).

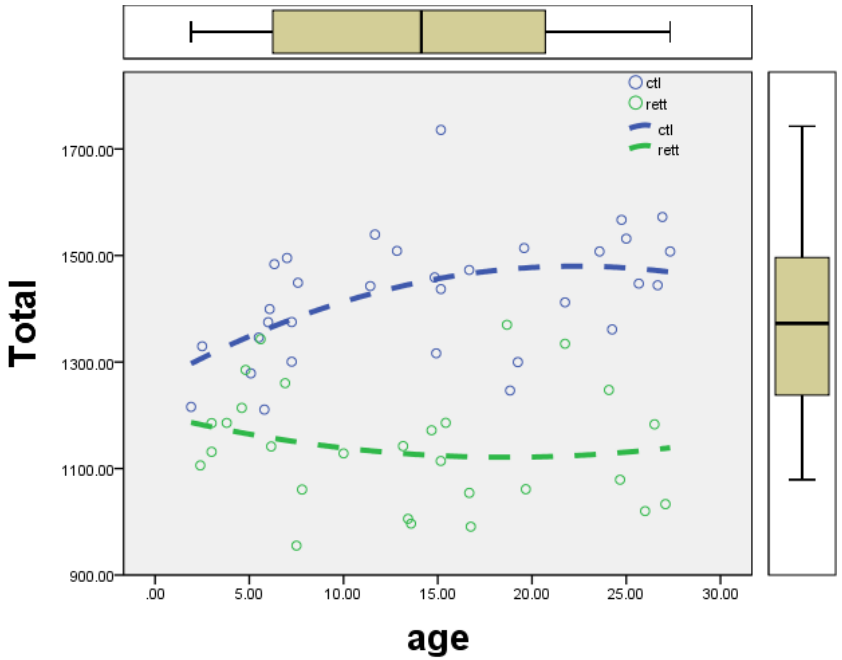

Total intracranial volume

	Adj. R^2	F	Sig.	Intercept	b1	b2
CTL	.241	4.605	.018	1261.109	19.61	-.43
RTT	.033	.431	.655	1202.385	-8.72	.23

doi:10.6342/NTU201702958

Figure 2. The different trajectories of development in gray matter and white matter. (A) Contrast to healthy controls (blue dots and blue line, p = 0.35), the development of gray matter in RTT patients began with a decline trajectory until it reached a plateau at age fifteen (green dots and green line, p = 0.012). (B) Both of healthy controls and RTT patients showed the increasing trajectories with age. However, the constant b1 in controls (b1 = 16.474) was higher than RTT patients (b1 = 5.283).

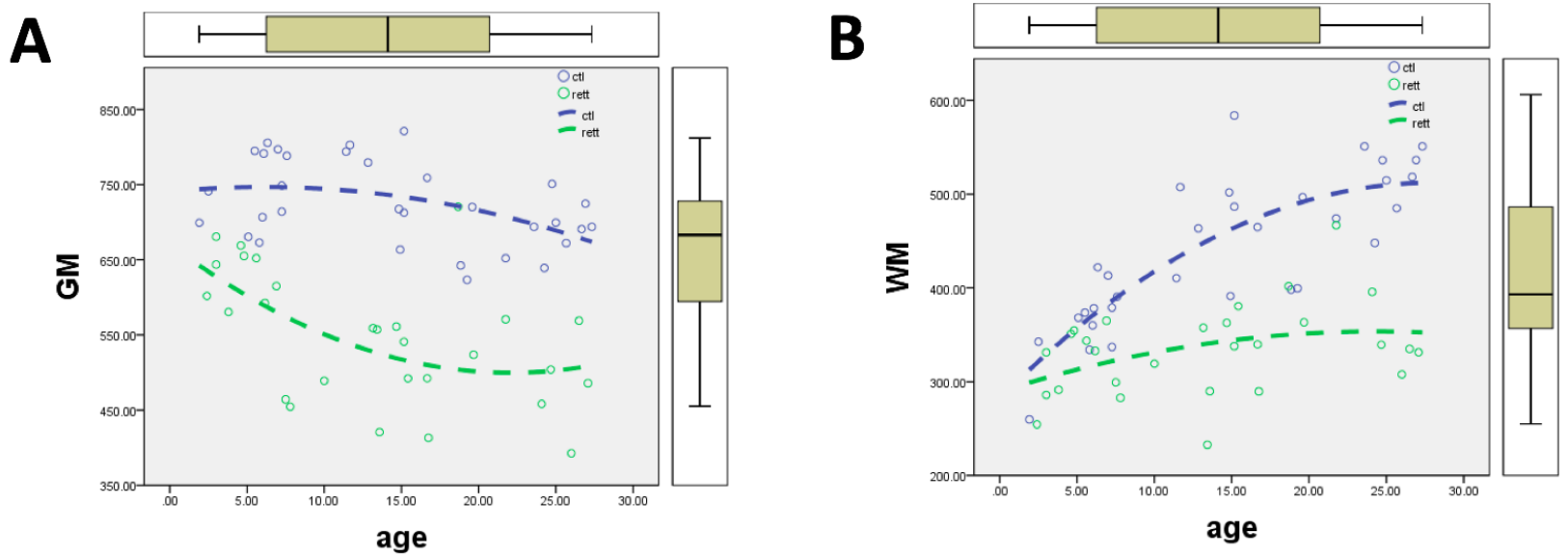

Gray matter volume

	Adj. R^2	F	Sig.	Intercept	b1	b2
CTL	.206	3.767	.035	740.671	1.99	-.16
RTT	.299	5.330	.012	670.703	-15.48	.35

White matter volume

	Adj. R^2	F	Sig.	Intercept	b1	b2
CTL	.664	28.68	.000	282.344	16.474	-.295
RTT	.148	2.165	.136	289.335	5.283	-.109

doi:10.6342/NTU201702958

Figure 3. The difference of developmental trajectories in frontal, parietal, temporal and occipital lobes. In four lobes, the development in gray matter in RTT patients began with a decline trajectory until it reached a plateau at age fifteen.

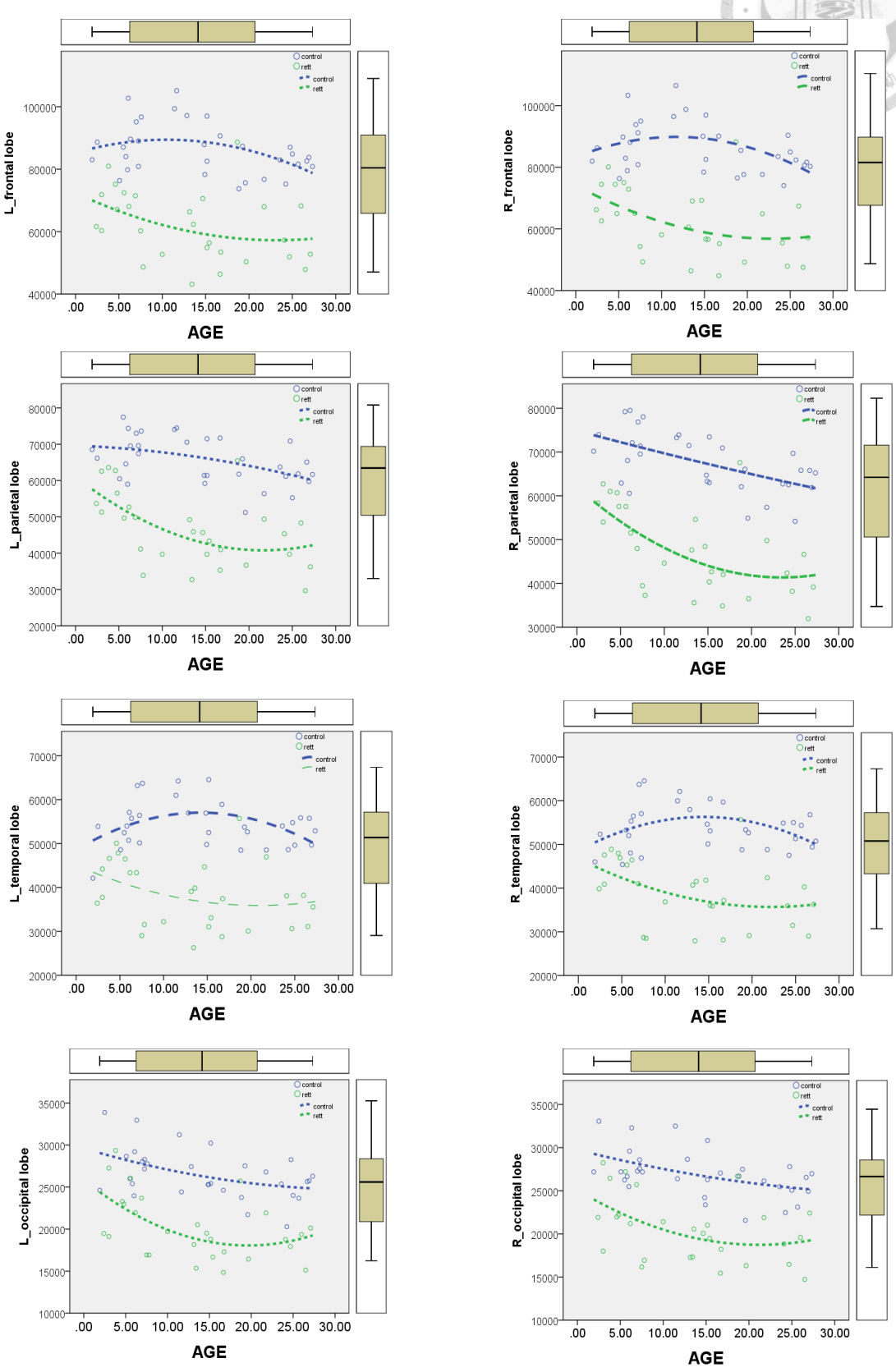

doi:10.6342/NTU201702958

Figure 4. Well-preservation of ROIs in two hemispheres in RTT patients. (a) and (b) showed the preserved gray matter regions in younger RTT patients in contrast to control in left and right hemispheres. (c) showed the preserved gray matter region in older RTT patients compared to controls in left hemisphere. However, in right hemisphere, the gray matter was globally reduced in older patients.

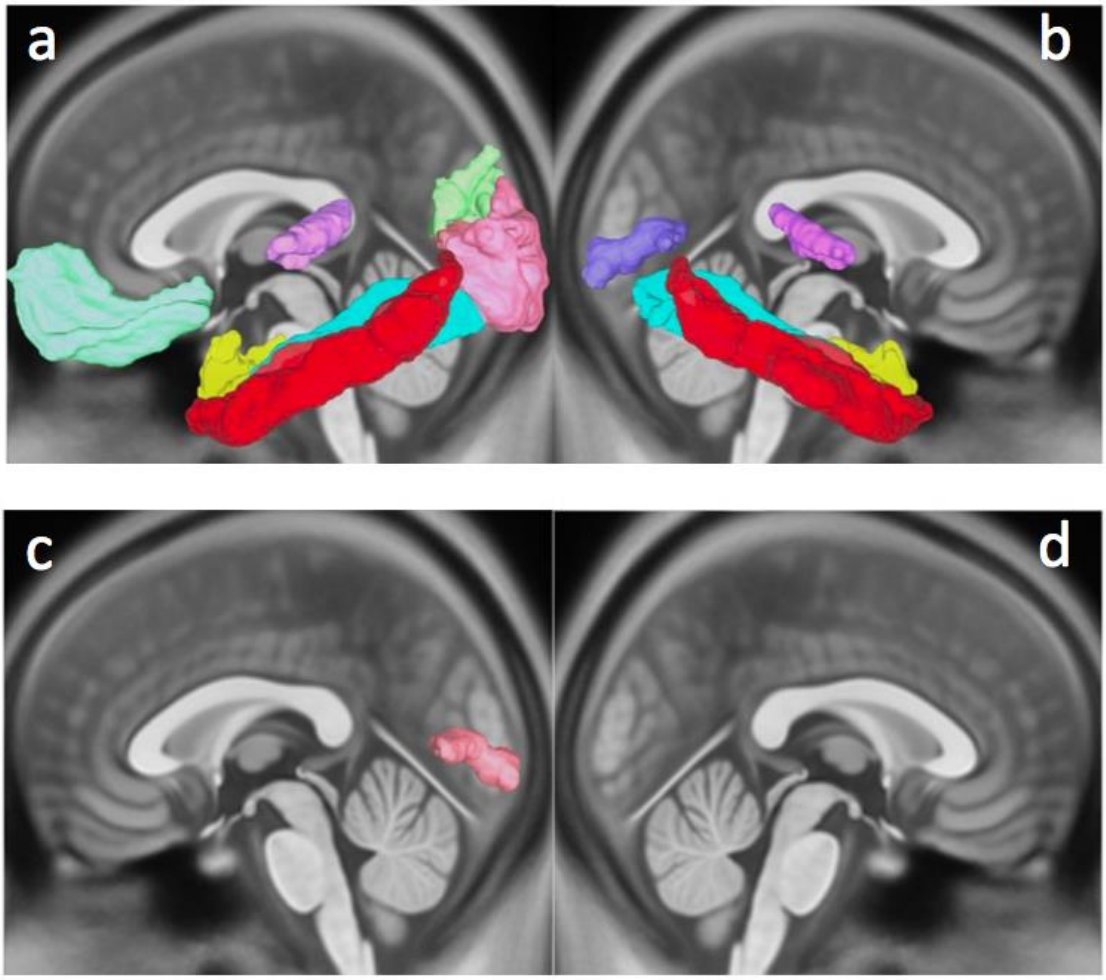

doi:10.6342/NTU201702958

Figure 5. The significant difference of GFA values in language related tracts compared among two speech groups in RTT patients and controls, analyzed by Kruskal Wallis H test. (a) The comparison of mean GFA values in left arcuate fasciculus showed the significant difference between mute and word groups in RTT (p = 0.027) and between mute group and control group (p = 0.003). (b) and (c) showed the significant difference between mute group and control group (p = 0.001 and p = 0.033) in left perpendicular fasciculus and superior longitudinal fasciculus. There was no difference among three groups in mean GFA values in left frontal aslent tract (d).

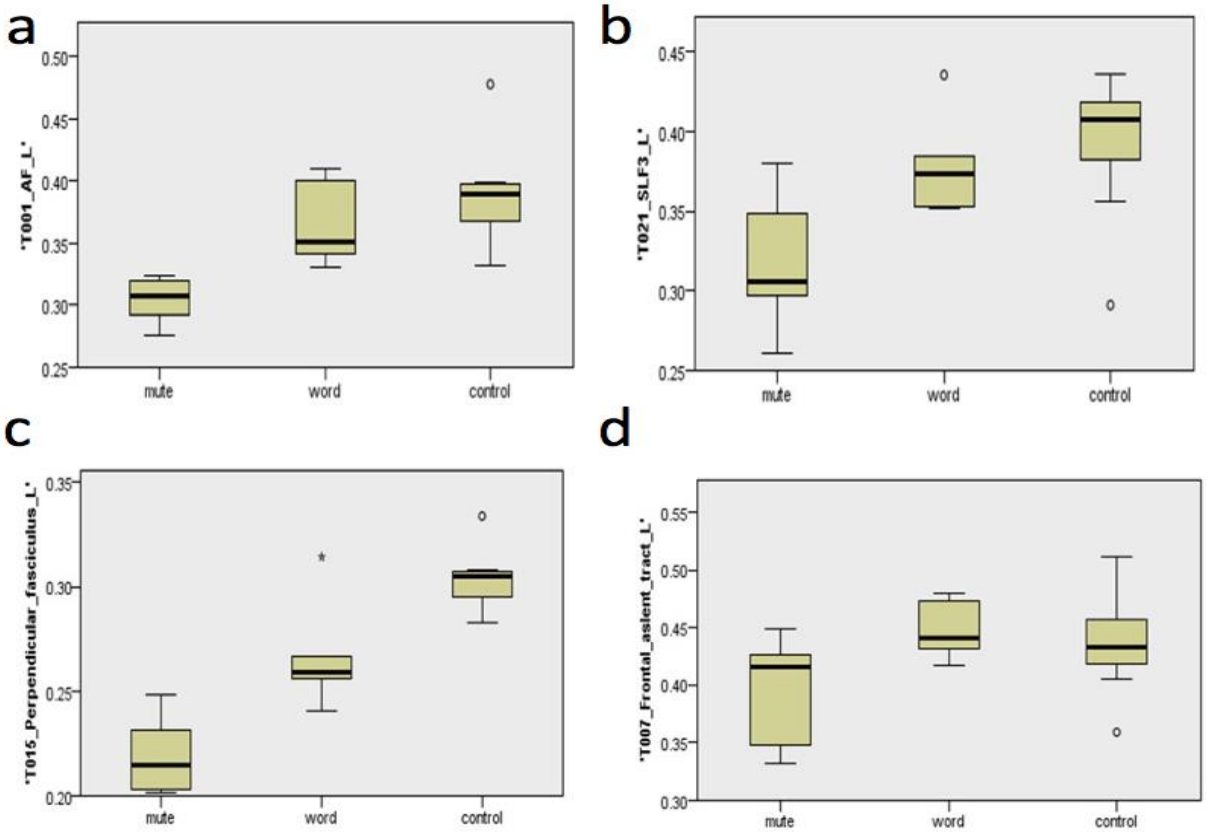

doi:10.6342/NTU201702958

Figure 6. The significant difference of GFA values in language related tracts compared among two speech groups in RTT patients and controls, analyzed by Kruskal Wallis H test. The mean GFA values in corticospinal tracts, connecting to mouth part of motor cortex, were not different among three groups. (c) and (d) showed the significant difference between mute group and control group (p = 0.003 and p = 0.033) in uncinate fasciculus and callosal fiber connecting bilateral superior temporal lobes.

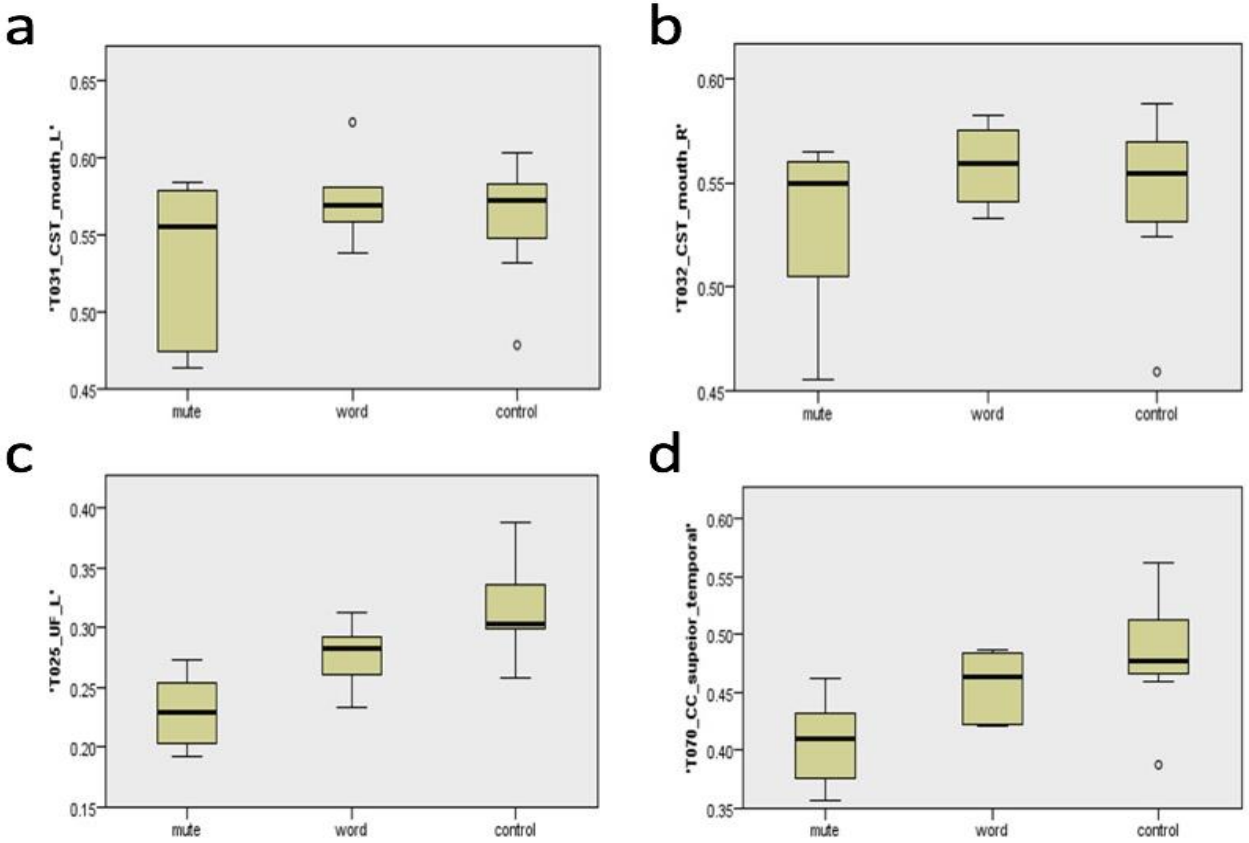

doi:10.6342/NTU201702958

Figure 7. The correlation between visual perceptions related tracts and visual-motor performance in older RTT patients. (a)The moderate correlation between mean GFA value in anterior commissure and visual motor scores was shown in older group (R = 0.531, p = 0.034). b). The mean GFA value in callosal fiber connecting bilateral splenium was correlated with visual motor scores in older group (R = 0.607, p = 0.013).

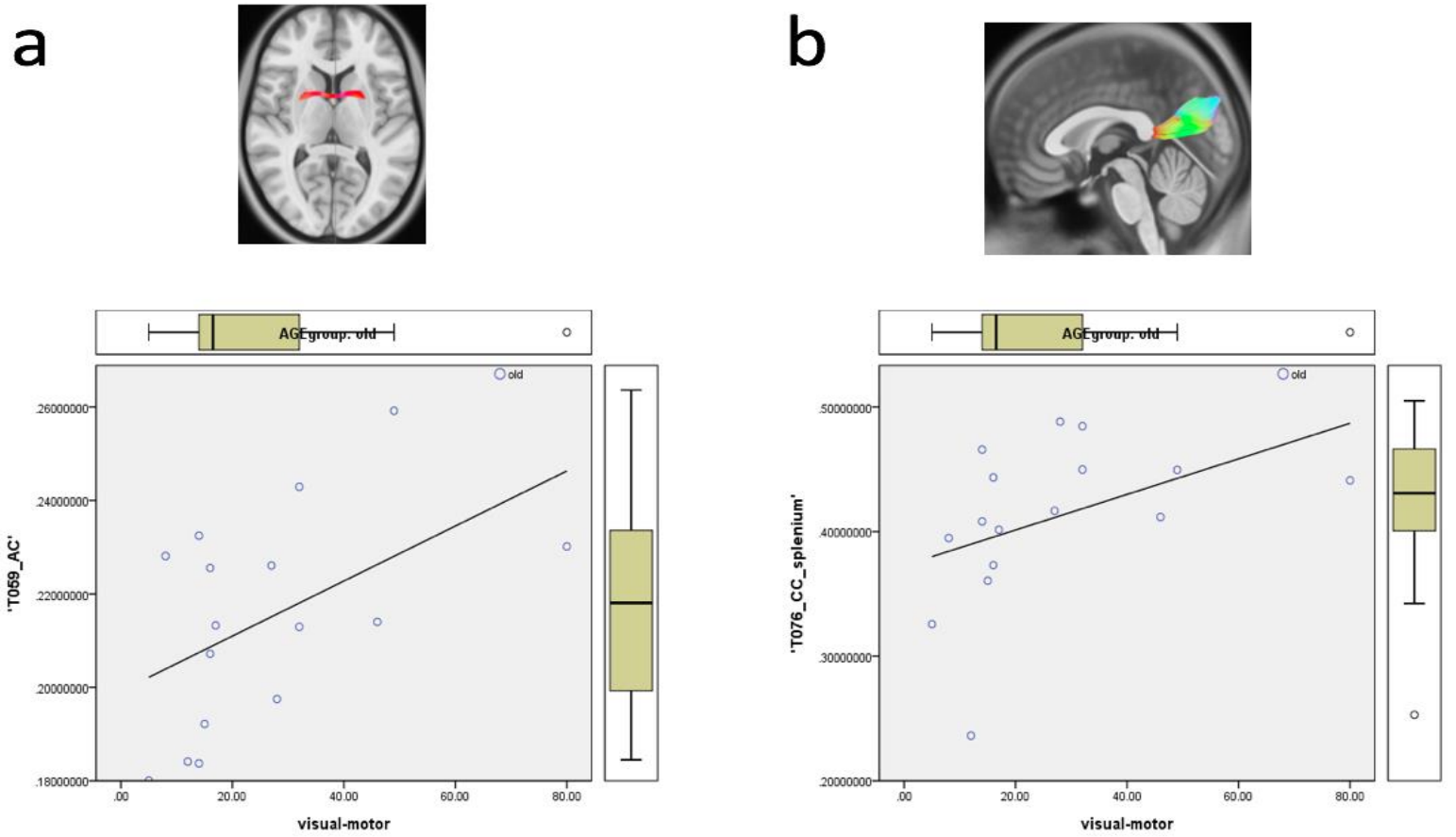

doi:10.6342/NTU201702958

Figure 8. The boxplots showed the comparisons in motor-related tracts among two mobility groups in RTT patients and controls, analyzed by Kruskal Wallis H test. (a) and (d) The comparison of mean GFA values in fiber tracts connecting frontal striatum to left orbitofrontal cortex and right motor precentral gyrus did not show difference among three groups (p = 0.54 and 0.052). (b) and (c). The comparison of mean GFA values in fiber tracts connecting frontal striatum to right orbitofrontal cortex and left motor precentral gyrus showed significant difference between RTT patients without mobility and control group (p = 0.02 and p = 0.023).

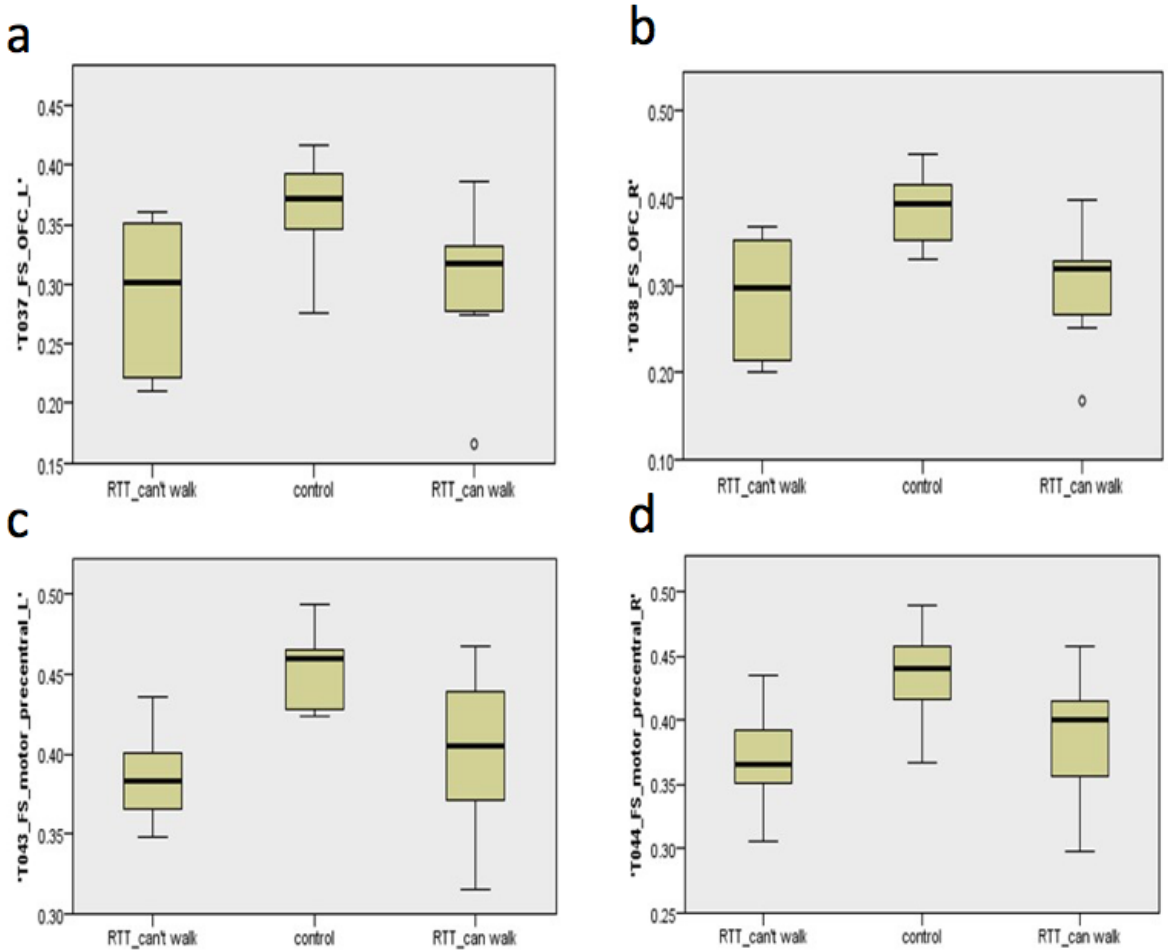

doi:10.6342/NTU201702958

Figure 9. The boxplots showed the comparisons in motor-related tracts among two mobility groups in RTT patients and controls, analyzed by Kruskal Wallis H test. (a)-(e) The comparison of mean GFA values in callosal fibers connecting to DLPFC (p = 0.01; p = 0.025), VLPFC (p = 0.004; p = 0.005), SMA (p =0.041; p = 0.032), motor precentral gyrus (p = 0.017; p = 0.024), and paracentral gyrus (p = 0.002; p = 0.024) showed significant differences between patients with mobility and controls, and between patients without mobility and controls, respectively.

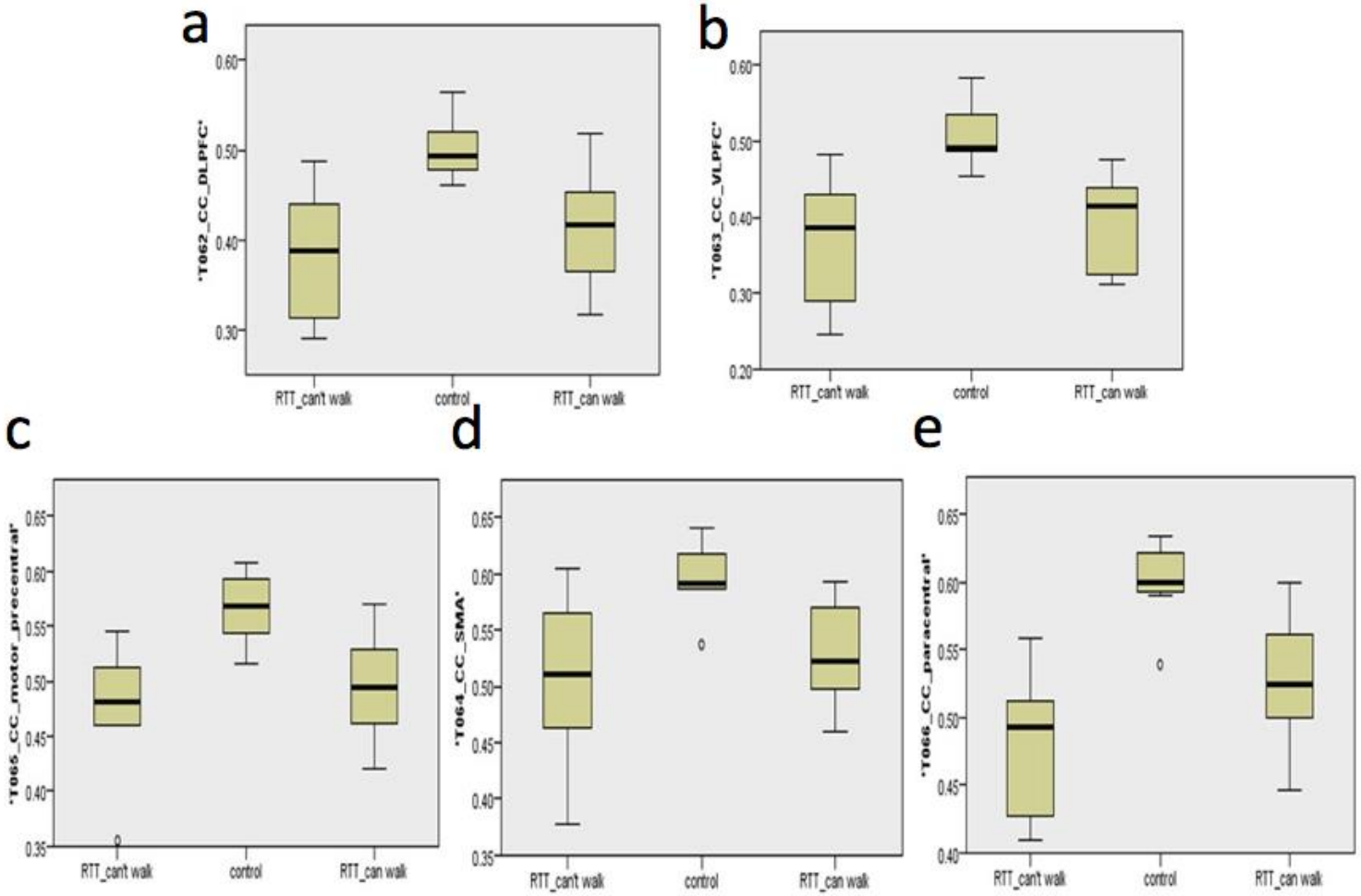

doi:10.6342/NTU201702958

Figure 10. The boxplots illustrated the significant differences in five ROIs in the midbrain. (b), (c), and (d) The contrast ratio of signal intensity was significantly different in caudate nucleus, putamen, and globus pallidus between RTT patients and controls. (a) and (e) The contrast ratio of substantia nigra and thalamus was not significantly different between RTT patients and controls.

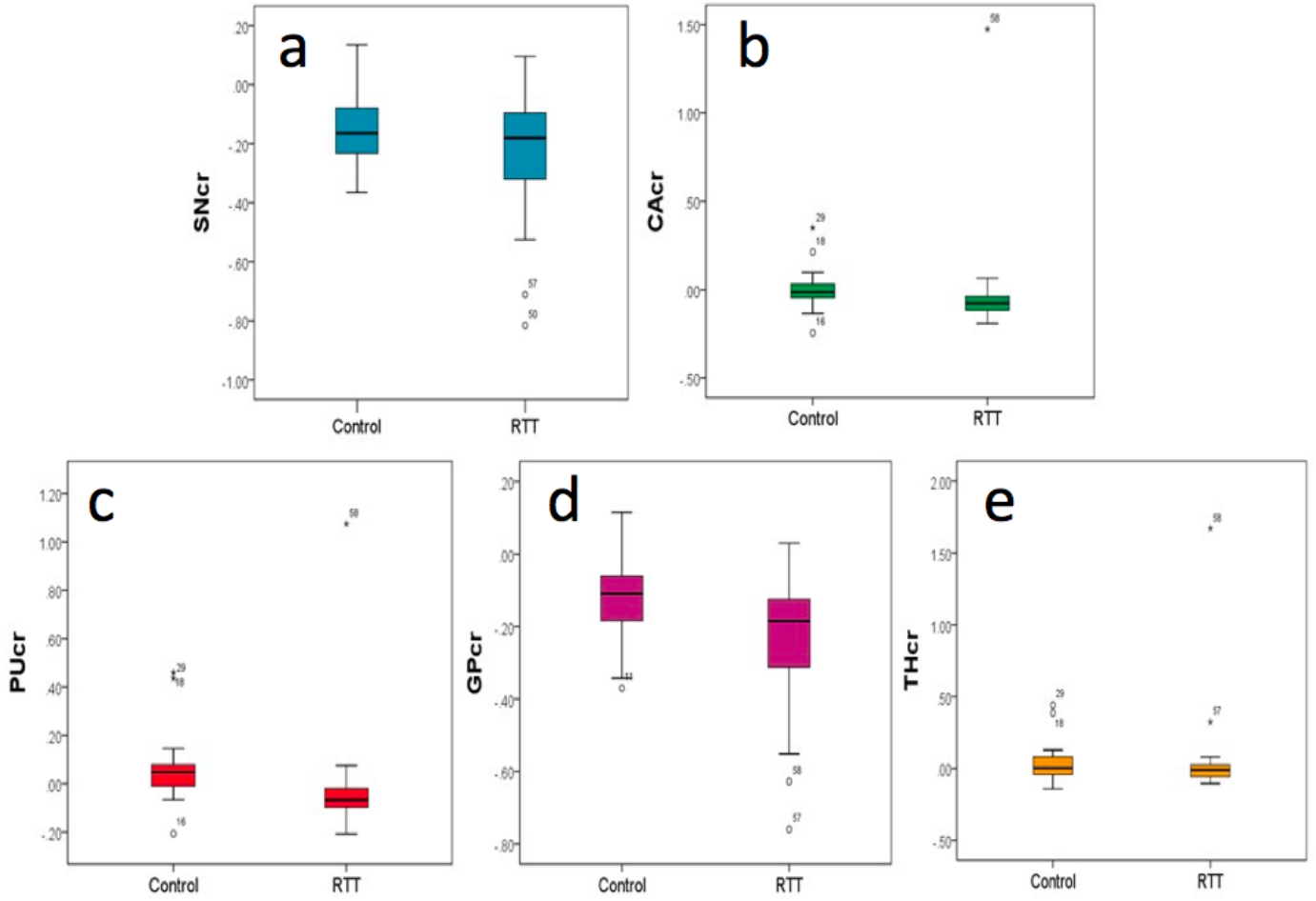

doi:10.6342/NTU201702958

Figure 11. The Spearman's correlation between age and contrast ratio of significant difference in 5 ROIs in the midbrain. The correlation between contrast ratio and age was significantly different in substantia nigra (R = -0.546; p = 0.001), caudate nucleus (R = -0.415; p = 0.020), putamen (R = -0.580; p = 0.001), globus pallidus (R = -0.740; p < 0.001), and thalamus (R = -0.489; p = 0.005) in control group (blue dots and blue line). On the other hand, the correlation in RTT group (green dots and green line) was significant different in substantia nigra (R = -0.652; p < 0.001), caudate nucleus (R = -0.404; p = 0.033), putamen (R = -0.585; p = 0.001), and globus pallidus (R = -0.680; p < 0.001). However, there was no correlation between contrast ratio in thalamus and age in RTT group (R = -0.356; p = 0.063).

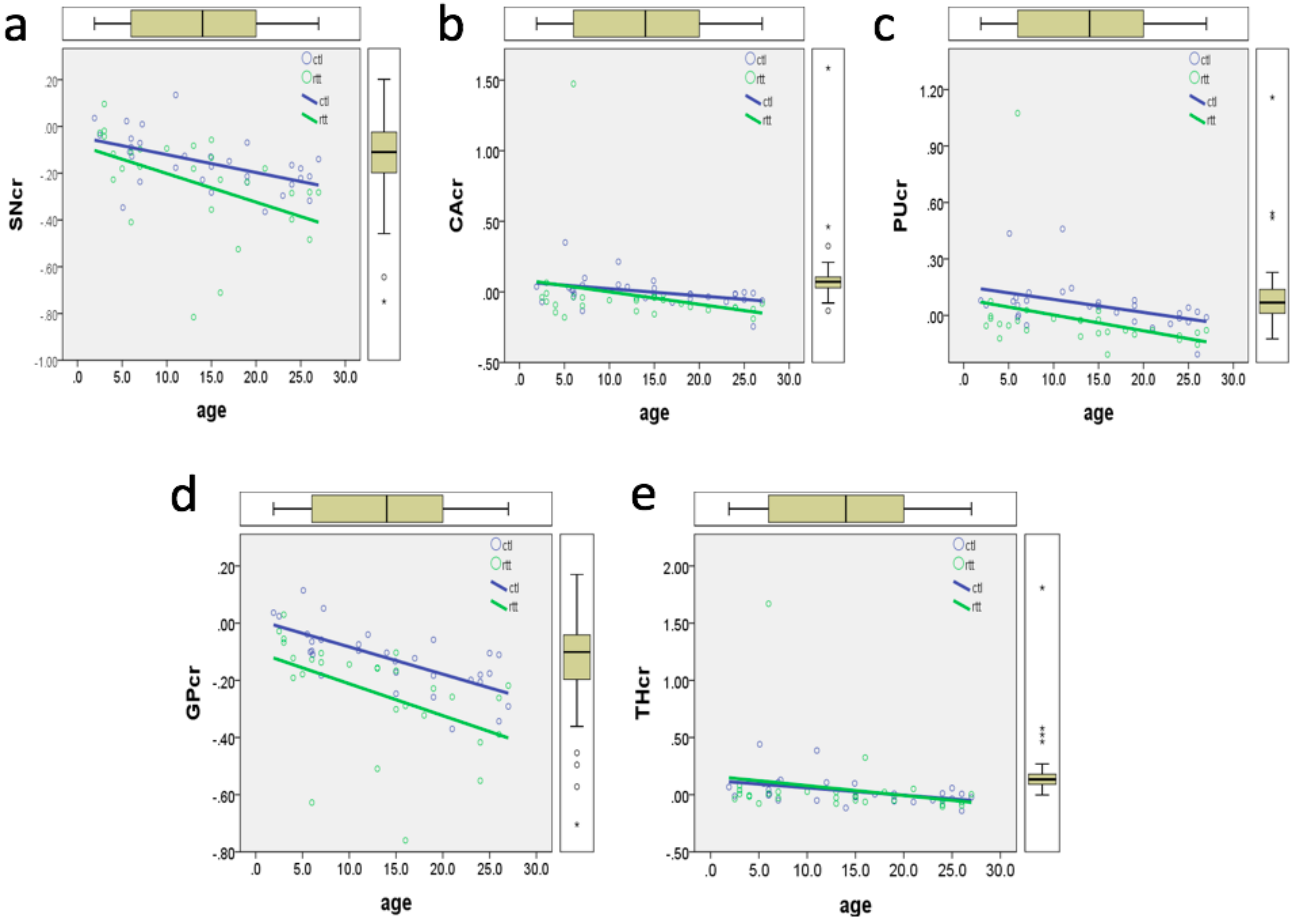

doi:10.6342/NTU201702958

Figure 12. The Spearman's correlation between clinical behavior and contrast ratio of significant difference in 5 ROIs in the midbrain. (b) and (e) showed the significant correlations with clinical behavior in caudate nucleus (R = 0.403; p = 0.033) and thalamus (R = 0.423; p = 0.025). However, there were no correlation with clinical behavior in contrast ratio in substantia nigra, putamen, and globus pallidus (p = 0.936; p = 0.136; p = 0.094).

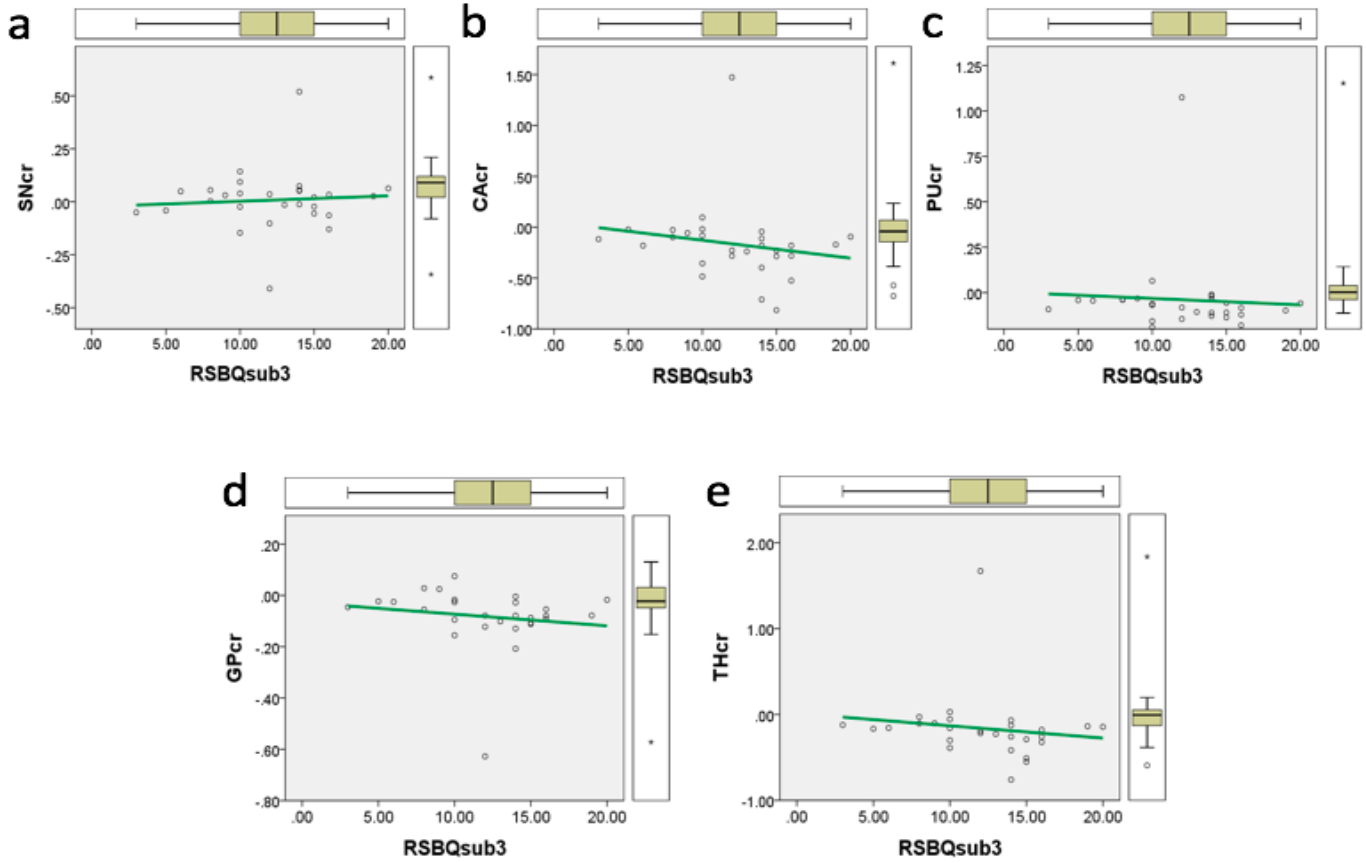

doi:10.6342/NTU201702958

Figure 13. Reconstruction of speech-language-related tracts with significant difference between RTT patients and controls. (* Survived after Bonferroni correction)

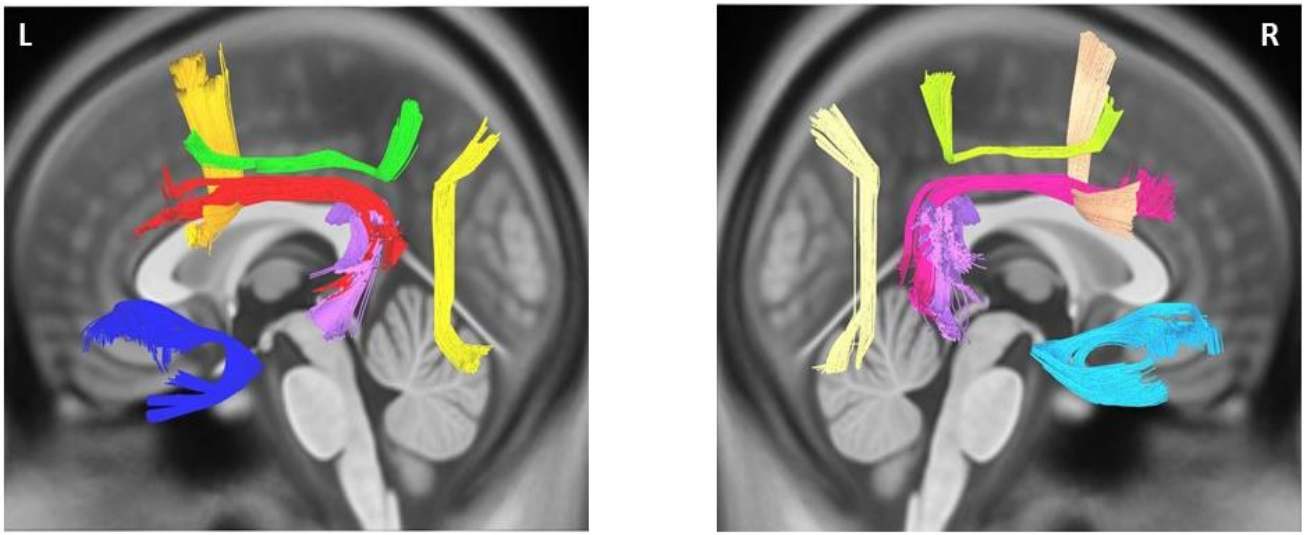

doi:10.6342/NTU201702958

Figure 14. Reconstruction of visual perception-related tracts with significant difference between RTT patients and controls. (* Survived after Bonferroni correction)

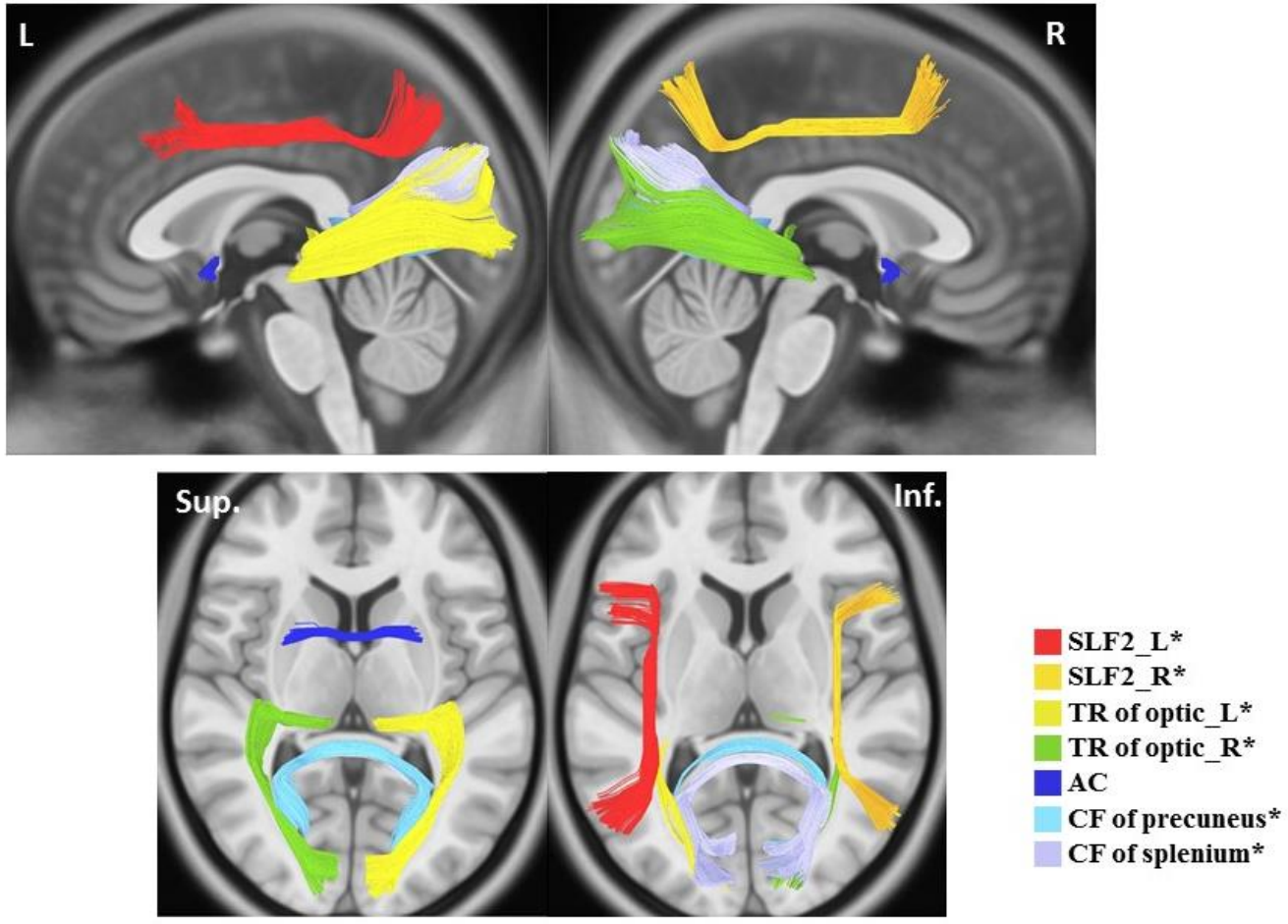

doi:10.6342/NTU201702958

Figure 15. Reconstruction of motor related tracts with significant difference between RTT patients and controls. (* Survived after Bonferroni correction)

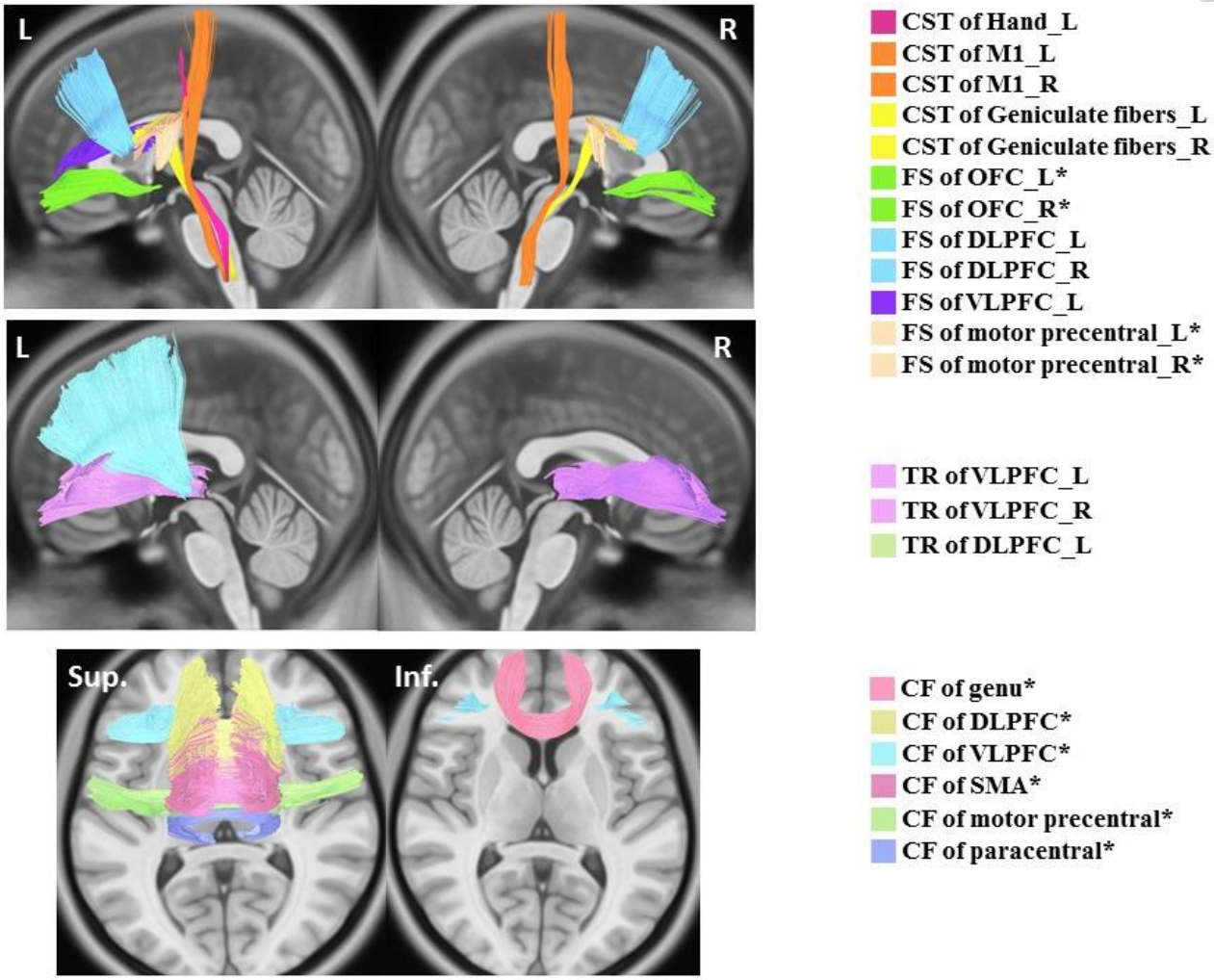

doi:10.6342/NTU201702958